UM-HSRI-76-26-2

Predicting the Braking Performance of Trucks and Tractor-Trailers

Phase III Technical Report
Appendices

C.B. Winkler
J.E. Bernard
P.S. Fancher
C.C. MacAdam
L. K. Johnson

Project 360932

Truck and Tractor-Trailer Braking and Handling Project

June 1976

Highway Safety Research Institute/University of Michigan

Technical Report Documentation Page

1. Report No.	2. Government Accession No.	3. Recipient's Catalog No.
UM-HSRI-76-26-2		

4. Title and Subtitle	5. Report Date
PREDICTING THE BRAKING PERFORMANCE OF TRUCKS AND TRACTOR-TRAILERS - Phase III Technical Report - Appendices A, B, C, D, E, F	June 15, 1976
	6. Performing Organization Code
7. Author(s) C. Winkler, J. Bernard, P. Fancher, C. MacAdam, L. Johnson	8. Performing Organization Report No. UM-HSRI-76-26-2
9. Performing Organization Name and Address Highway Safety Research Institute The University of Michigan Huron Parkway and Baxter Road Ann Arbor, Michigan 48109	10. Work Unit No. (TRAIS) 360932 11. Contract or Grant No.
12. Sponsoring Agency Name and Address Motor Vehicle Manufacturers Association 320 New Center Building Detroit, Michigan 48202	13. Type of Report and Period Covered 14. Sponsoring Agency Code
15. Supplementary Notes	

16. Abstract

This report documents three digital computer programs for predicting the braking performance of commercial highway vehicles. The computer programs were developed by the Highway Safety Research Institute of The University of Michigan under the sponsorship of the Motor Vehicle Manufacturers Association. The three programs are applicable to straight trucks, tractor-semitrailers, and doubles combination vehicles. The programs model these vehicle types in detail and include the effects of tandem suspension dynamics, air brake system dynamics, brake fade, antilock system performance, and sprung mass dynamics.

The research studies leading to the development of the programs are discussed. The report concludes with a discussion of appropriate applications of these programs, and with a recommendation for further research into the areas of truck tire mechanics, the mechanical friction brake, and antilock systems.

17. Key Words	18. Distribution Statement
commercial vehicles, truck, tractor-trailer, doubles, braking performance, tandem suspension, fade, antilock, simulation, tires, dynamics, brakes	Unlimited

19. Security Classif. (of this report)	20. Security Classif. (of this page)	21. No. of Pages	22. Price
None	None	154	

Form DOT F 1700.7 (8-72) Reproduction of completed page authorized

* U. S. GOVERNMENT PRINTING OFFICE : 1973 725-504/328

UM-HSRI-76-26-2

PREDICTING THE BRAKING PERFORMANCE OF TRUCKS AND TRACTOR-TRAILERS

Phase III Technical Report

Appendices A, B, C, D, E, F

C. B. Winkler
J. E. Bernard
P. S. Fancher
C. C. MacAdam
L. K. Johnson

Project 360932

Truck and Tractor-Trailer Braking
and Handling Project

June 1976

Sponsored by

The Motor Vehicle Manufacturers Association

EDITOR'S NOTE

The reader should note that Appendix F, included in the Table of Contents in this volume, was not listed in the Table of Contents of Volume 1. This is because the optional fifth wheel models discussed in Appendix F were implemented into the Phase III computer programs in October 1976, following the printing of Volume 1.

TABLE OF CONTENTS

APPENDIX A - THE PROGRAMS. 1

APPENDIX B - THE SUSPENSION MODELS 11

B.1 General Suspension Program Format. 11

B.2 The Single-Axle Suspension 21

B.3 The Walking Beam Suspension. 24

B.4 The Basic Four Spring Suspension 33

B.5 The Four Spring Suspension with Spring-Type Torque Rods. 53

B.6 The Four Spring Suspension with Long Load Leveler. 58

B.7 The Multiple-Torque Rod Four Spring Suspension 64

B.8 The MTRFSS with a Leaf Spring-Type Lower Torque Rod 76

B.9 Air Suspension Model 78

APPENDIX C - THE SPRUNG MASSES 109

C.1 Introduction 109

C.2 Static Considerations. 109

C.3 The Dynamic Sprung Mass Models 119

APPENDIX D - THE BRAKE MODELS. 127

D.1 Introduction 127

D.2 Brake Torque Calculation 127

D.3 Brake Factor Calculations. 130

D.4 User Input for Brake Modules 134

D.5 References 136

APPENDIX E - THE ANTILOCK MODEL. 139

APPENDIX F - OPTIONAL FIFTH WHEEL MODELS 151

APPENDIX A

THE PROGRAMS

The Phase III programs consist of three different digital computer programs, one each for the simulation of the braking performance of straight trucks, tractor-semitrailers, and doubles combination vehicles. Each of the three programs consists of a MAIN program and INPUT, OUTPUT, and FCTl subprograms, i.e., there is a different version of each of these programs associated with each of the three vehicle types. In addition, a group of "support" subprograms, which include HPCG, ANTLKR, PRINT, BRAKE, TABLE, ROAD, INPOAl, INP5A6, and INPAIR, are used by these three programs.

All the programs are written in FORTRAN IV. The core storage requirements for the programs are:

Straight truck programs:	89912 bytes
Tractor-Semitrailer programs:	135616 bytes
Doubles programs:	162032 bytes
Support programs:	148656 bytes

A general flow diagram for the Phase III programs was presented in Section 2.0 (Figure 2.1). To further assist the user in understanding the program flow, Table A-l reviews the various subroutines, presenting their entry points, the programs from which they are called, and their functions. Also, Figures A-l through A-5 present flow diagrams for various subroutines.

TABLE A-1

THE PHASE III SUBROUTINES

Subroutine	Entry Points	Called From	Function
INPUT	INPUT	MAIN	Read and echo all data exclusive of optional suspension, antilock, time increment and rerun parameters.
	RERUN		Read the rerun parameter and CALL EXIT or restart program.
OUTPUT	OUTPUT	MAIN	Read time increment and initialize constants and variables.
	OUTP	HPCG	Update variables, write onto output buffer, print output buffer when appropriate, signal HPCG for termination of integration when appropriate.
	OUTP1	MAIN	Print output buffer.
	TORQUE	FCT	Determine brake pressures and torques including hysteresis.
FCT1	FCT1	MAIN	Initialize and static calculation.
	FCT	HPCG	Performs the majority of dynamic calculations including those concerning the sprung mass, front suspension, tire forces and brake fade.
HPCG	HPCG	MAIN	IBM Scientific Subroutine Package program which performs the integration of state variables and controls program flow.

TABLE A-1 (Cont.)

Subroutine	Entry Points	Called From	Function
ANTLKR	ANTLKR	INPUT	Read antilock parameters.
	ANTLKW	INPUT	Echo antilock parameters.
	ANTLK	TORQUE	Modify brake pressure depending on antilock performance.
PRINT	PRINT	ANTLKW	Assist in printing antilock parameters.
BRAKE	BRAKE	INPUT	Read brake module parameters.
	BRAKE1	INPUT	Echo brake module parameters.
	BINIT	OUTPUT	Initialization calculation for brake modules.
	BCALCU	TORQUE	Calculate brake torque using brake modules.
	FINAL	OUTP	For debug purposes.
TABLE	TABLE	A variety of places	Handle tabular data.
ROAD	ROAD	FCT1	Accept data describing the sprung mass.
	ROADS	ONEOA1, ONE5A6, ONEAIR	Calculate axle positions on the vehicle.

TABLE A-1 (Cont.)

Subroutine	Entry Points	Called From	Function
	ROADS2	FCT	Calculate road height at each axle.
INPOA1	INPOA1	INPUT	Read and echo data and initialize constants for single-axle or walking beam suspension.
	ONEOA1	FCT1	Perform static calculations for single-axle or walking beam suspensions.
	SUS1AX	FCT	Perform dynamic calculation for single-axle suspension.
	SUSWLK	FCT	Perform dynamic calculation for walking beam suspension.
INP5A6	INP5A6	INPUT	Read and echo data and initialize constants for all variations of the four spring suspension.
	ONE5A6	FCT1	Perform static calculations for all variations of the four spring suspension.
	SUS2A3	FCT	Perform dynamic calculations for the basic four spring and four spring with spring-type torque rod suspension.
	SUS4	FCT	Perform dynamic calculation for the four spring suspension with long load leveler.

TABLE A-1 (Cont.)

Subroutine	Entry Points	Called From	Function
	SUS5A6	FCT	Perform dynamic calculations for the MTRFSS and MTRFSS with spring-type lower torque rod.
INPAIR	INPAIR	INPUT	Read and echo data and initialize constant for air suspensions.
	ONEAIR	FCT1	Perform static calculations for air suspensions.
	SUSAIR	FCT	Perform dynamic calculations for air suspensions.

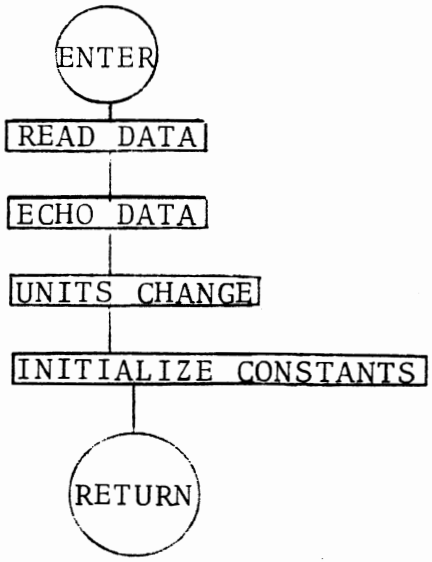

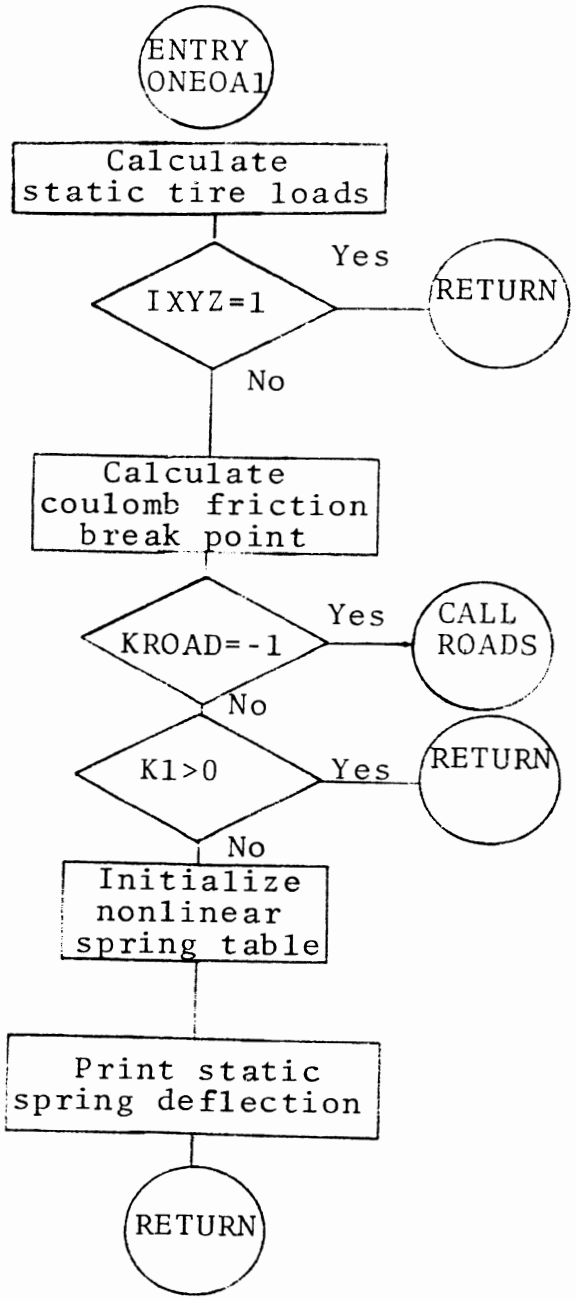

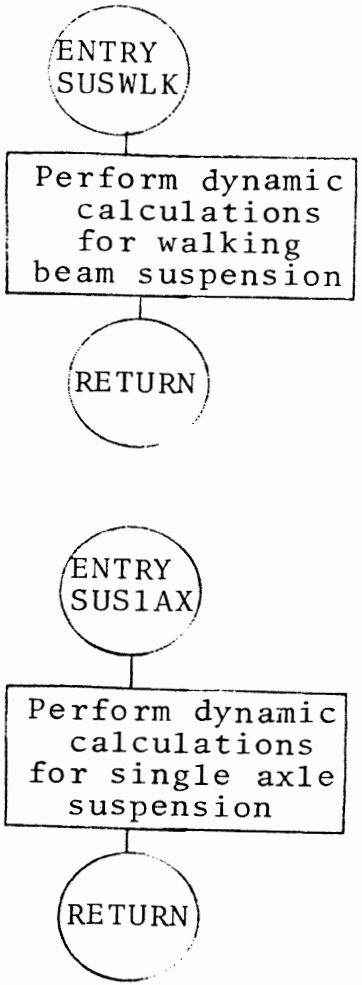

Figure A-1. Flow diagram of INPOA1

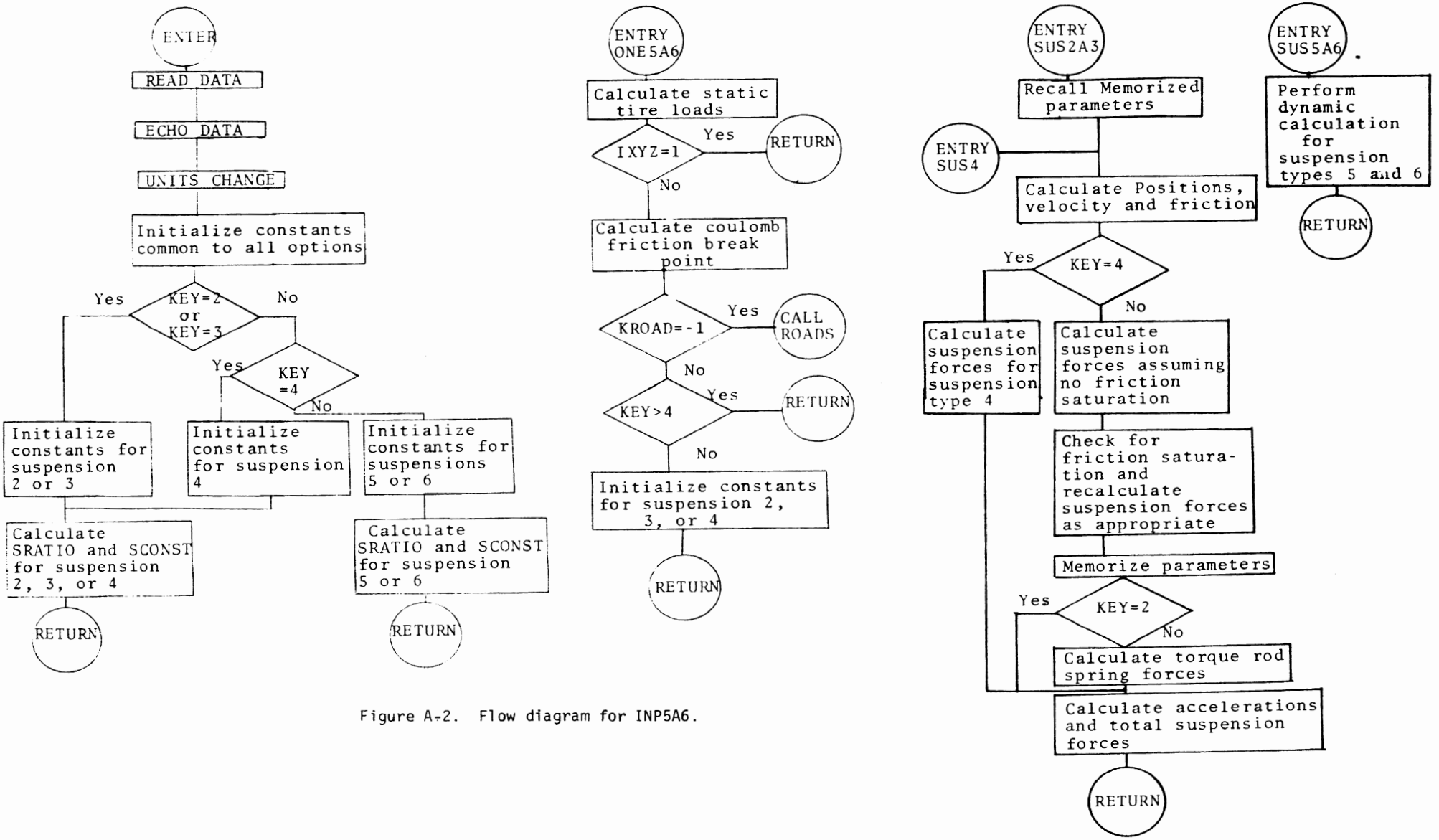

Figure A-2. Flow diagram for INP5A6.

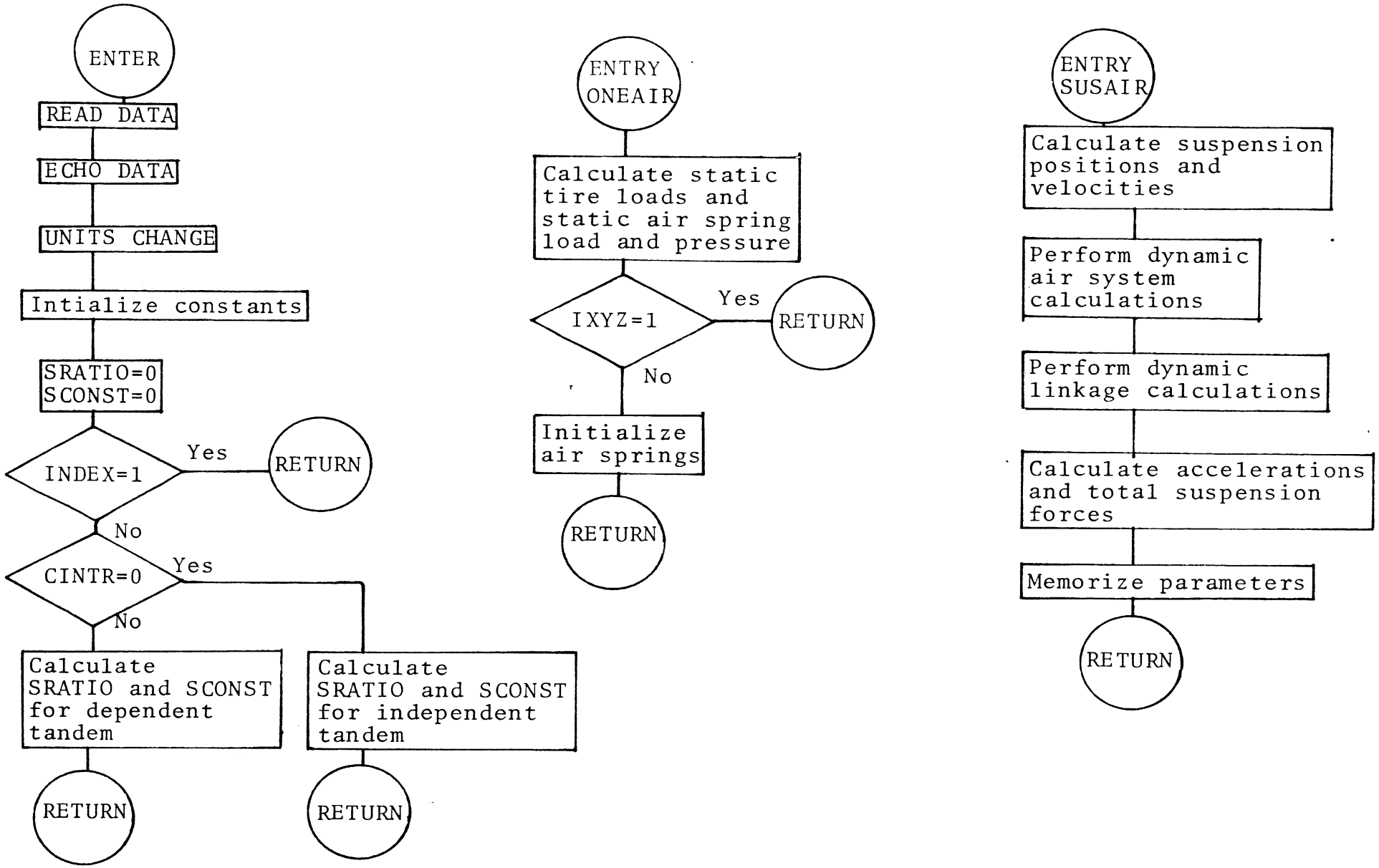

Figure A-3. Flow diagram for INPAIR.

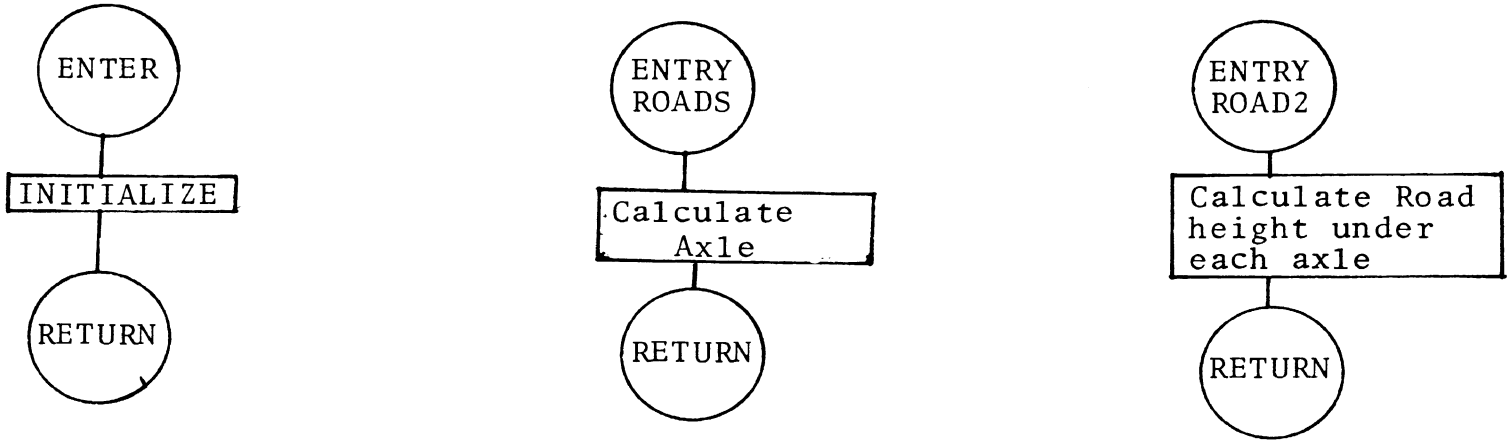

Figure A-4. Flow diagram for ROAD.

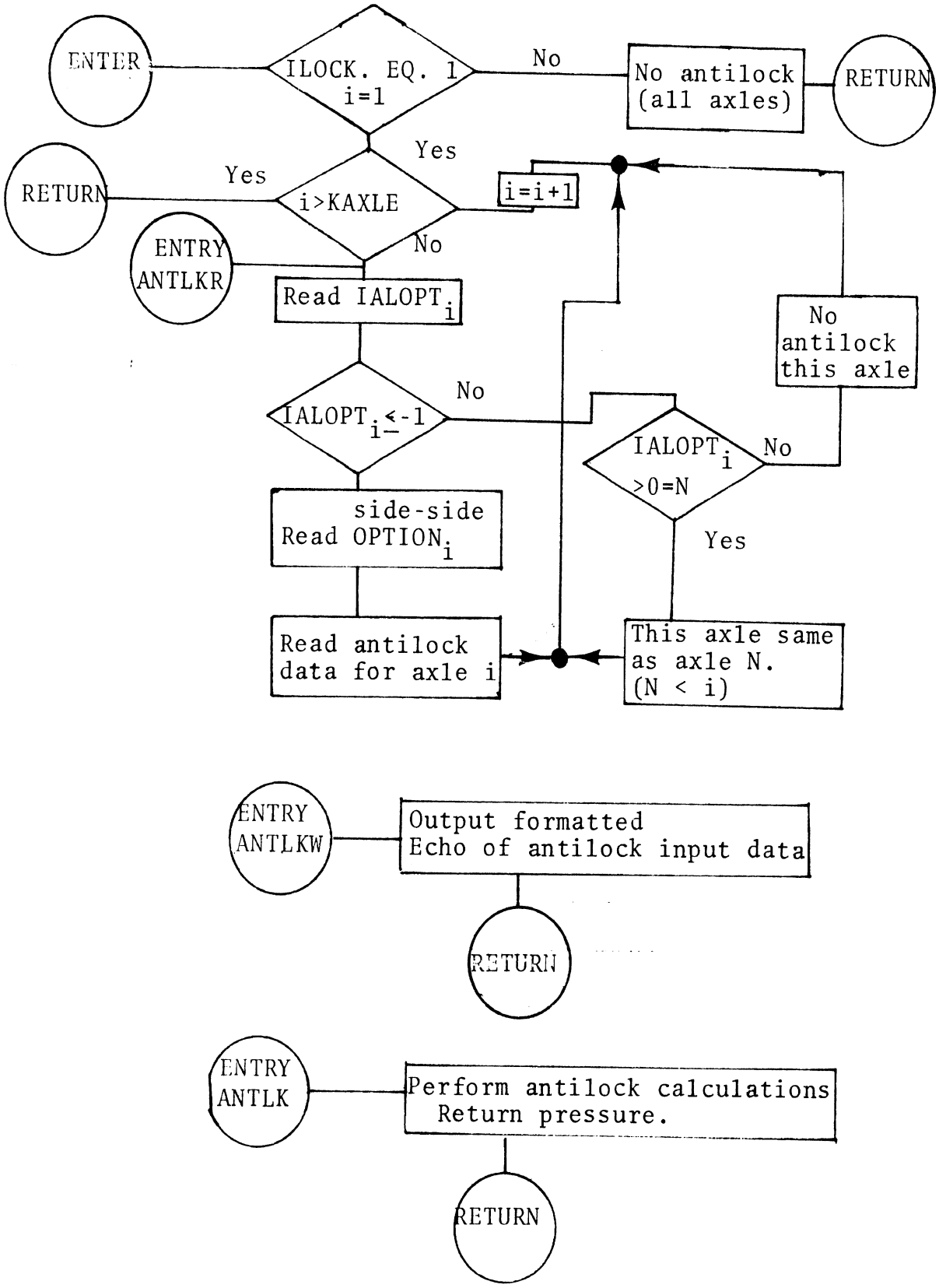

Figure A-5. Flow diagram for ANTLKR

APPENDIX B

THE SUSPENSION MODELS

B.1 General Suspension Program Format

In this appendix, the mathematical models used to simulate each of the optional suspension types available to the user will be reviewed. In this first section of the appendix, certain considerations common to various suspension types will be considered.

Because of the variety of options available, all suspension calculations are performed in suspension subprograms which are part of the total simulation program. To facilitate the manipulation of suspension options within the program, all individual forces (i.e., torque rod, spring, friction, etc.) which a suspension applies to the sprung mass are summed into a generalized vertical force, horizontal force, and moment which act through and about the "Suspension Reference Point.*" These generalized forces and moment are then passed from the suspension subprogram to the main portion of the program for the sprung mass calculations. This general format is employed by the simulation for both static and dynamic calculations.

For dynamic calculation the generalized forces and moment are named TSFV (total suspension force, vertical), TSFH (total suspension force, horizontal), and TSTORQ (total suspension torque). Sign conventions for these generalized forces are:

TSFV	is positive for tensile forces between sprung and unsprung masses (springs extended from their static length)
TSFH	is positive for forces between sprung and unsprung masses which tend to accelerate the sprung mass

*The Suspension Reference Point for each of the suspension options was defined in Section 2.

TSTORQ is positive for moments which tend to produce a positive pitch of the sprung mass (i.e., front up, rear down).

Note that each of these variables is the dynamic component of the generalized force, i.e., these variables are zero at static equilibrium.

In the static calculation the variables SSFV and STORQ are the equivalents of TSFV and TSTORQ, respectively. For any suspension, two constants, SRATIO and SCONST are also defined such that:

$$STORQ = SRATIO \cdot SSFV + SCONST \qquad (B\text{-}1)$$

These two constants are properties of a suspension which are calculated using parametric input supplied by the user. The values of SRATIO and SCONST are determined during the first of two initialization entries to the suspension subprogram. These values are passed to the main portion of the program which then calculates the distribution of static suspension loads about the vehicle (i.e., SSFV for each of the various suspensions). SSFV is passed to the suspension subprogram at the time of the second initialization entry and the static wheel loads are calculated.

In the latter sections of this appendix, the mathematics of each suspension model will be discussed. These discussions will be confined to the equations of motion of the unsprung masses and to the calculation of SRATIO, SCONST, STORQ, TSFV, TSFH, and TSTORQ.* The manner in which these functions are employed in sprung mass-related calculations will be considered in Appendix C.

In deriving the equations for the suspension models, the following assumptions were made: (1) the force in the suspension is the sum of the forces due to coulomb friction, viscous friction

*Note that SSFV is deleted from this list for it is calculated in the sprung mass portion of the program.

and the spring force; (2) the suspension forces are always in the "z" direction. The differences between results derived using this assumption and results derived assuming that the forces are perpendicular to the frame of the vehicle are negligible for small pitch angles.

Most of the suspension options allow for the inclusion of coulomb friction. The classic expression usually denoted by the term "coulomb friction" is

$$f \leq \mu N \tag{B-2}$$

where

f is the force of friction,

μ is an experimentally derived parameter,

N is the contact "normal force" between two sliding surfaces.

Equation (B-2) is empirical in nature, and describes approximately an observed phenomenon. To illustrate this point, consider the simple system shown in Figure B-1.

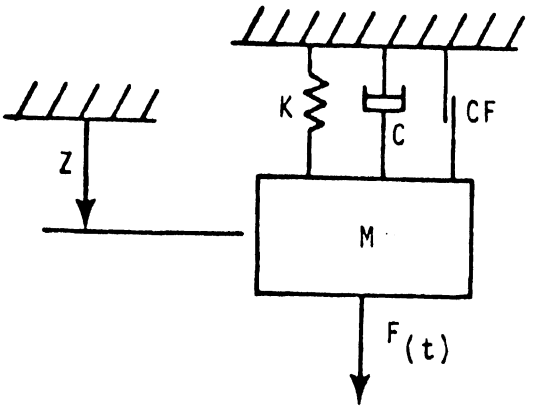

Figure B-1. Mass spring system with viscous damping and coulomb friction.

The equation of motion of the mass M shown is

$$\overline{CF} = Mg + F(t) - Kz \qquad \text{(B-3a)}$$

for $\dot{z} = 0 , \quad |\overline{CF}| < CF$

otherwise,

$$M\ddot{z} + Kz + C\dot{z} + CF \frac{|\dot{z}|}{\dot{z}} = Mg + F(t) \qquad \text{(B-3b)}$$

where CF is the maximum allowable magnitude of the coulomb friction force $\overline{CF}$, F(t) is the driving force on the system, K is the spring rate, C is the viscous damping coefficient, z is the displacement of the mass M (z=0 at the free length of the spring), and g is the gravity constant.

From Equation (B-3a), it can be seen that no motion is possible for the system initially at rest until the magnitude of the quantity Mg + F(t) - Kz becomes greater than |CF|. At this point, motion ensues, which is described by Equation (B-3b), until the system again meets the conditions of Equation (B-3a).

In developing a digital simulation of a system with coulomb friction, Equations (B-3a) and (B-3b) present special problems. Since the velocity $\dot{z}$ is known only at discrete points, the time when $\dot{z}$ equals zero cannot easily be found. Thus, the actual time to switch from solution of Equation (B-3a) to solution of Equation (B-3b) is not known. There are a variety of ways to circumvent this problem, some of which are considered below:

(a) Continuously solving Equation (B-3b). This method is unsatisfactory (especially for large amounts of coulomb friction) since the system will "chatter" around the static equilibrium position. A slightly negative $\dot{z}$ produces large coulomb friction, which

causes large positive $\ddot{z}$. When the large positive $\ddot{z}$ is integrated over a short time, positive $\dot{z}$ results. The cycle then repeats with opposite signs. The period of this "chatter" is twice the integration time step.

(b) Use an "equivalent viscous damping." By this method an increased value of C is chosen to compensate for the elimination of coulomb friction. This method can be useful when the coulomb friction forces are small compared to the velocity sensitive forces, but, in general, it cannot yield satisfactory results in truck dynamics since the forces of coulomb friction are normally much larger than those of viscous friction.

(c) Introduce a "dead zone" around static equilibrium. This method is shown schematically in Figure B-2. This method has proven quite satisfactory for suspensions in which both viscous and coulomb friction are present. In the event that the viscous coefficient C is zero, however, the simulation allows velocity up to $|\dot{z}| = \delta$ with no energy loss. In digital computation this can cause the same type of chatter described in (b) above.

(d) Use a limiting (saturation) function. A schematic diagram showing the function used in the simulation is given in Figure B-3. This function effectively eliminates the problems with the methods described in (a), (b), and (c).

There is no free zone around static equilibrium. Thus, given large enough δ, all chatter is eliminated. The value of δ should be small enough, however, to preserve the character of coulomb friction. A method for the computation of δ is given below:

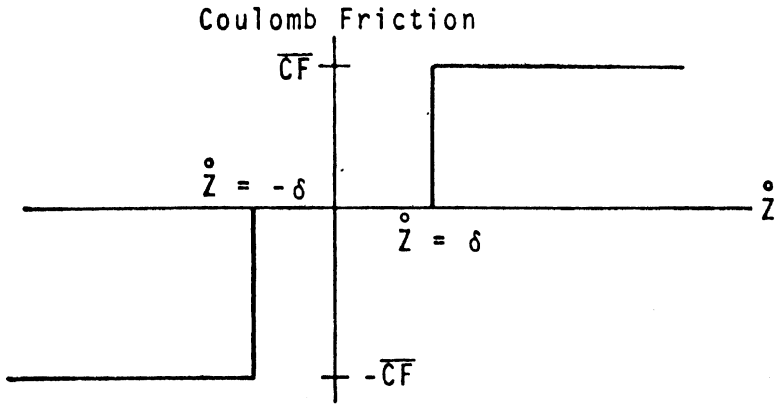

Figure B-2. Coulomb friction with dead zone.

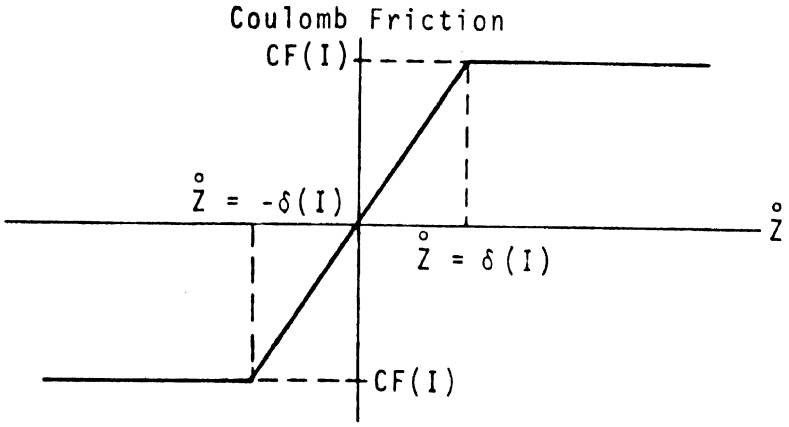

Figure B-3. Coulomb friction represented by limiting (saturation) functions.

δ should be large enough so that if the coulomb friction were the only force applied to the unsprung mass and the sprung mass, the velocity in the suspension could not change from δ to a negative value in one integration time step. This precludes the onset of chatter.

The free-body diagram of a system of sprung and unsprung masses, which can represent a truck or a tractor, is shown in Figure B-4. The relative velocity between the sprung mass and the unsprung mass may be written:

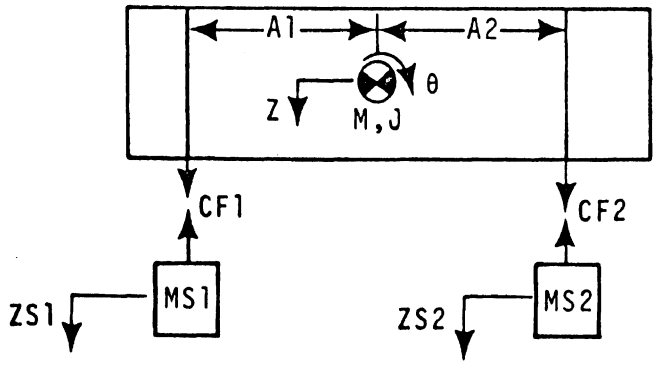

Figure B-4. System used in sample calculations of δ.

$$SD1 = \dot{ZS1} + A1\dot{\theta} - \dot{Z} \tag{B-4}$$

$$SD2 = \dot{ZS2} - A2\dot{\theta} - \dot{Z} \tag{B-5}$$

Thus:

$$|\ddot{Z}| \leq \frac{1}{M}(CF1+CF2) \tag{B-6}$$

$$|\ddot{\theta}| \leq \frac{1}{J}(CF1(A1)+CF2(A2)) \tag{B-7}$$

$$|\ddot{ZS1}| \leq \frac{CF1}{MS1} \tag{B-8}$$

$$|\ddot{ZS2}| < \frac{CF2}{MS2} \tag{B-9}$$

During a time interval, Δt, the change in suspension velocities are

$$|\Delta S1D| \leq \Delta t \left[CF1\left(\frac{1}{MS1}+\frac{1}{M}+\frac{A1^2}{J}\right)+CF1\left(\frac{1}{M}+\frac{(A2)A1}{J}\right)\right] \tag{B-10}$$

$$|\Delta S2D| \leq \Delta t \left[CF2\left(\frac{1}{MS2}+\frac{1}{M}+\frac{A2^2}{J}\right)+CF2\left(\frac{1}{M}+\frac{(A1)A2}{J}\right)\right] \tag{B-11}$$

The coulomb friction break points, $\pm\delta(I)$ in Figure B.3 for suspensions 1 and 2 are set at

$$DEL1 = |\Delta S1D| \tag{B-12}$$

$$DEL2 = |\Delta S2D| \tag{B-13}$$

In a similar manner, it can be shown that, for a trailer suspension

$$DEL3 \leq \Delta t \left[CF3 \left(\frac{1}{MT} + \frac{A4^2}{J} \right) \right] \qquad \text{(B-14)}$$

Since, in the program, the integration time step, Δt, is always .0025 second, calculations lead to typical values for the break points in the neighborhood of 3 inches/second. Thus, the simulated "frozen" suspension will allow small relative velocities (less than, say, 3 inches/second) rather than holding relative velocity to zero, and the possibility of numerical instability due to the coulomb friction is thereby eliminated.

Several of the suspension options include viscous damping due to the use of shock absorbers. The viscous friction coefficient is the slope of the force-velocity curve for the shock absorber. The user may select the slope in rebound and compression as is shown in Figure B-5.* If no damping is desired, the user may enter values of zero.**

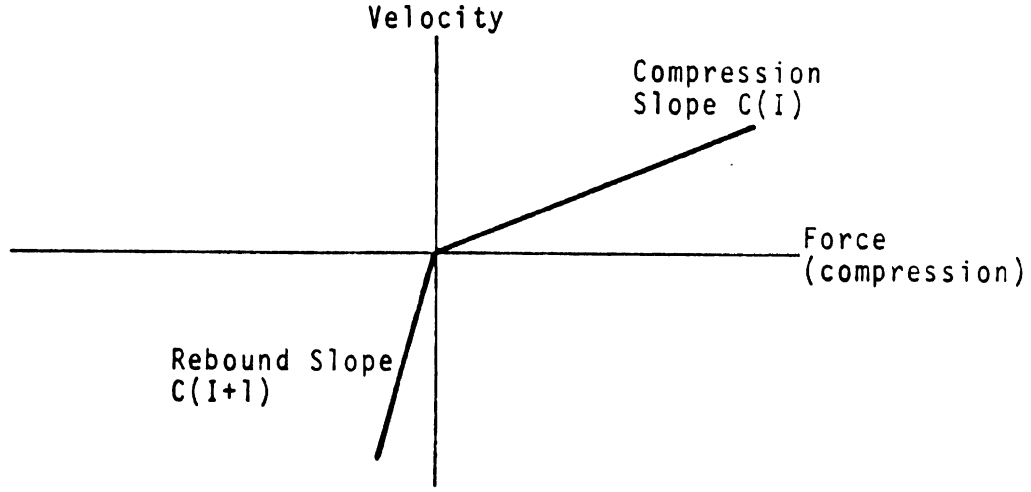

Figure B-5. Force-velocity characteristic of shock absorbers.

*To conform with popular shock absorber test practice, compression is shown positive.

**Further considerations in the use of viscous damping were referred to in Section 3.

The spring force at an axle may be denoted by a linear relationship

$$F(I) = K(I) * S(I) \qquad \text{(B-15)}$$

where

K(I) is the slope of the force-deflection curve in pounds/inch

S(I) is the suspension deflection from its static length in inches.

Alternatively, in the single axle and walking beam suspensions, a nonlinear force-deflection relationship may be used. An example is shown in Figure B-6, in which four points are used. The force in the spring will then be found through linear interpolation. (Use of spring tables was discussed in Section 2.0.)

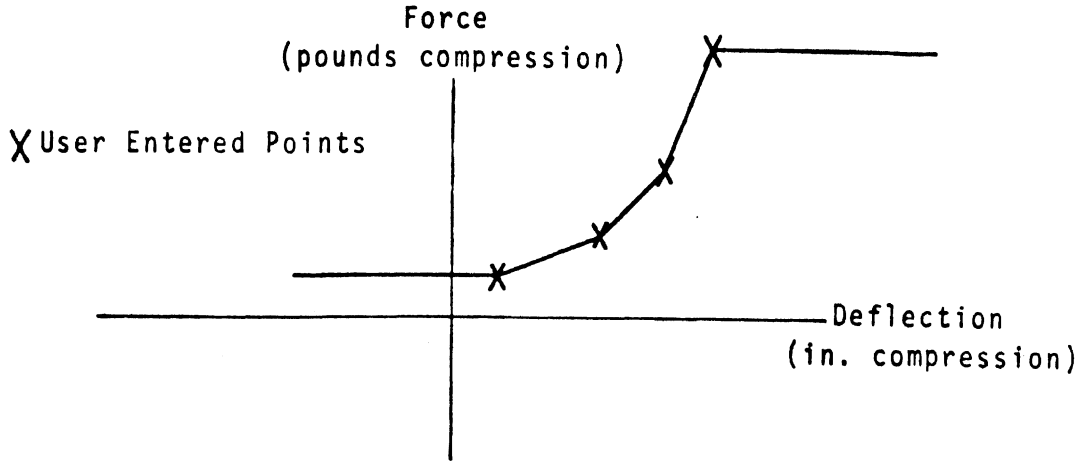

Figure B-6. Nonlinear spring force-deflection characteristics.

As a final preliminary point to the discussion of the individual suspension models, mention of the coordinate system to be employed is appropriate. The fore/aft motion of the unsprung masses is labeled "X" with the positive direction forward. It is assumed that the X motions of both the sprung and all unsprung masses are rigidly coupled. The vertical motions of the unsprung masses are labeled "ZS" (subscripted by "1" and "2" to denote leading and trailing axle, respectively, where appropriate), with the positive direction downward. To simplify the following presentations, it is assumed that the vehicle frame remains at a fixed vertical position, however, in the actual calculations of the Phase III programs, vertical motions of the frame are properly considered in calculating spring and frictional forces.

B.2 The Single-Axle Suspension

A schematic diagram of the single-axle model appears in Figure B-7. Table B-1 presents the nomenclature used in association with this model.

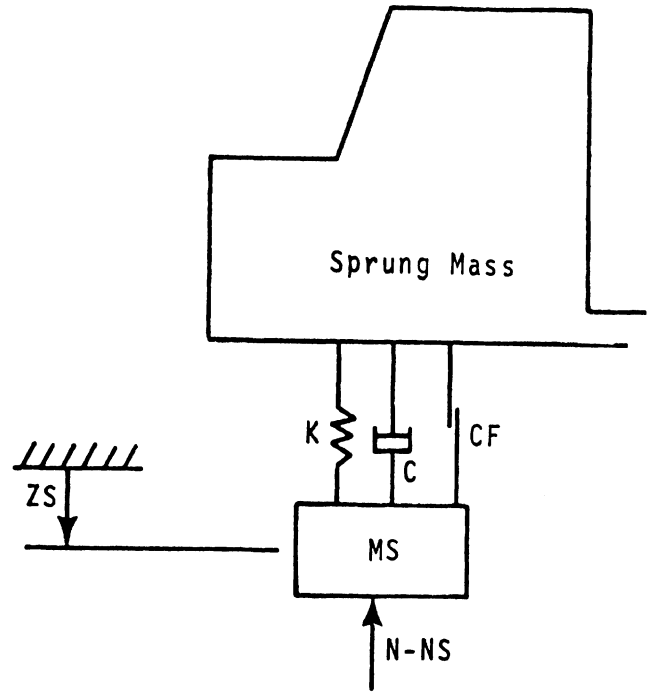

Figure B-7. Single-axle suspension model.

Table B-1. Single-Axle Model Nomenclature.

C1	Viscous damping coefficient in jounce
C2	Viscous damping coefficient in rebound
CF	Coulomb friction
K1	Vertical suspension spring rate
WS1	Weight of the unsprung mass

Figure B-8 shows a free-body diagram of the unsprung mass as applies to the static calculations. As the diagram shows, in the static condition there can be no moments about the suspension reference point (axle center) and therefore by definition

$$STORQ \equiv 0.0 \qquad \text{(B-16)}$$

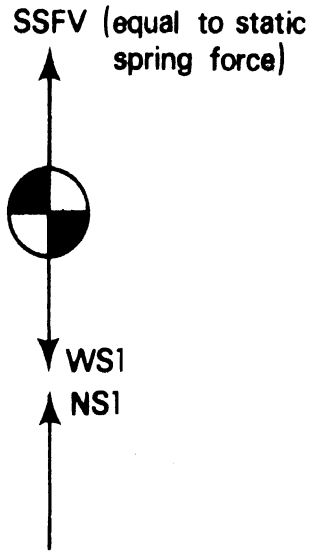

Figure B-8. Static free-body diagram: Single-axle suspension.

From Equations (B-1) and (B-16)

$$0 = SRATIO \cdot SSFV + SCONST \tag{B-17}$$

The solution to Equation (B-17) for all values of SSFV is

$$SRATIO = SCONST = 0 \tag{B-18}$$

Also, by summing vertical forces in the free-body of Figure B-8, the static normal load on the tire is

$$NS1 = WS1 - SSFV \tag{B-19}$$

where SSFV is calculated in the sprung mass portion of the program using SRATIO and SCONST.

The dynamic free-body diagram for this suspension appears in Figure B-9. From the free-body, and the definitions of the generalized dynamic suspension forces and moments:

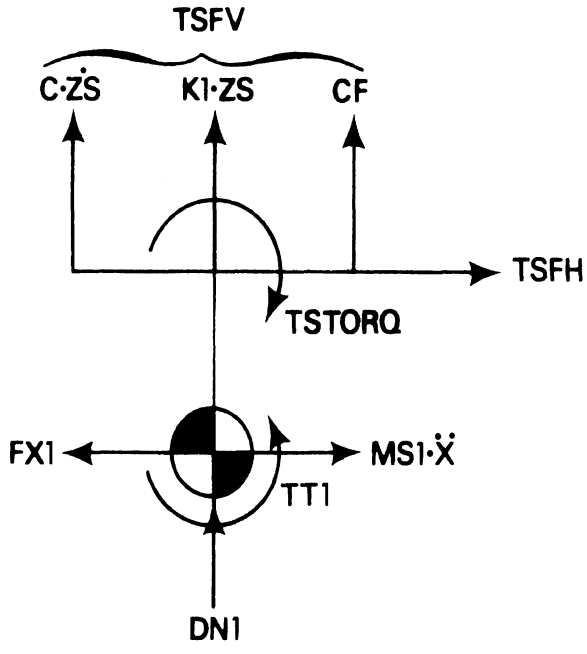

Figure B-9. Dyanmic free-body diagram: Single-axle suspension.

$$TSFV = K1 \cdot ZS + C \cdot \dot{ZS} + CF \quad * \tag{B-20}$$

$$TSFH = FX1 - MS1 \cdot \ddot{X} \tag{B-21}$$

$$TSTORQ = - TT1 \tag{B-22}$$

and the unsprung mass equation of motion is

$$MS1 \cdot \dot{ZS} + TSFV + DN1 = 0 \tag{B-23}$$

B.3 The Walking Beam Suspension

A diagram of the walking beam suspension is shown in Figure B-10. Nomenclature used in association with this suspension type appears in Table B-2. It should be noted that the torque rods are assumed to remain horizontal and the center of mass of the tandem is assumed to be on the line of the wheel centers.

Table B-2. Walking Beam Model Nomenclature.

AA1	Horizontal distance from walking beam pin to leading axle (in)
AA2	Horizontal distance from walking beam pin to trailing axle (in)
AA4	Vertical distance from axle to W.B. (in)
AA5	Vertical distance from axle to torque rod (in)
C1	Viscous damping: jounce on rear axle(s) (lb-sec/in)
C2	Viscous damping: rebound on rear axle(s) (lb-sec/in)
CF	Maximum coulomb friction, rear suspension (lb)
K	Spring rate, rear suspension (lb/in)
PERCNT	Percent effectiveness of torque rods
WS1	Weight of front tandem (lbs)
WS2	Weight of rear tandem (lbs)

*The parameters K1 and C may be functions of ZSPR and $\dot{ZSPR}$, respectively, as discussed in Section A.1, and CF is taken from the functional relationship analogous to that shown in Figure B.3.

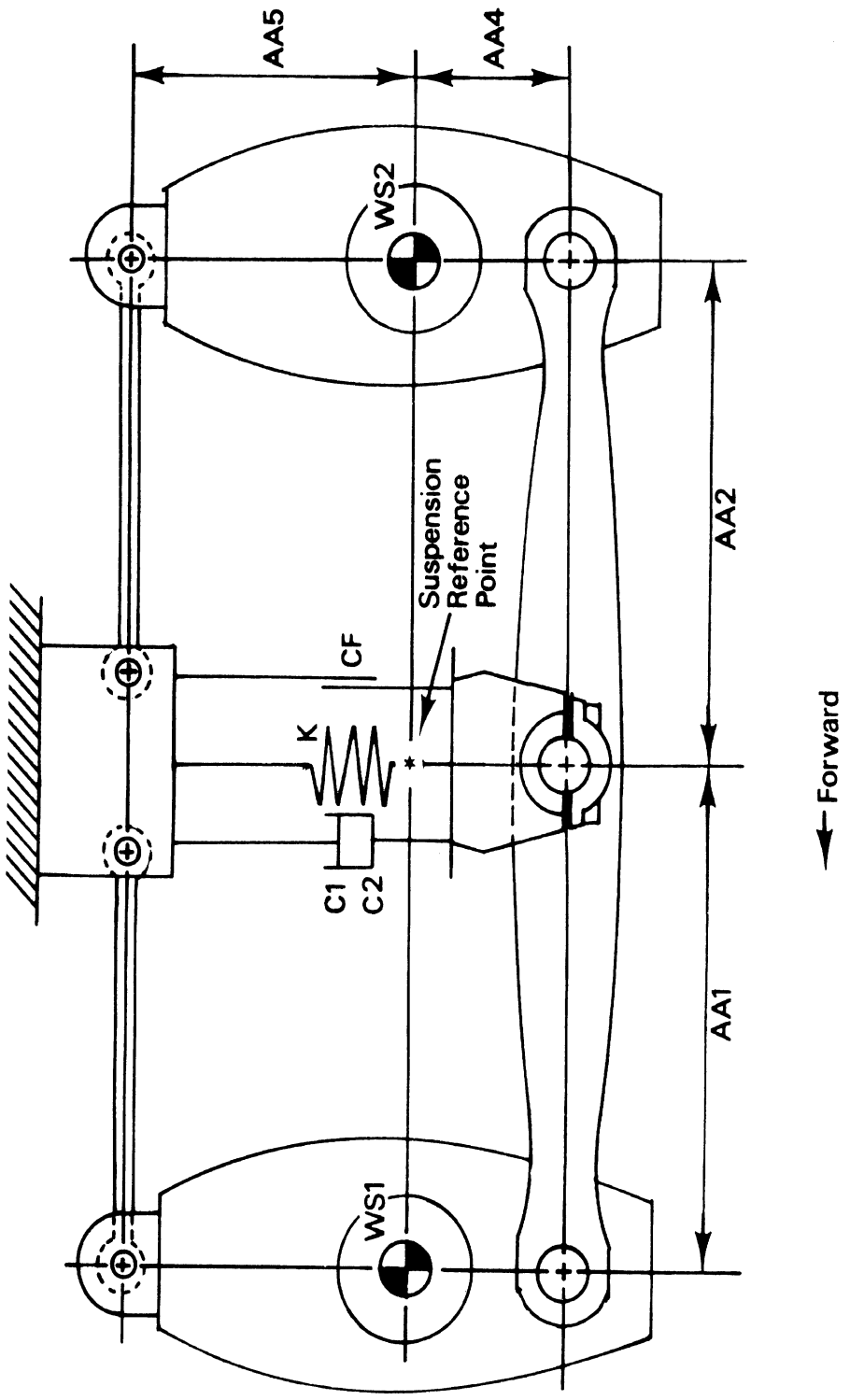

Figure B-10. The walking beam suspension model.

Addressing first the static considerations for this suspension, refer to the free-body diagram of Figure B-11. Since the suspension reference point is directly above the walking beam pin, zero moment (about the reference point) will be passed to the sprung mass in the static condition, i.e.,

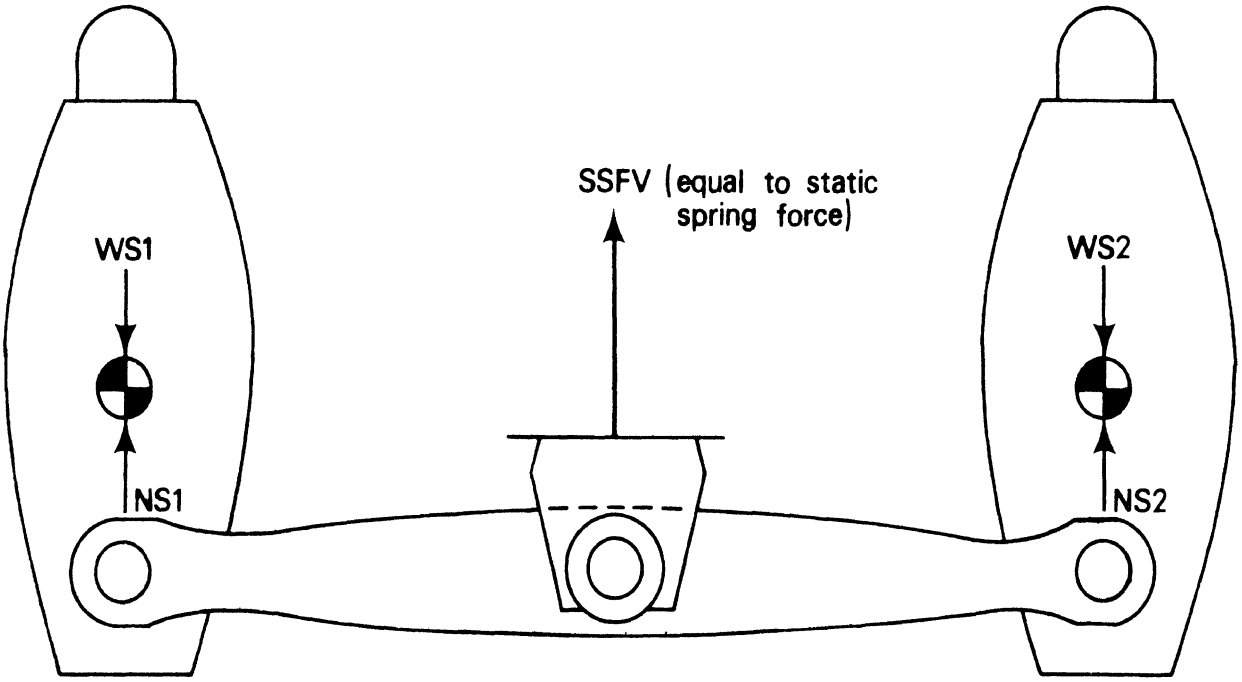

Figure B-11. Static free-body diagram: the walking beam suspension.

$$STORQ = 0 \tag{B-24}$$

Therefore, as for the single-axle suspension

$$SRATIO = SCONST = 0 \tag{B-25}$$

To obtain the static tire normal loads, sum forces in the vertical direction and moments about the walking beam pin to obtain, respectively,

$$NS1 + NS2 - WS1 - WS2 + SSFV = 0 \quad \text{(B-26)}$$

and

$$(NS1-WS1)AA1 - (NS2-WS2)AA2 = 0 \quad \text{(B-27)}$$

Solving for (B-26) and (B-27) for NS1 and NS2 yields

$$NS1 = WS1 - \frac{AA2}{AA1+AA2} \cdot SSFV \quad \text{(B-28)}$$

$$NS2 = WS1 + WS2 - SSFV - NS1 \quad \text{(B-29)}$$

where SSFV is known from calculations performed in the sprung mass portion of the program using SRATIO and SCONST.

A dynamic free-body diagram of the suspension appears in Figure B-12. Note that the suspension applies forces to the sprung mass only through the walking beam pin and the torque rods. Therefore, the generalized suspension forces and moment are defined by these forces. Since the torque rods are horizontal, vertical forces are passed to the sprung mass only at the torque rod pin. Therefore, TSFV is the sum of spring and frictional forces. That is

$$TSFV = K1 \cdot ZS + C \cdot \dot{Z}S + CF \quad \text{(B-30)}$$

where the parameters C and K may be functions of $\dot{Z}S$ and ZS, respectively, as discussed in Section A.1, and the dependence of CF on $\dot{Z}S$ is taken from a functional relationship analogous to that shown in Figure B-3.

Summing the horizontal forces acting on the sprung mass

$$TSFH = TR1 + TR2 - L \quad \text{(B-31)}$$

but applying Newton's second law in the horizontal direction yields:

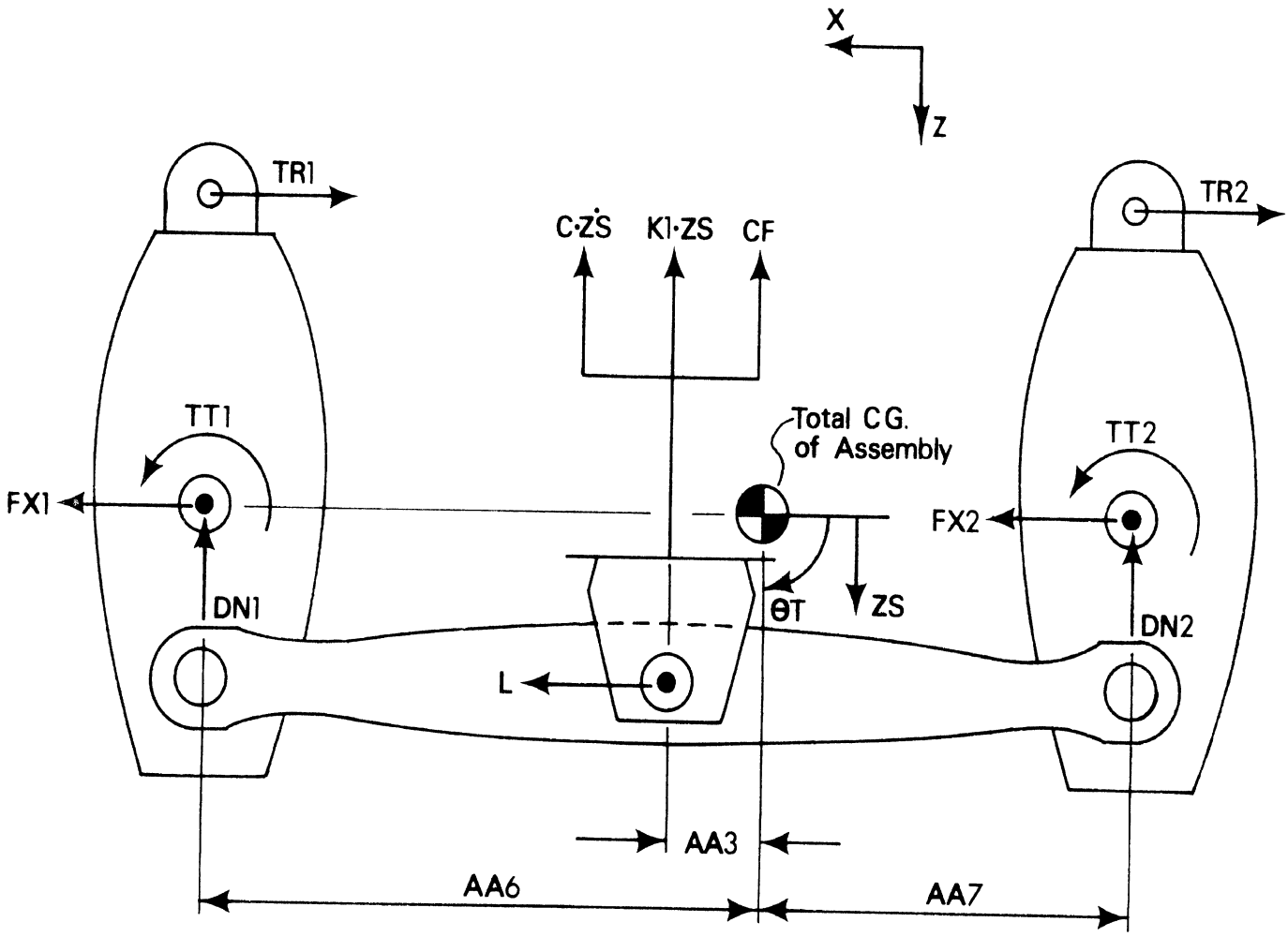

Figure B-12. Dynamic free-body diagram: the walking beam suspension.

$$TR1 + TR2 - L - (FX1-MS1\cdot\ddot{X})-(FX2-MS2\cdot\ddot{X}) = 0 \qquad (B-32)$$

From (B-31) and (B-32)

$$TSFH = FX1 - MS1 \cdot \ddot{X} + FX2 - MS2 \cdot \ddot{X} \qquad (B-33)$$

The walking beam suspension model has two degrees of freedom which we will interpret in this analysis as the vertical and pitch motion of the center of mass of the tandem assembly (ZS and θT as shown in Figure B-12). The following analysis will derive the two equations of motion for these degrees of freedom.

Applying Newton's second law in the ZS direction of Figure B-12:

$$-(DN1 + DN2 + TSFV) = \ddot{ZS} (MS1 + MS2) \qquad (B-34)$$

The moment of momentum of MS1 and MS2 about the center of mass of the tandem is

$$MS1(AA6)^2 + MS2(AA7)^2 \qquad (B-35)$$

where

$$AA6 = \frac{MS2}{MS1+MS2} (AA1+AA2) \qquad (B-36)$$

$$AA7 = (AA1+AA2) - AA6 \qquad (B-37)$$

Summing moments about the mass center and employing Equation (B-30)

$$DN1(AA6) - DN2(AA7) + (TR1+TR2)AA5 + TSFV(AA3)$$
$$+ L(AA4) - TT1 - TT2 = (MS1(AA6)^2 + MS2(AA7)^2)\ddot{\theta}T \qquad (B-38)$$

Referring now to Figure B-13, which shows the free-bodies of the individual parts of the suspension, we see that, by summing moments about the centers of the axle housings,

$$TT1 - TR1(AA5) - H1(AA4) - V1 \cdot \alpha 1 \cdot AA4 = 0 \qquad (B\text{-}39)^*$$

$$TT2 - TR2(AA5) - H2(AA4) - V2 \cdot \alpha 2 \cdot AA4 = 0 \qquad (B\text{-}40)^*$$

and by summing horizontal forces on the walking beam

$$L = H1 + H2 \qquad (B\text{-}41)$$

From (B-39) through (B-41), then,

$$L(AA4) = (H1+H2)AA4 = TT1+TT2 - (TR1+TR2)AA5 - (V1 \cdot \alpha 1 + V2 \cdot \alpha 2)AA4 \qquad (B\text{-}42)$$

Substituting (B-42) into (B-38)

$$DN1(AA6) - DN2(AA7) + TSFV(AA3) - (V1 \cdot \alpha 1 + V2 \cdot \alpha 2)AA4 = (MS1 \cdot AA6^2 + MS2 \cdot AA7^2)\ddot{\theta}T \qquad (B\text{-}43)$$

To obtain $\ddot{\theta}T$ from Equation (B-43), the terms $V1 \cdot \alpha 1$ and $V2 \cdot \alpha 2$ must be found (all other terms being known). These unknown terms are a function of many compliances in the suspension. Since V may be very large and α quite small, these terms are very difficult to model analytically. Rather, it is assumed that

*Small values of $\alpha 1$ and $\alpha 2$ have been assumed.

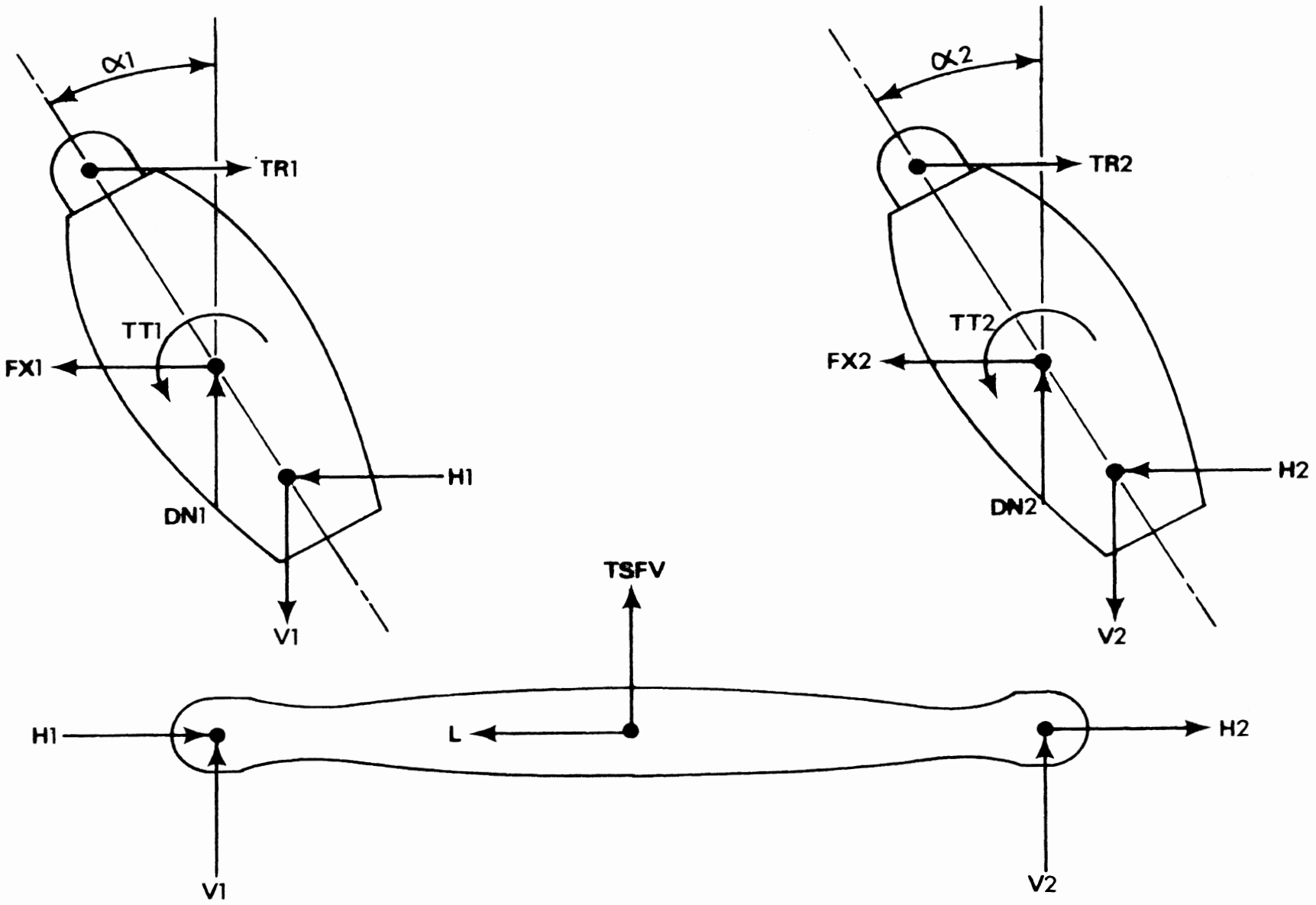

Figure B-13. Individual dynamic free-body diagram: the walking beam suspension.

$$V1 \cdot \alpha 1 \cdot AA4 = P(TR1)AA5 \quad \text{(B-44)}$$

$$V2 \cdot \alpha 2 \cdot AA4 = P(TR2)AA5 \quad \text{(B-45)}$$

i.e., the moment of V about the axle will be proportional to the moment of the torque rod force about the axle. With these assumptions, Equation (B-43) can be rewritten as

$$DN1(AA6) - DN2(AA7) + TSFV(AA3) - (TR1+TR2)P \cdot AA5$$

$$= (MS1(AA6)^2 + MS2(AA7)^2)\ddot{\theta}T \quad \text{(B-46)}$$

Equations (B-34) and (B-46) are then the equations of motion for the suspension, but we still need to determine the TR forces. By summing horizontal forces on the two axle housings, we obtain:

$$-TR1 + FX1 - MS1 \cdot \ddot{X} + H1 = 0 \quad \text{(B-47)}$$

$$-TR2 + FX2 - MS2 \cdot \ddot{X} + H2 = 0 \quad \text{(B-48)}$$

By combining Equations (B-39), (B-44), and (B-47) and combining (B-40), (B-45), and (B-48) we obtain, respectively,

$$TR1 = \frac{TT1 - AA4(MS1 \cdot \ddot{X} - FX1)}{AA4 + (1+P)AA5} \quad \text{(B-49)}$$

$$TR2 = \frac{TT2 - AA4(MS2 \cdot \ddot{X} - FX2)}{AA4 + (1+P)AA5} \quad \text{(B-50)}$$

Lastly, it remains to determine TSTORQ, the generalized moment which the suspension applies to the sprung mass (about the reference point). By definition

$$TSTORQ \equiv - (TR1+TR2)AA5 - L(AA4) \quad \text{(B-51)}$$

Substituting (B-42) into (B-51)

$$TSTORQ = -TT1 - TT2 + (V1 \cdot \alpha 1 + V2 \cdot \alpha 2)AA4 \qquad (B\text{-}52)$$

Substituting (B-44) and (B-45) into (B-52)

$$TSTORQ = -TT1 - TT2 + (TR1+TR2) \cdot P \cdot AA5 \qquad (B\text{-}53)$$

This completes the walking beam suspension model. By way of review, the static model consists of the values of SCONST, SRATIO, and STORQ and the expressions for the static normal tire loads as functions of SSFV. The dynamic model consists of the two equations of motion plus expressions for TSFV, TSFH, and TSTORQ.

B.4 The Basic Four Spring Suspension

In this section, the model of the basic four spring suspension will be developed. The section begins with a simplified discussion of the physical behavior of the suspension during braking. This discussion is intended to provide an intuitive basis for certain fundamental assumptions of the mathematical model.

Figure B-14 illustrates a four spring suspension in its static loaded condition. When brake torque is applied to the axles of this suspension, two mechanisms by which brake torque is resisted come into play. In Figure B-15 it is shown that a portion of the brake torque is resisted by moments arising from horizontal forces. The horizontal forces at points H and J in the figure are components of the torque rod reactions. The horizontal forces at points D, E, F, and G result primarily from spring/frame contact friction. Figure B-16 illustrates that the remaining portion of the brake torque is resisted by vertical force couples, primarily composed of the dynamic components of vertical spring/frame contact forces at points D, E, F, and G.

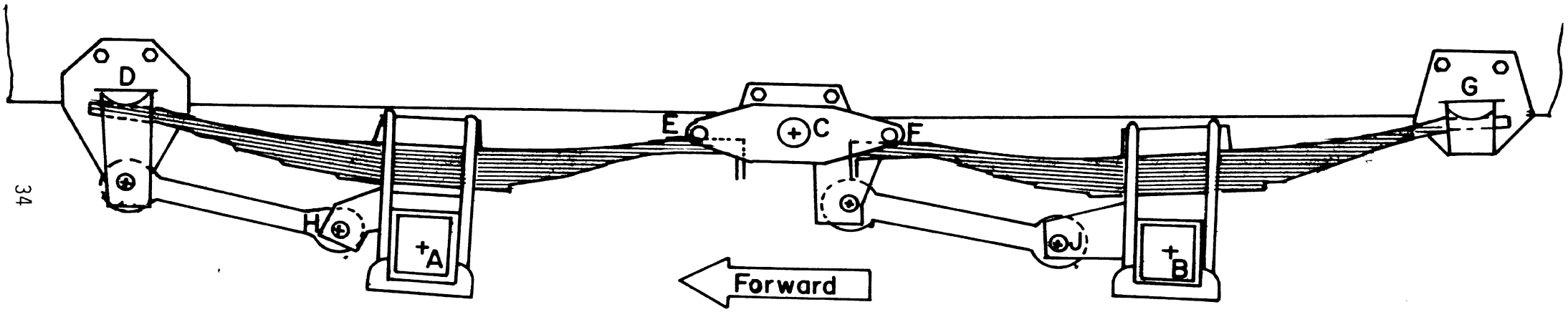

Figure B-14. The basic four spring suspension.

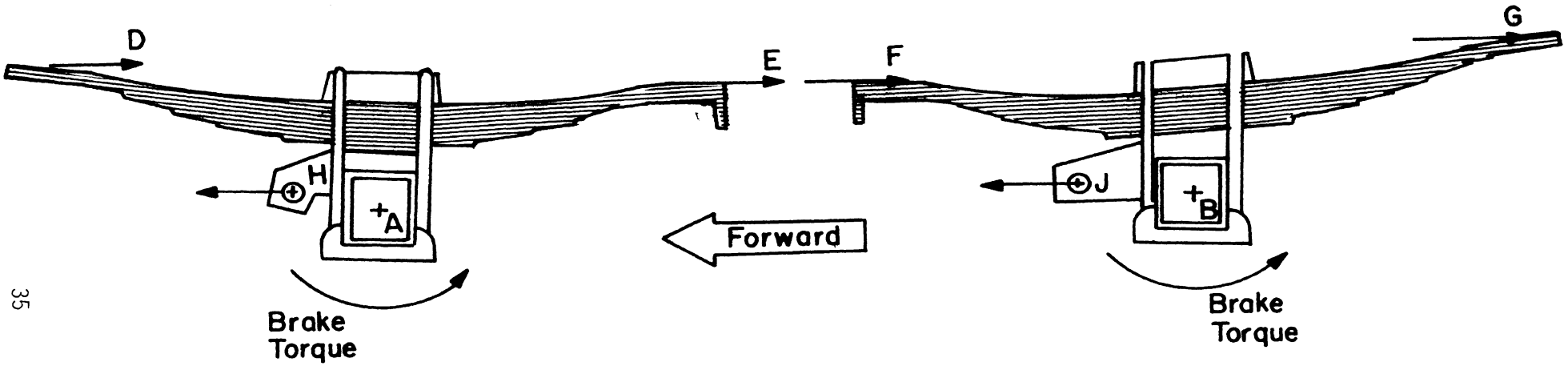

Figure B-15. Part of the brake torque is resisted by moments due to horizontal forces.

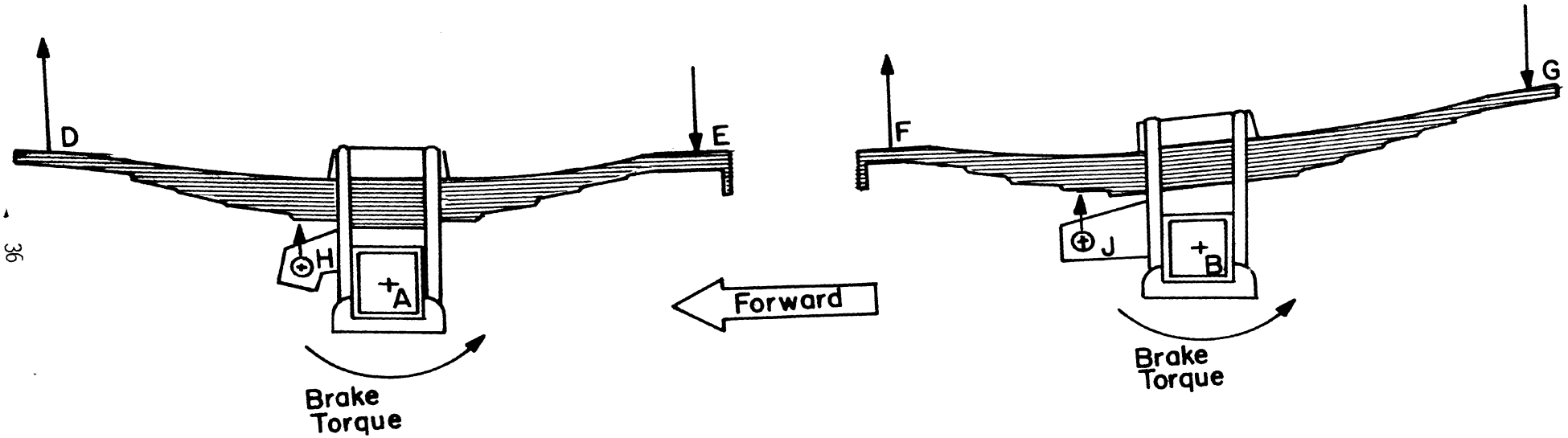

Figure B-16. Part of the brake torque is resisted by moments due to vertical forces.

The development of the vertical force couples is primarily responsible for the occurrence of interaxle load transfer. These forces act in opposite directions at either end of the same spring. Because the leaf spring is a compliant member in the vertical direction, these forces can only develop as a result of spring wrap-up as illustrated in Figure B-17.* In turn, Figure B-18 illustrates that spring wrap-up cannot occur until some small sliding action between the spring and frame has taken place at their contact points. (During this action, the springs slide forward with respect to the vehicle.) In order for this sliding to occur, friction must first be overcome. Therefore, we hypothesize that, as increasing brake torque is applied to the axles, the horizontal forces will develop until they are of sufficient magnitude to saturate spring/frame contact friction. Only after this has taken place may spring sliding and spring wrap-up occur, resulting in the development of the vertical force couples.

A mathematical model based on the following assumptions will now be developed.

1. Longitudinal acceleration of the unsprung masses relative to the sprung masses are neglected.

2. The slight shifts of spring, axle, and torque rod positions due to the rotation of the load leveler, horizontal movement of the spring/frame contact points, and spring flexture are neglected in calculating suspension forces.

3. The connection between the load leveler and the frame is considered to be a frictionless pin.

---

*Figures B-17 and B-18 indicate that as spring wrap-up occurs, the axle housings rotate around points H and J. This is because the nearly horizontal attitude of the torque rods results in the horizontal positions of H and J being virtually fixed while vertical motions of H and J are not germane to this part of the discussion.

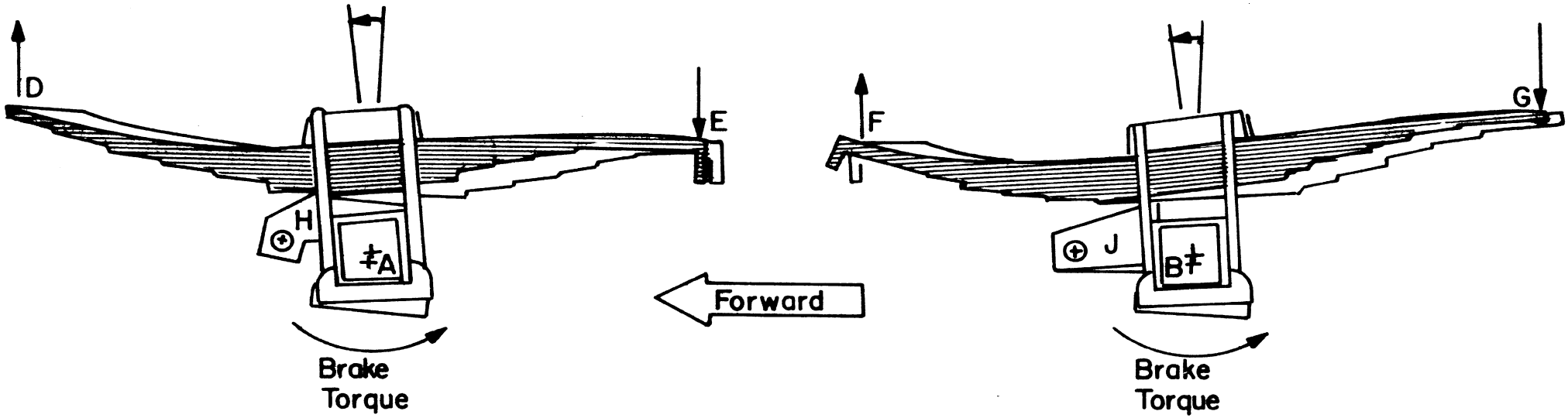

Figure B-17. Spring wrap-up must occur to produce vertical spring contact forces.

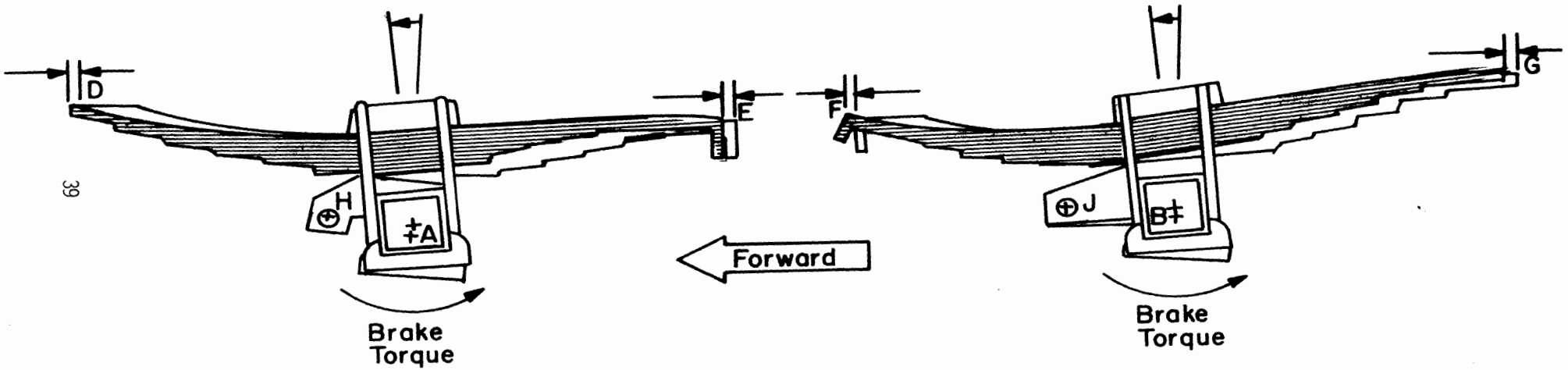

Figure B-18. Spring contact points must slide forward for wrap-up to occur.

4. The coefficient of friction is assumed to be identical and constant at all spring/frame contact points.

5. Spring/frame contact areas are assumed to be oriented such that frictional forces are horizontal and normal forces are vertical.

6. The summation of moments about an axle center due to the vertical forces at the spring/frame contact points (of the spring associated with the axle) can change only at points in time during which the frictional forces at those same spring/frame contact points are saturated.

7. Only vertical forces are significant in the load leveler equations. (Justification for this assumption is given at the end of this section.)

8. Coulomb friction contained in the vertical deflection properties of the leaf springs are applied between frame and axle housing.*

Note that it is assumption 6 that follows from the preceding discussion.

Addressing first the static consideration regarding this suspension, reference the schematic and static free-body diagrams of Figures B-19 and B-20, respectively.

From Figure B-20, summing moments on the two axle assemblies and the load leveler individually yields

$$TN1S(AA2A) = TN2S(AA1\text{-}AA2A) \tag{B-54}$$

$$TN3S(AA1 - AA2B) = TN4S(AA2B) \tag{B-55}$$

*The method for calculating these coulomb friction forces was reported earlier in this appendix.

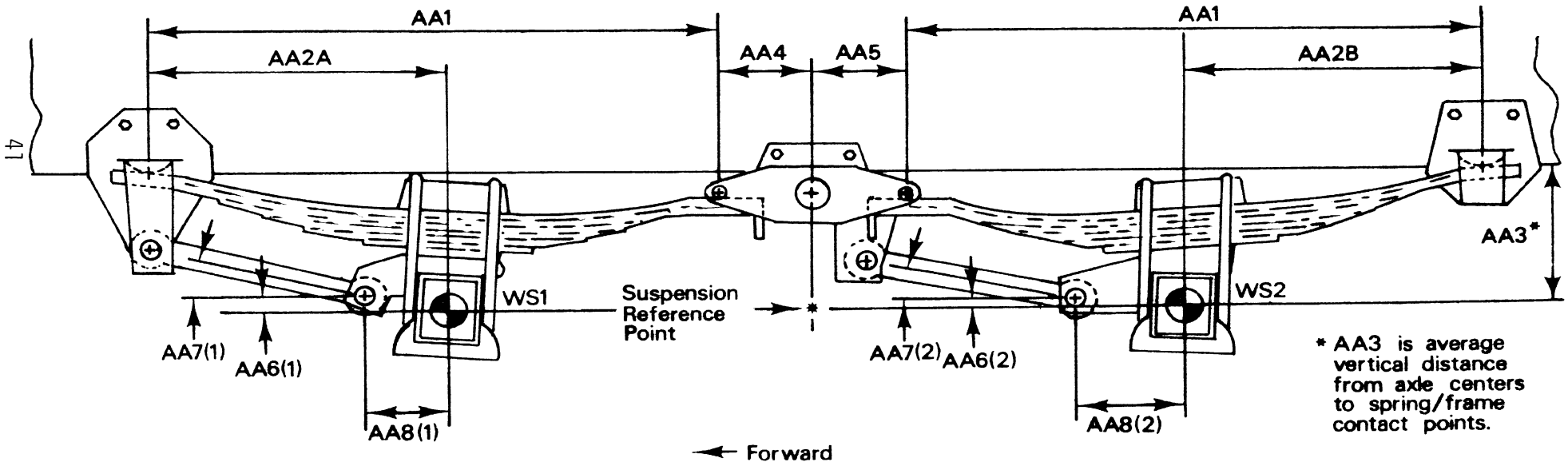

Figure B-19. The basic four spring suspension model.

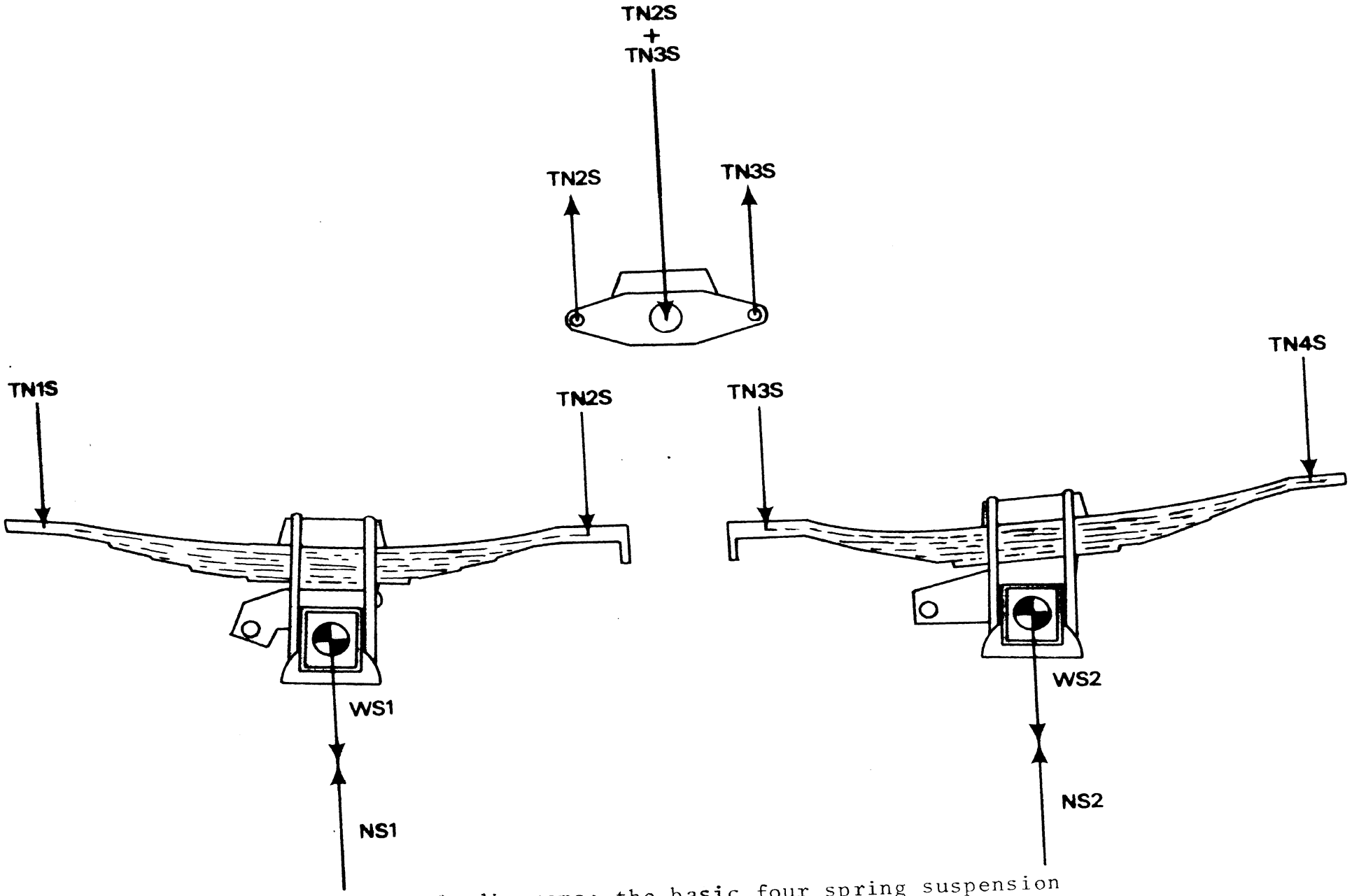

Figure B-20. Static free-body diagrams: the basic four spring suspension

$$TN2S(AA4) = TN3S(AA5) \tag{B-56}$$

By the definitions of SSFV and STORQ

$$SSFV = -TN1S - TN2S - TN3S - TN4S \tag{B-57}$$

$$STORQ = TN1S(AA1+AA4) - TN4S(AA1+AA5) \tag{B-58}$$

Substituting (B-54), (B-55), and (B-56) into (B-57) and (B-58) yields

$$SSFV = -\left[\frac{AA1-AA2A}{AA2A} + 1 + \frac{AA4}{AA5}\left(1 + \frac{AA1-AA2B}{AA2B}\right)\right] TN2S \tag{B-59}$$

$$STORQ = \left[\frac{AA1-AA2A}{AA2A}(AA1+AA4) - \frac{AA1-AA2B}{AA2B} \cdot \frac{AA4}{AA5}(AA1+AA5)\right]TN2S \tag{B-60}$$

Now by the definition of SRATIO and SCONST

$$STORQ = SSFV \cdot SRATIO + SCONST \tag{B-61}$$

Substituting (B-58) and (B-59) into (B-60)

$$\left[\frac{AA1-AA2A}{AA2A}(AA1+AA4) - \frac{AA1-AA2B}{AA2B} \cdot \frac{AA4}{AA5}(AA1+AA5)\right]TN2S =$$

$$-\left[\frac{AA1-AA2A}{AA2A} + 1 + \frac{AA4}{AA5}\ 1 + \frac{AA1-AA2B}{AA2B}\right] TN2S \cdot SRATIO + SCONST \tag{B-62}$$

The general solution for (B-62) for all values of TN2S is

$$SCONST = 0 \tag{B-63}$$

$$SRATIO = -\frac{\frac{AA1-AA2A}{AA2A}(AA1+AA4) - \frac{AA1-AA2B}{AA2B} \cdot \frac{AA4}{AA5}(AA1+AA5)}{\frac{AA1-AA2A}{AA2A} + 1 + \frac{AA4}{AA5}\left(1 + \frac{AA1-AA2B}{AA2B}\right)} \tag{B-64}$$

Simplifying (B-64) yields

$$SRATIO = \frac{(-AA1 - AA2A + AA4) + (AA1-AA2B+AA5)\frac{AA4}{AA5}\frac{AA2A}{AA2B}}{1 + \frac{AA4}{AA5}\frac{AA2A}{AA2B}} \quad (B-65)$$

To complete the static calculations we must determine the static normal tire loads as a function of SSFV.

Summing vertical forces and moments on the entire suspension yields

$$SSFV + NS1 + NS2 - WS1 - WS2 = 0 \quad (B-66)$$

$$(NS1-WS1)(AA1-AA2A+AA4) - (NS2-WS2)(AA1-AA2B+AA5) - STORQ = 0 \quad (B-67)$$

Solving these two equations simultaneously for NS1 and NS2 yields:

$$NS1 = WS1 + \frac{STORQ - SSFV(AA1-AA2B+AA5)}{(AA1-AA2A+AA4) + (AA1-AA2B+AA5)} \quad (B-68)$$

$$NS2 = WS1 + WS2 - NS1 - SSFV \quad (B-69)$$

Turning now to the dynamic suspension model, consider the free-body diagram of Figure B-21. Note that all the forces shown in these diagrams are dynamic components only. In the case of the vertical spring forces, these dynamic components are expressed as the total force minus the static component, i.e.,

$$(TNi - TNiS)$$

where i = 1,2,3,4. This method is used to facilitate calculations involving the relationships of leaf/frame frictional forces and normal forces, i.e., relationships of the form

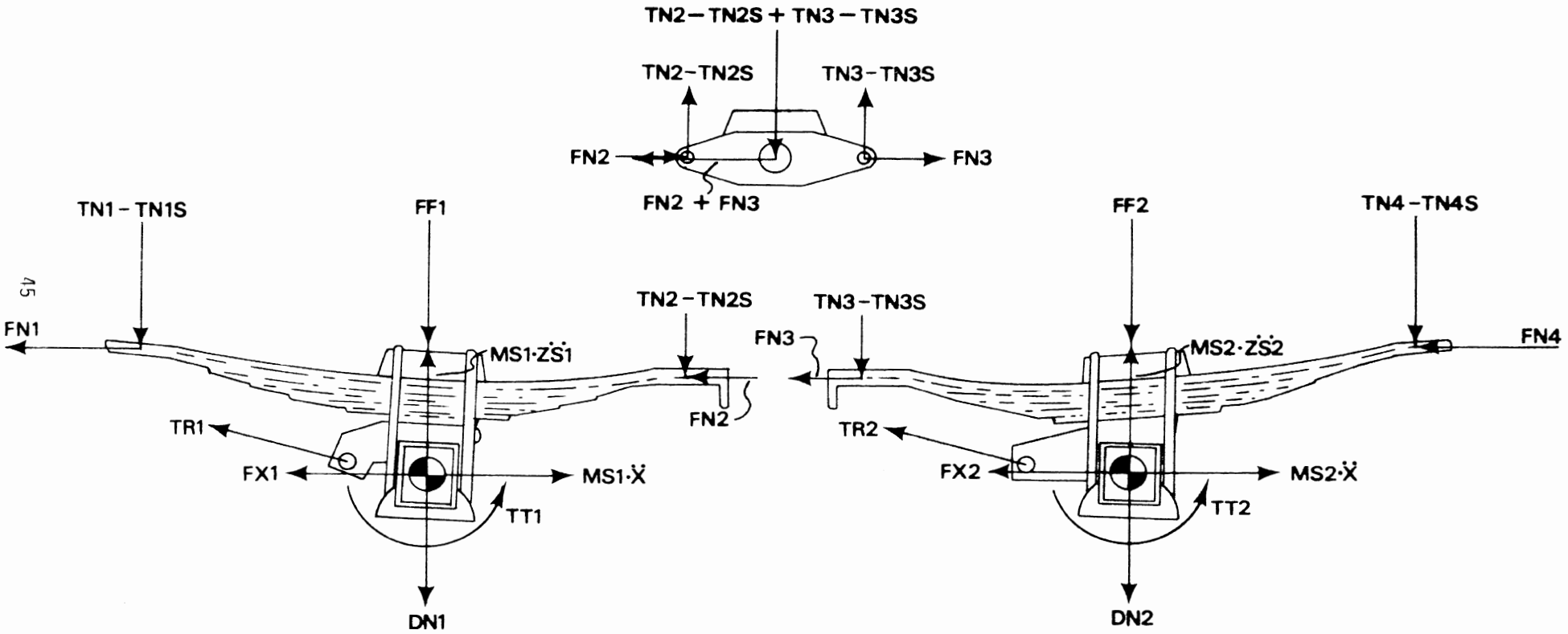

Figure B-21. Dynamic free-body diagrams: the basic four spring suspension.

$$FNi \leq MUS \cdot TNi$$

where MUS is the coefficient of friction and i = 1,2,3,4.

Applying Newton's second law in the "X" direction to each of the axles in Figure B-21 yields

$$TR1(\cos AA7(1)) + FX1 - MS1(\ddot{x}) + (FN1+FN2) = 0 \qquad (B\text{-}70)$$

$$TR2(\cos AA7(2)) + FX2 - MS2(\ddot{x}) + (FN3+FN4) = 0 \qquad (B\text{-}71)$$

where $\ddot{x}$ is longitudinal acceleration, MS1 is the unsprung mass of the leading axle, and MS2 is the unsprung mass of the trailing axle.

Summing moments about the axle centers yields

$$TT1 - TR1(ARM1) + TN1(AA2A) - TN2(AA2A) + (FN1+FN2)AA3 = 0 \qquad (B\text{-}72)$$

$$TT2 - TR2(ARM2) + TN3(AA1-AA2B) - TN4(AA2B) + (FN3+FN4)AA3 = 0 \qquad (B\text{-}73)$$

where all the TNiS terms have been removed by substitution of Equations (B-54) and (B-55), and where ARM1 and ARM2 are the distances from the torque rod to the axle center, in a direction perpendicular to the torque rod, for the leading and trailing axle, respectively.

Now, with KK designated as the sum of the spring rates of all four leaf springs, the following expression is assumed:

$$TN1 + TN2 + TN3 + TN4 = -KK(\delta) + TN1S+TN2S+TN3S+TN4S = SUMTN \qquad (B\text{-}74)$$

where δ is the average vertical displacement of the axle centers relative to the sprung mass.*

Summing moments on the load leveler and envoking assumption (7) yields

$$TN2(AA4) - TN3(AA5) = 0 \qquad \text{(B-75)}$$

where the TNiS terms have been removed by the substitution of Equation (B-56).

At this point, Equations (B-70) through (B-75) represent six equations in eight unknowns, these unknowns being TN1, TN2, TN3, TN4, TR1, TR2, and the quantities (FN1+FN2) and (FN3+FN4). (Note that $\sum_{I=1}^{4} TN(1)$, FX1, FX2, TT1, TT2, and $\ddot{x}$ are known quantities provided by previous calculations made in the program.)

Assumption (6) can now be used with respect to each of the two axle assemblies to obtain the two additional equations required. For example, for the leading axle it is initially assumed that the forces FN1 and FN2 will not saturate the friction capability of the spring/frame contact points. It then follows from assumption (6) that

$$TN1(AA2A) - TN2(AA1\text{-}AA2A) = TN1_0(AA2A) - TN2_0(AA1\text{-}AA2A) \qquad \text{(B-76)}$$

where the subscript (o) indicates "from the preceding time step." And likewise, for the trailing axle,

$$TN3(AA1\text{-}AA2B) - TN4(AA2B) = TN3_0(AA1\text{-}AA2B) - TN4_0(AA2B) \qquad \text{(B-77)}$$

Equations (B-70) through (B-77) may now be solved for the eight unknowns listed above. If, upon completing these calculations,

---

*The use of this form of equation has been discussed in the Phase I report [1].

it is determined that

$$|(FN1+FN2)| \leq MUS(|TN1| + |TN2|) \qquad \text{(B-78a)}$$

and

$$|(FN3+FN4)| \leq MUS(|TN3| + |TN4|) \qquad \text{(B-78b)}$$

where MUS is the coefficient of friction of spring/frame contact, then friction is, indeed, not saturated and the solution is acceptable as calculated. If either criteria indicated by Equation (B-78) fail, then recalculation of the solution is called for. In this case, if, for example, Equation (B-78a) is not met, then friction is saturated at the leading axle. Equation (B-76) must then be replaced by

$$(FN1+FN2) = \pm MUS(|TN1| + |TN2|) \qquad \text{(B-79)}$$

where the appropriate sign is indicated by the sign of (FN1+FN2) as found by the preliminary calculations just described (i.e., using Equations (B-70) through (B-77)).

Similarly, if Equation (B-78b) is not satisfied, Equation (B-77) is replaced by

$$(FN3+FN4) = \pm MUS(|TN3| + |TN4|) \qquad \text{(B-80)}$$

Thus, Equations (B-70) through (B-75) plus the appropriate two equations from (B-76), (B-77), (B-79), and (B-80), as determined by the criteria of Equation (B-78), will always provide eight equations which may be solved for the eight unknowns.

With all the suspension forces calculated, the appropriate accelerations of the sprung and unsprung masses may now be calculated.

Summing forces in the vertical direction on each of the unsprung masses yields the equations of vertical wheel motions, viz.:

$$-FF1 - TR1 \sin(AA7(1)) + (TN1-TN1S) + (TN2-TN2S) - DN1 = MS1(\ddot{Z}S1) \quad (B\text{-}81)$$

$$-FF2 - TR2 \sin(AA7(2)) + (TN3-TN3S) + (TN4-TN4S) - DN2 = MS2(\ddot{Z}S2) \quad (B\text{-}82)$$

where the "FF" terms are the sum of the coulomb and viscous friction forces, calculated as described in Section B.1, and the "DN" forces are the dynamic normal tire loads.

To complete the model we must determine the generalized suspension forces and moments.

By definition

$$TSFV = -[(TN1+TN1S) + (TN2-TN2S) + (TN3-TN3S) + (TN4-TN4S)] + FF1+FF2 + TR1 \sin(AA7(1)) + TR2 \sin(AA7(2)) \quad (B\text{-}83)$$

and

$$TSFH = -[FN1+FN2+FN3+FN4] - TR1 \cos(AA7(1)) - TR2 \cos(AA7(2)) \quad (B\text{-}84)$$

But from Equations (B-70) and (B-71), we see that the right-hand side of Equation (B-84) is equal to:

$$FX1 - MS1 \cdot \ddot{x} + FX2 - MS2 \cdot \ddot{x}$$

Therefore

$$TSFH = FX1 + FX2 - (MS1 + MS2)\ddot{x} \quad (B\text{-}85)$$

We can now determine TSTORQ. By definition

$$TSTORQ = (TN1-TN2S)(AA1+AA4) + (TN2-TN2S)(AA4) - (TN3-TN3S)(AA5)$$
$$- (TN4-TN4S)(AA1+AA5) + (FN1+FN2+FN3+FN4)AA3$$
$$- TR1[ARM1 + \sin(AA7(1))\ (AA1-AA2A+AA4)] \qquad (B\text{-}86)$$
$$- TR2[ARM2 - \sin(AA7(2))\ (AA1-AA2B+AA5)]$$
$$- CF1(AA1-AA2A+AA4) + CF2(AA1-AA2B+AA5)$$

By substituting Equations (B-72) and (B-73) and the equations

$$AA2A - AA2A = 0 \qquad (B\text{-}87)$$

$$AA2B - AA2B = 0 \qquad (B\text{-}88)$$

into Equation (B-86), we can show that

$$TSTORQ = (AA1-AA2A+AA4)[(TN1-TN1S) + (TN2-TN2S) - FF1$$
$$- TR1 \sin(AA7(1))] - (AA1-AA2B+AA5)$$
$$[(TN3-TN3S) + (TN4-TN4S) - FF2 - TR2 \sin(AA7(2))]$$
$$- TT1 - TT2 \qquad (B\text{-}89)$$

As a final point in this section, the mathematical justification to assumption (7), referred to early in this section, will be presented.

Consider the summation of moments equation for the load leveler (see Fig. B-22):

$$TN2(AA4)\cos\varepsilon - TN3(AA5)\cos\varepsilon + FN2(AA4)\sin\varepsilon$$
$$- FN3(AA5)\sin\varepsilon = 0 \qquad (B\text{-}90)$$

Qualitatively, there are three conditions under which this equation will generally operate:

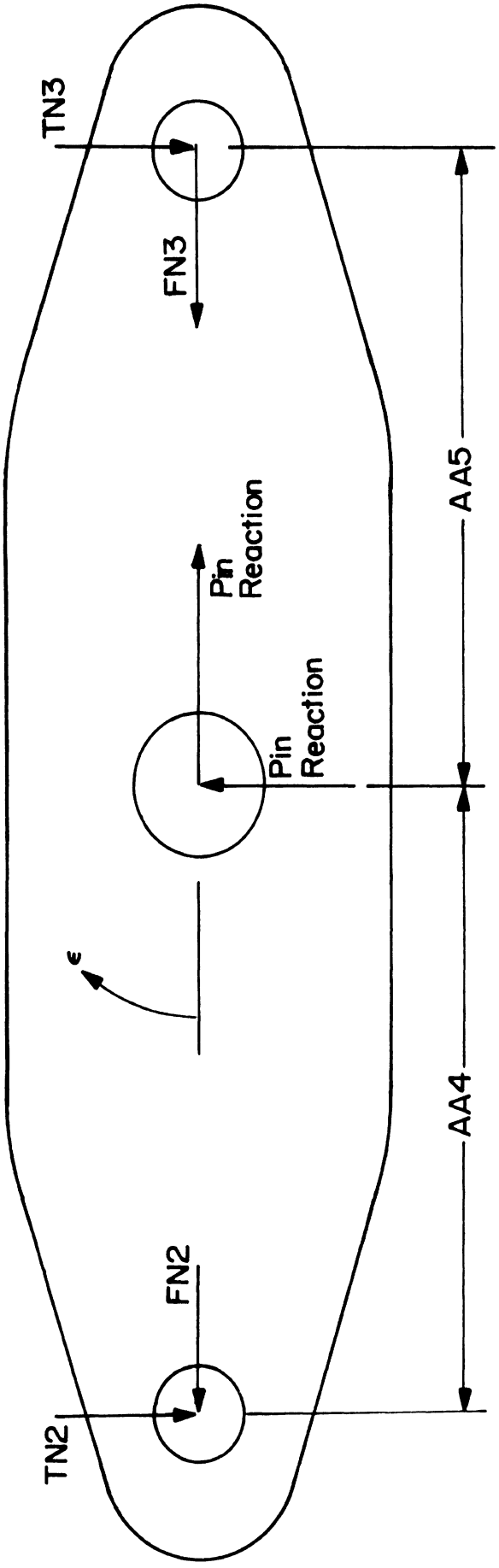

Figure B-22. Free-body diagram: the load leveler

1. Low level brake torque applications during which forces FN2 and FN3 do not saturate the friction capability of the spring/frame contacts.
2. Severe brake application in which FN2 and FN3 saturate friction.
3. Moderate conditions under which either, but not both, FN2 and FN3 may saturate friction.

During condition 1, the preceding discussion would indicate that, because spring/frame contact friction has not saturated, very little load transfer has occurred. Consequently, it would be true that the angle ε is small and that Equation (B-90) would be well approximated by

$$TN2(AA4) - TN3(AA5) = 0 \tag{B-91}$$

During condition 2 friction is saturated. Designating MUS as the coefficient of friction at the contact points

$$FN2 = \pm (MUS)\,|TN2| \tag{B-92a}$$

$$FN3 = \pm (MUS)\,|TN3| \tag{B-92b}$$

where, generally, the signs of the right-hand side of Equations (B-92a) and (B-92b) will be the same. With this limitation, substituting Equations (B-92a) and (B-92b) into (B-90) yields

$$[TN2(AA4)-TN3(AA5)][\cos \varepsilon \pm MUS(\sin \varepsilon)] = 0 \tag{B-93}$$

with solutions

$$TN2(AA4) - TN3(AA5) = 0 \tag{B-94}$$

or

$$\cos \varepsilon \pm MUS(\sin \varepsilon) = 0 \tag{B-95}$$

For a positive sign in Equation (B-95), the solution for ε lies in the second or fourth quadrants; this is not in agreement with observed behavior. If the sign were negative, a solution exists in the first quadrant but, since MUS < 1, then ε > 45 deg. for all cases, which again does not agree with observed behavior. A solution also would exist in the third quadrant. This also is not compatible with observed behavior. Thus, the proper solution is represented by Equation (B-94) (which is identical to Equation (B-91).

Under the third condition, that of moderate braking, where friction is saturated at one, but not both, contact points, it may be reasonably assumed that the angle ε would be relatively small. In addition, the quantity FN2(AA4) - FN3(AA5) would be small. Consequently,

$$[FN2(AA4)-FN3(AA5)]\sin\varepsilon = FN2(AA4)\sin\varepsilon - FN3(AA5)\sin\varepsilon \approx 0 \qquad \text{(B-96)}$$

Therefore, Equation (B-91) can be assumed. Consequently, Equation (B-91) is assumed for all cases.

B.5 The Four Spring Suspension with Spring-Type Torque Rods

The mathematical model of the four spring suspension with spring-type torque rods is virtually identical to that of the basic four spring suspension with the addition of the torque rod "spring force." For this reason, the model will not be reviewed in detail here; only changes with respect to the basic four spring model will be noted. To do this, we will develop, from the free-body diagram of Figure B-23, certain new equations for the subject suspension and note the equations (of the basic four spring suspension model) which they replace. Development of the new model would then proceed analogously to the old. The changes to be described apply only to the dynamic suspension model. The static model is unchanged from

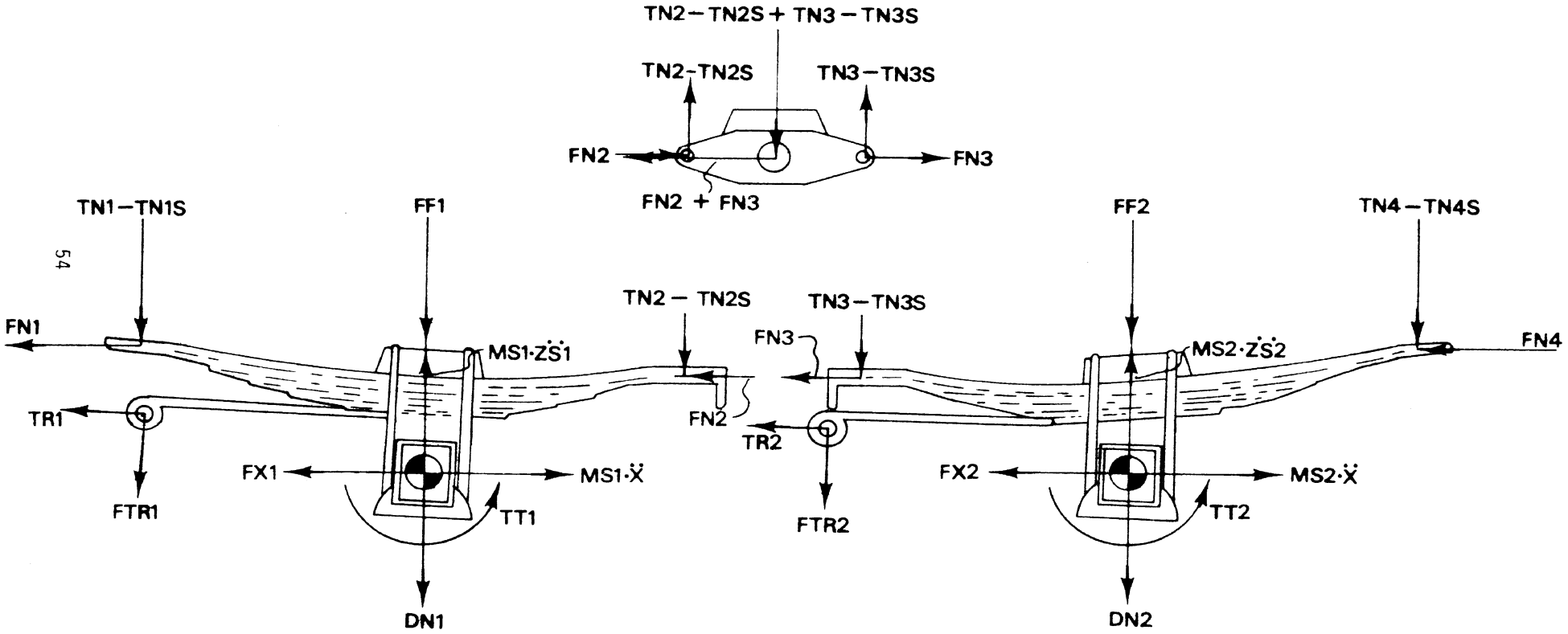

Figure B-23. Dynamic free-body diagram: the four spring suspension with spring-type torque rods.

that of the basic four spring suspension (i.e., the static torque rod spring forces are assumed to be small).

Applying Newton's second law in the "X" direction to each of the axles in Figure B-23 yields

$$TR1(\cos AA7(1)) - FTR1(\sin AA7(1)) + FX1 - MS1(\ddot{x}) + (FN1+FN2) = 0 \quad \text{(B-97)}$$

$$TR2(\cos AA7(2)) - FTR2(\sin AA7(2)) + FX2 - MS2(\ddot{x}) + (FN3+FN4) = 0 \quad \text{(B-98)}$$

(replacing Equations (B-70) and (B-71) where the new "FTR" forces are the "spring forces" of the torque rods.

Summing moments about the axle center yields:

$$TT1-TR1(ARM1) - FTR1\{\cos AA7(1) \cdot AA9(1) - \sin AA7(1) [AA6(2) - (AA9(2))\tan AA7(2)]\} + TN3(AA1-AA2B) - TN4(AA1) + (FN3+FN4)AA3 = 0 \quad \text{(B-99)}$$

$$TT2-TR2(ARM2) - FTR2\{\cos AA7(2) \cdot AA9(2) - \sin AA7(2) [AA6(2) - (AA9(2))\tan AA7(2)]\} + TN3(AA1-AA2B) - TN4(AA1) + (FN3+FN4)AA3 = 0 \quad \text{(B-100)}$$

(Equations (B-99) and (B-100) replace Equations (B-72) and (B-73).

With the substitution of these four equations, the analysis proceeds basically as it did for the basic four spring suspension up to Equation (B-81). However, we note that there are now two additional unknowns. FTR1 and FTR2, in the equation set which is solved to determine suspension forces. Thus, in effect we have

eight equations in ten unknowns. To resolve this dilemma, the FTR forces are calculated at the end of each integration time step, to be used as known values in the calculations for the next time step. (Prior to the first time step, these forces are assumed to be zero.) As an example of this calculation, consider Figure B-24 depicting the leading axle assembly. Note that the leaf spring is assumed to be symmetric such that one-half of the total spring rate may be attributed to each half of the spring. Using the notation of the figure, and assuming that $\theta 1$ is small (i.e., $\cos \theta 1 \approx 1$), we may write equations for TN1 and FTR1 as:

$$TN1 = - K1/2 \cdot ZS1 + K1/2 \cdot AA2A \sin \theta 1 \qquad \text{(B-101)}$$

$$FTR1 = (KTR1 \cdot ZS1 - KTR1 \cdot AA9(1) \cdot \sin \theta 1/\cos AA7(1) \qquad \text{(B-102)}$$

Solving for FTR1 yields

$$FTR1 = \frac{KTR1}{\cos AA7(1)} \left(1 - \frac{AA9(1)}{AA2A}\right) ZS1 - 2 \frac{KTR1}{K1} \cdot \frac{AA9(1)}{AA2A} \cdot \frac{TN1}{\cos AA7(1)} \qquad \text{(B-103)}$$

In completing the dynamic model, the additional torque rod spring forces alter Equations (B-81), (B-82), (B-83), and (B-89) (of the basic model), respectively, as follows:

$$-FF1-TR1 \sin AA7(1) + (TN1-TN1S) + (TN2-TN2S) - DN1 - FTR1 \cos AA7(1) = MS1(\ddot{ZS}1) \qquad \text{(B-104)}$$

$$-FF2-TR2 \sin AA7(2) + (TN3-TN3S) + (TN4-TN4S) - DN2 - FTR2 \cos AA7(2) = MS2(\ddot{ZS}2) \qquad \text{(B-105)}$$

$$TSFV = [(TN1-TN1S) + (TN2-TN2S) + (TN3-TN3S) + (TN4-TN4S)] + FF1+FF2 + TR1 \cdot \sin AA7(1) + TR2 \cdot \sin AA7(2) + FTR1 \cdot \cos AA7(1) + FTR2 \cdot \cos AA7(2) \qquad \text{(B-106)}$$

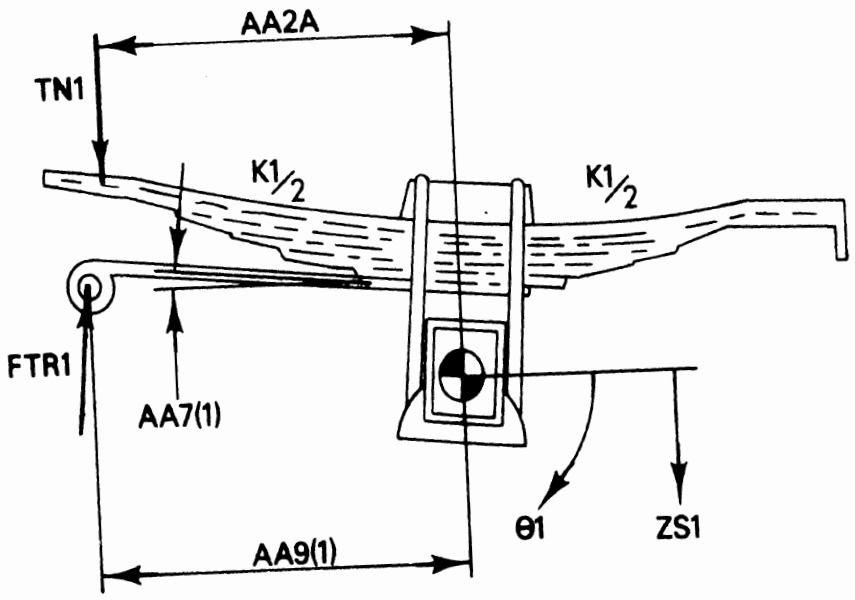

Figure B.24. Determining the torque rod spring forces.

$$TSTORQ = (AA1-AA2A+AA4)[(TN1-TN1S) + (TN2-TN2S)$$
$$- FF1-TR1 \cdot \sin AA7(1) - FTR1 \cdot \cos AA7(1)]$$
$$- (AA1-AA2B+AA5)[(TN3-TN3S) + (TN4-TN4S)$$
$$- FF2-TR2 \cdot \sin AA7(2) - FTR2 \cdot \cos AA7(2)] \quad \text{(B-107)}$$

B.6 The Four Spring Suspension with Long Load Leveler

This section presents the mathematical and digital computer models of the four spring suspension with long load leveler (FSS-LLL) as they apply to the Phase III braking performance programs. The suspension was illustrated in Figure 2-15.

The mathematical model is similar to the four spring suspension model of Phase I [1]. As such, it is considerably simplified as compared to the other four spring suspension model described in Section B.4.

In particular, spring/frame contact frictional forces of the FSS-LLL are ignored. Modeling of these forces greatly complicates the suspension model, and consequently increases the expense of its use. In the case of the FSS-LLL, the geometry of the suspension greatly reduces interaxle load transfer and correspondingly reduces the significance of spring/frame friction. For these reasons, the model presented does not include spring/frame frictional forces.

The mathematical model is based on the following assumptions:

1) Vertical motions of the axle assemblies (ZS1 and ZS2, Figure B-24) are the only independent motions of the suspension (longitudinal motion is coupled to the sprung mass) in which inertia is significant.

2) The slight shifts of spring, axle, and torque rod positions due to suspension motions are neglected in calculating suspension forces.

3) The connection between load leveler and frame is a frictionless pin.

4) Motions ZS1 and ZS2 (Fig. B-24) are assumed to remain vertical for all suspension/vehicle motions.

5) Only vertical forces exist at the spring/frame contact points.

The equations which follow use the notation presented in Figures 2-15 and B-25. The free-body diagrams of Figure B-25 illustrate only the dynamic components of all forces.

Applying Newton's second law in the "X" direction to each of the axles yields:

$$TRH1 = MS1\ \ddot{x} - FX1 \qquad \text{(B-108)}$$

$$TRH2 = MS2\ \ddot{x} - FX2 \qquad \text{(B-109)}$$

where FX1 and FX2 are the brake forces at the leading and trailing axles, respectively.

In the "Z" direction, Newton's second law yields

$$(TN1-TN1S) + (TN2-TN2S) + FF1 - TRV1 - DN1 = MS1 \cdot \ddot{ZS}1 \qquad \text{(B-110)}$$

$$(TN3-TN3S) + (TN4-TN4S) + FF2 - TRV2 - DN2 = MS2 \cdot \ddot{ZS}2 \qquad \text{(B-111)}$$

Forces FF1 and FF2 are the "friction forces" including both coulomb friction and viscous damping forces for the leading and trailing axles, respectively. Their method of calculation was discussed in Section 2.1. Forces DN1 and DN2 are the dynamic components of the tire-road normal forces.

Summing moments about each axle center and about the load leveler pin (and employing static equilibrium equations to remove the TNiS terms) yields, respectively:

$$TT1 + TN1 \cdot AA2A - TN2(AA1-AA2A) + TRH1 \cdot AA6(1) - TRV1 \cdot AA8(1) = 0 \qquad \text{(B-112)}$$

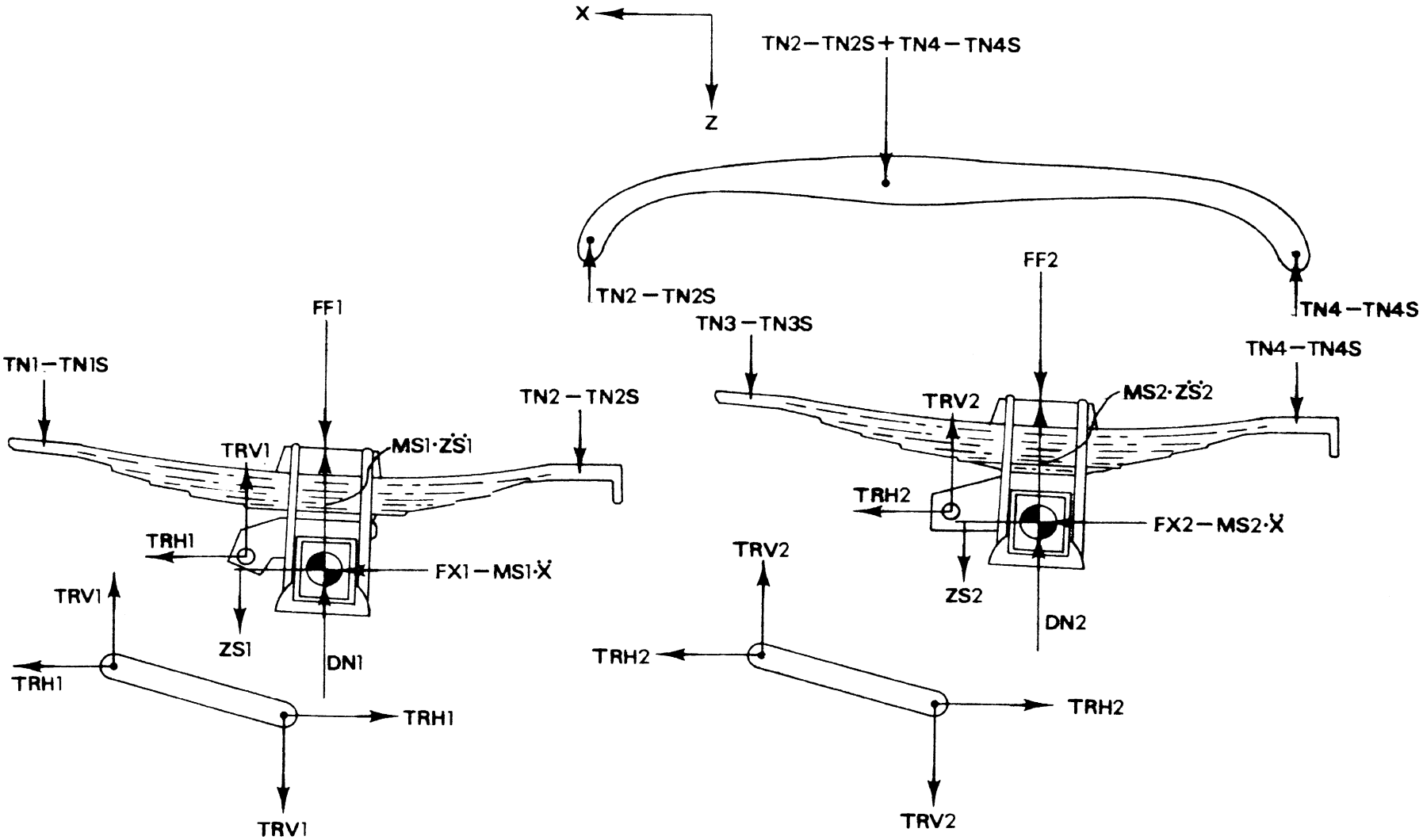

Figure B-25. Dynamic free-body diagram: the four spring suspension with long load leveler

$$TT2 + TN3 \cdot (AA1-AA2B) - TN4 \cdot AA2B + TRH2 \cdot AA6(2) - TRV2 \cdot AA8(2) = 0 \quad \text{(B-113)}$$

and

$$TN2 \cdot AA4 = TN4 \cdot AA5 \quad \text{(B-114)}$$

And by summing moments on each of the torque rods:

$$TRV1 = TRH1 \cdot TAN[AA7(1)] \quad \text{(B-115)}$$

$$TRV2 = TRH2 \cdot TAN[AA7(2)] \quad \text{(B-116)}$$

Now, with KK defined as the sum of the spring rates of all four leaf springs, the following expression is assumed:

$$TN1 + TN2 + TN3 + TN4 = KK \cdot \delta \equiv SUMTN \quad \text{(B-117)}$$

where δ is the average vertical displacement of the axle centers. This assumption is similar to assumptions used in earlier models. Use of this assumption requires that the difference between spring rates of leading and trailing axles be small.

In the context of the Phase III programs employing modularized suspension subprograms, the values of $\ddot{X}$, FX1, FX2, TT1, TT2, DN1, DN2, FF1, FF2, and δ (i.e., SUMTN) are inputs to the suspension model, having been calculated elsewhere in the simulations. Thus Equations (B-108) through (B-117) can be solved for each of the ten unknowns (TN1, TN2, TN3, TN4, TRV1, TRV2, TRH1, TRH2, $\dot{Z}\dot{S}1$, $\dot{Z}\dot{S}2$). These solutions are

$$TRH1 = MS1\ \ddot{X} - FX1 \quad \text{(B-118)}$$

$$TRH2 = MS2\ \ddot{X} - FX2 \quad \text{(B-119)}$$

$$TRV1 = TRH1 \cdot TAN[AA7(1)] \quad \text{(B-120)}$$

$$TRV2 = TRH2 \cdot TAN[AA7(2)] \quad \text{(B-121)}$$

$$TN4 = \left[\frac{1}{1 + \frac{AA5}{AA4}\left(1 - \frac{AA1 - AA2A}{AA2A}\right) + \frac{AA2B}{AA1-AA2B}}\right] \cdot$$

$$\left[\frac{TT1}{AA2A} + \frac{TT2}{AA1-AA2B} + TRH1\left(\frac{AA6(1) - TAN[AA7(1)] \cdot AA8(1)}{AA2A}\right)\right.$$

$$\left. + TRH2\left(\frac{AA6(2) - TAN[AA7(2)] \cdot AA8(2)}{AA1 - AA2B}\right) + SUMTN\right] \qquad \text{(B-122)}$$

$$TN2 = TN4 \cdot \frac{AA5}{AA4} \qquad \text{(B-123)}$$

$$TN3 = TN4 \cdot \frac{AA2B}{AA1-AA2B} - \left[\frac{TT2 + TRH2(AA6(2) - TAN[AA7(2)] \cdot AA8(2)}{AA1 - AA2B}\right] \qquad \text{(B-124)}$$

$$TN1 = TN2 \cdot \frac{AA1 - AA2A}{AA2A}$$

$$- \left[\frac{TT1 + TRH1(AA6(1) - TAN[AA7(1)] \cdot AA8(1))}{AA1 - AA2B}\right] \qquad \text{(B-125)}$$

$$\ddot{ZS}1 = \frac{(TN1-TN1S) + (TN2-TN2S) + FF1 - TRV1 - DN1}{MS1} \qquad \text{(B-126)}$$

$$\ddot{ZS}2 = \frac{(TN3-TN3S) + (TN4-TN4S) + FF2 - TRV2 - DN2}{MS2} \qquad \text{(B-127)}$$

The dynamic outputs required of the suspension model for use by the Phase III simulation programs are $\ddot{ZS}1$, $\ddot{ZS}2$, TSFV, TSFH, TSTORQ. The accelerations $\ddot{ZS}1$ and $\ddot{ZS}2$ have already been solved for, and by definition

$$TSFV = TRV1 + FF1 - (TN1-TN1S) - (TN2-TN2S) + TRV2 + FF2 - (TN3-TN3S) - (TN4-TN4S) \qquad \text{(B-128)}$$

$$TSFH = TRH1 + TRH2 \qquad \text{(B-129)}$$

$$TSTORQ = TN1 \cdot (AA1+AA4) - TN4 \cdot AA5 - FF1 \cdot (AA1-AA2A+AA4)$$
$$+ FF2 \cdot (AA5-AA2B) + TRH1 \cdot AA6(1) + TRH2 \cdot AA6(2)$$
$$- TRV1 \cdot [AA1 - AA2A + AA4 + AA8(1)] + TRV2$$
$$\cdot [AA5 - AA2B - AA8(2)] \qquad (B\text{-}130)$$

Consequently, Equations (B-126) through (B-130) represent the output of the dynamic model.

The static load calculations are similar to the dynamic model. The variables SSFV and STORQ are the static equivalents of TSFV and TSTORQ, respectively. The two constants SRATIO and SCONST are defined such that

$$STORQ = SRATIO \cdot SSFV + SCONST \qquad (B\text{-}131)$$

In the Phase III programs, the suspension model is required to determine SRATIO and SCONST. With these values, the main program determines SSFV and the suspension model in turn calculates STORQ and NS1 and NS2 (the static normal tire loads for the leading and trailing axles, respectively). It can be shown that, for the FSS-LLL

$$SRATIO = \frac{\left[-(AA1 - AA2A + AA4) + (AA5 - AA2B)\,\frac{AA4}{AA5} \cdot \frac{AA2A}{AA1-AA2B}\right]}{\left[1 + \frac{AA4}{AA5} \cdot \frac{AA2A}{AA1-AA2B}\right]} \qquad (B\text{-}132)$$

$$SCONST = 0 \qquad (B\text{-}133)$$

and

$$NS1 = WS1 + \left[\frac{1}{(AA5-AA2B) + (AA1-AA2A+AA4)}\right]\left[STORQ - SSFV \cdot (AA5-AA2B)\right] \qquad (B\text{-}134)$$

$$NS2 = WS2 + WS1 - SSFV - NS1 \quad \text{(B-135)}$$

where WS1 and WS2 are the unsprung weights of the leading and trailing axles, respectively.

B.7 The Multiple-Torque Rod Four Spring Suspension

A sketch of the multiple-torque rod four spring suspension (MTRFSS) under discussion appeared in Figure 2-18. The mathematical model of this suspension which will be developed is, in part, based on the hypothesis that there are two significant mechanisms by which this suspension reacts brake torques. These mechanisms are:

1) The development of couples composed of vertical forces located at the spring/frame contact points. These couples develop via "spring wrap-up."

2) The development of couples composed of tensile and compressive forces developed in the torque rods.

Conspicuous in their absence are the frictional (horizontal) forces at the spring/frame contact points. Although these forces are significant in the basic four spring suspension, we believe that it is reasonable to ignore them in the MTRFSS. In the basic model, frictional forces are significant inasmuch as their participation in the horizontal force couples reduces that portion of the brake torque which must be reacted by the vertical spring/frame contact force couples. However, the introduction of the upper torque rod greatly reduces the importance of frictional forces in determining the apportionment of brake torque reaction effort. With the introduction of this new element, the interrelationship between the torsional compliance of the leaf spring (manifest in "spring wrap-up"), the torsional compliance of the torque rod assembly* (due to the use of rubber bushings, etc.) and the geometric constraints represented by load leveler and torque rod assembly angular positions, become paramount in determining the apportionment of brake torque

*Herein, the "torque rod assembly" is defined as the four-bar linkage composed of the upper and lower torque rods, the axle housing, and the vehicle frame.

reaction effort. Frictional forces, then, are relegated to second-order importance.

A conceptualized sketch of the MTRFSS, showing the dynamic components and motions of interest, appeared in Figure 2.19*. As shown in the figure, each leaf spring has been reduced to four elements. Namely, a rigid link with angular position, θK, a linear spring with rate K, a torsional spring with rate KTQ, and a coulomb friction member which saturates at CF. Note that this coulomb friction member is assumed to be located between the sprung mass and unsprung mass. A viscous damping member is also provided. Each unsprung mass, MS, has a vertical position, ZS, and angular position, θS. The torque rod assembly is reduced to a massless four-bar linkage pinned to the unsprung mass at the center of torsional compliance of the torque rod assembly. (The center of torsional compliance is defined as follows: Consider the torque rod assembly separately, i.e., remove the leaf springs from Figure 2-18. If the angle AA7 were held fixed and a moment applied to the axle housing, a slight rotation of the axle housing would result due to compliance in the torque rod assembly. The center of this rotation is defined as the center of torsional compliance. A torsional spring of rate KTRTQ (a property of the torque rod assembly) is located between this link and the unsprung mass. The angle θSN (read θS-nominal) is defined as the nominal angular position of the unsprung mass, i.e., the angular position (defined by the torque rod assembly geometry) which the unsprung mass would assume, for a given vertical position, if it were under no load. Therefore, θSN is a function of ZSP where the function is established independently by the geometry of the torque rod assembly. Finally, the load leveler is shown as a rigid link with angular position θL.)

*In Figure 2.18 and in Figure 2.19, various labels appear with the subscripts (1) and (2) denoting the leading and trailing axles, respectively. In the following discussion, wherever it is not important to distinguish between axles, these subscripts will be dropped.

We will now develop a mathematical model of the MTRFSS based on the conceptual model of Figure 2-19. The model is based on the following assumptions:

1) In general, the modeling concepts of Figure 2-19 are valid.

2) Vertical motions of the unsprung mass are the only independent motions of the suspension (longitudinal motion is coupled to the sprung mass) in which inertia is significant.

3) Displacements shown in Figure 2-19 are the only suspension motions of significance and are important only with respect to the development of spring forces; i.e., slight changes in all other dimensions (see Figure 2-18) due to motions of the suspension are ignored.

4) Motion (ZS) is assumed to remain vertical for all suspension/vehicle motions.

5) All pin connections are frictionless.

6) Only vertical forces exist at the spring/frame and spring/load leveler contact points.

7) $\theta SN(1) = NACOEF(1) \cdot ZS(1)$ (a)

$\theta SN(2) = NACOEF(2) \cdot ZS(2)$ (b)

where NACOEF(1) and NACOEF(2) (read nominal axle angle coefficient) are constants.

Assumption (7) represents a further restricting on the functional relationship between θSN and ZS discussed earlier. The value of NACOEF is parametric input to the model.

We will begin with the dynamic portion of the model. Refer to the free-body diagram of Figure B-26 and note that all forces shown in the figure are dynamic components. Applying Newton's second law to each of the unsprung masses, respectively:

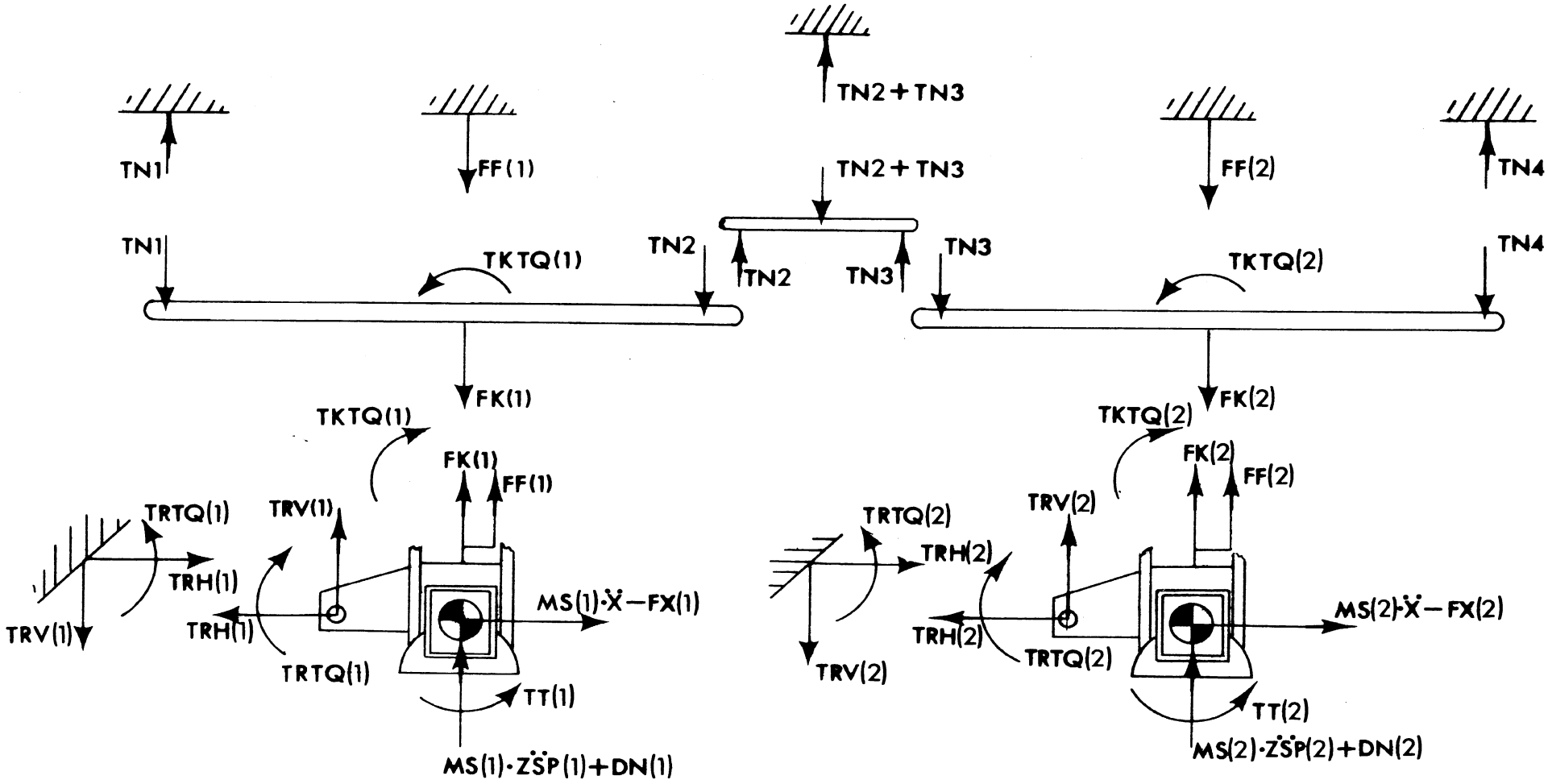

Figure B-26. Dynamic free-body diagram: the MTRFSS

$$MS(1) \cdot \ddot{x} - FX(1) = TRH(1) \quad (a)$$
$$MS(2) \cdot \ddot{x} - FX(2) = TRH(2) \quad (b) \qquad \text{(B-136)}$$

where FX is the brake force input to the axle. Now, in the Z direction,

$$MS(1) \cdot \ddot{ZS}(1) = - FK(1) - FF(1) - DN(1) - TRV(1) \quad (a)$$
$$MS(2) \cdot \ddot{ZS}(2) = - FK(2) - FF(2) - DN(2) - TRV(2) \quad (b) \qquad \text{(B-137)}$$

where DN is the dynamic portion of the tire normal load and FF is the total frictional force on the axle (coulomb plus viscous).*

Summing moments on the unsprung masses about the axle centers:

$$TRTQ(1) + TKTQ(1) - TRH(1) \cdot AA6(1) + TRV(1) \cdot AA8(1) - TT(1) = 0 \quad (a)$$

$$TRTQ(2) + TKTQ(2) - TRH(2) \cdot AA6(2) + TRV(2) \cdot AA8(2) - TT(2) = 0 \quad (b) \qquad \text{(B-138)}$$

From the geometry of the suspension model, the various spring forces and moments can be expressed as follows:

$$FK(1) = K(1) \cdot [ZS(1) + \frac{AA2A \cdot AA4}{AA1} \sin \theta L] \quad (a)$$
$$FK(2) = K(1) \cdot [ZS(2) - \frac{AA2B \cdot AA5}{AA1} \sin \theta L] \quad (b) \qquad \text{(B-139)}$$

*See Section B.1 for the technique used in modeling coulomb friction.

$$TRTQ(1) = KTRTQ(1)\cdot[\theta SN(1) - \theta S(1)] \quad (a)$$
$$TRTQ(2) = KTRTQ(2)\cdot[\theta SN(2) - \theta S(2)] \quad (b) \qquad (B\text{-}140)$$

$$TKTQ(1) = KTQ(1)\cdot[\theta K(1) - \theta S(1)] \quad (a)$$
$$TKTQ(2) = KTQ(2)\cdot[\theta K(2) - \theta S(2)] \quad (b) \qquad (B\text{-}141)$$

where, assuming small values of $\theta K(1)$ and $\theta K(2)$,

$$\theta K(1) = -\frac{AA4}{AA1}\sin\theta L \quad (a)$$
$$\theta K(2) = -\frac{AA5}{AA1}\sin\theta L \quad (b) \qquad (B\text{-}142)$$

Consider the "nominal axle position link" free-body diagram of Figure B-27. Summing moments about point A,

$$TRTQ + TRH[(1\text{-}c)\cdot d + (1\text{-}c)\cdot b\cdot\tan AA7] - P[b\cdot c\cdot\sin AA7 + (d + (1\text{-}c)\cdot b\cdot\tan AA7)\cdot\cos AA7] = 0 \qquad (B\text{-}143)$$

where c is a proportionality constant. Rearranging

$$P = \frac{TRTQ + (1\text{-}c)\cdot(d+b\cdot\tan AA7)\cdot TRH}{b\cdot\sin AA7 + d\cdot\cos AA7} \qquad (B\text{-}144)$$

Summing moments about point B,

$$TRTQ + (1\text{-}c)\cdot d\cdot TRH + (1\text{-}c)\cdot b\cdot TRV - P\cdot(b\cdot\sin AA7 + d\cdot\cos AA7) = 0 \qquad (B\text{-}145)$$

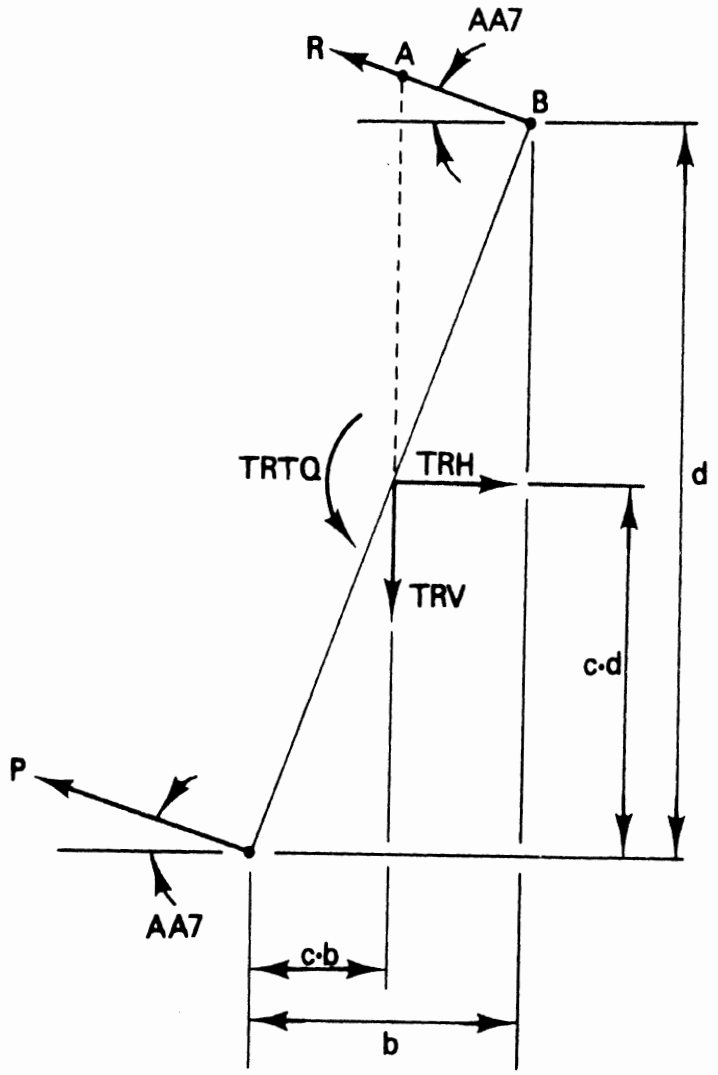

Figure B-27. Free-body diagram: the "nominal axle position link."

Substituting Equation (B-144) into (B-145) yields

$$TRTQ + (1-c)\cdot d\cdot TRH + (1-c)\cdot b\cdot TRV - TRTQ - (1-c)\cdot(d+b\cdot \tan AA7)\cdot TRH = 0 \qquad \text{(B-146)}$$

or

$$TRV = TRH \cdot \tan AA7 \qquad \text{(B-147)}$$

Equation (B-147) applies to both axles and may be written

$$TRV(1) = TRH(1)\cdot \tan AA7(1) \quad \text{(a)}$$
$$TRV(2) = TRH(2)\cdot \tan AA7(2) \quad \text{(b)} \qquad \text{(B-148)}$$

Referring again to Figure B-26, sum moments on the spring links and rearrange to find:

$$TN2 = \frac{-FK(1)\ AA2A + TKTQ(1)}{AA1} \quad \text{(a)}$$
$$TN3 = \frac{-FK(2)\ AA2B + TKTQ(2)}{AA1} \quad \text{(b)} \qquad \text{(B-149)}$$

Summing moments on the load leveler:

$$TN2 \cdot AA4 = TN3 \cdot AA5 \qquad \text{(B-150)}$$

Substituting Equation (B-149) into (B-150)

$$[TKTQ(1) - FK(1)\cdot AA2A]AA4 = -AA5[TKTQ(2) - FK(2)\cdot AA2B] \qquad \text{(B-151)}$$

Substituting Equation (B-139), (B-140), (B-141), (B-142), and (B-148) into Equation (B-138) and rearranging

$$\theta S(1) = \frac{KTRTQ(1)\cdot\theta SN(1) - \frac{AA4}{AA1}\cdot KTQ(1)\cdot\sin\theta L + TRH(1)\cdot[AA8(1)\cdot\tan AA7(1) - AA6(1)] - TT(1)}{KTQ(1) + KTRTQ(1)} \quad (a)$$

$$\theta S(2) = \frac{KTRTQ(2)\cdot\theta SN(2) - \frac{AA5}{AA1}\cdot KTQ(2)\cdot\sin\theta L + TRH(2)\cdot[AA8(2)\cdot\tan AA7(2) - AA6(2)] - TT(2)}{KTQ(2) + KTRTQ(2)} \quad (b)$$

(B-152)

Finally, Equations (B-135), (B-139), (B-141), (B-142), (B-151), and (B-152) may all be solved for sin θL yielding

$$\sin\theta L = \left\{AA1/\left[AA4^2\left\{AA2A^2\cdot K(1) + KTQ(1)\cdot\left(1 - \frac{KTQ(1)}{KTQ(1) + KTRTQ(1)}\right)\right\}\right.\right.$$

$$\left.\left. + AA5^2\left\{AA2B^2\cdot K(2) + KTQ(2)\cdot\left(1 + \frac{KTQ(2)}{KTQ(2) + KTRTQ(2)}\right)\right\}\right]\right\}$$

$$\cdot\left\{-\frac{AA4\ KTQ(1)}{KTQ(1) + KTRTQ(1)}\ [KTRTQ(1)\cdot NACOEF(1\cdot ZSP(1) + TRH(1)\right.$$

$$\cdot\{AA8(1)\cdot\tan AA7(1) - AA6(1)\} - TT(1)]$$

$$-\frac{AA5\ KTQ(2)}{KTQ(2) + KTRTQ(2)}\ [KTRTQ(2)\cdot NACOEF(2)\cdot ZSP(2) + TRH(2)$$

$$\cdot\{AA8(2)\cdot\tan AA7(2) - AA6(2)\} - TT(2)]$$

$$\left. - AA4\cdot AA2A\cdot K(1)\cdot ZSP(1) + AA5\cdot AA2B\cdot K(2)\cdot ZSP(2)\right\} \quad (B\text{-}153)$$

The necessary suspension model outputs are the total vertical suspension force (TSFV), the total horizontal suspension force (TSFH), the total suspension torque about the suspension reference point (TSTORQ), plus $\ddot{Z}SP(1)$ and $\ddot{Z}SP(2)$.

Define SFV(1) as the vertical suspension force associated with axle 1, that is

$$\begin{aligned} SFV(1) &= TRV(1) + FK(1) + FF(1) \quad (a) \\ SFV(2) &= TRV(2) + FK(2) + FF(2) \quad (b) \end{aligned} \tag{B-154}$$

By definition

$$TSFV = TRV(1) + FF(1) - TN1-TN2 + TRV(2) + FF(2) - TN3-TN4 \tag{B-155}$$

Summing vertical forces on the leaf spring links*

$$\begin{aligned} FK(1) + TN1 + TN2 &= 0 \quad (a) \\ FK(2) + TN3 + TN4 &= 0 \quad (b) \end{aligned} \tag{B-156}$$

From (B-154), (B-155) and (B-156)

$$TSFV = SFV(1) + SFV(2) \tag{B-157}$$

By definition:

$$\begin{aligned} TSTORQ &= TN1(AA1 + AA4) - TN4(AA1 + AA5) \\ &- FF(1)\cdot(AA1 - AA2A + AA4) + FF(2)\cdot(AA1 - AA2B + AA5) \\ &+ TRH(1)\cdot AA6(1) + TRH(2)\cdot AA6(2) \\ &- TRV(1)\cdot[AA1 - AA2A + AA4 + AA8(1)] + TRV(2) \\ &\cdot [AA1 - AA2B + AA5 - AA8(2)] - TRTQ(1) - TRTQ(2) \end{aligned} \tag{B-158}$$

But by summing moments about the suspension reference point for the free-body diagram of Figure B-27,

---

*Note that in this model, unlike in the basic four spring model, the "TN" forces are dynamic components only, not the total force.

$$TN1(AA1 + AA4) - TN4(AA1 + AA5)$$
$$- FF(1)\cdot(AA1 - AA2A + AA4) + FF(2)\cdot(AA1 - AA2B + AA5)$$
$$+ TRH(1)\cdot AA6(1) + TRH(2)\cdot AA6(2)$$
$$- TRV(1)\cdot[AA1 - AA2A + AA4 + AA8(1)] + TRV(2)\cdot[AA1 - AA2B$$
$$+ AA5 - AA8(2)]$$
$$- TRTQ(1) - TRTQ(2) - [DN(1) + MS(1)\cdot\ddot{Z}SP(1)]\cdot(AA1 - AA2A + AA4)$$
$$+ [DN(2) + MS(2)\cdot\ddot{Z}SP(2)]\cdot(AA1 - AA2B + AA5) + TT(1) + TT(2) = 0 \qquad \text{(B-159)}$$

Substituting Equations (B-137), (B-154), and (B-158) into (B-159) yields

$$TSTORQ = - TT(1) - TT(2)$$
$$- SFV(1)\ (AA1 - AA2A + AA4) + SFV(2)\ (AA1 - AA2B + AA5) \qquad \text{(B-160)}$$

By definition

$$TSFH = TRH(1) + TRH(2) \qquad \text{(B-161)}$$

From Equations (B-137) and (B-154)

$$\ddot{Z}SP(1) = - [SFV(1) + DN(1)]/MS(1) \qquad \text{(a)}$$
$$\ddot{Z}SP(2) = - [SFV(2) + DN(2)]/MS(2) \qquad \text{(b)} \qquad \text{(B-162)}$$

By way of review, the entire suspension model output can be represented by:

$$TSFV = SFV(1) + SFV(2) \qquad \text{(a)}$$
$$TSFH = TRH(1) + TRH(2) \qquad \text{(b)} \qquad \text{(B-163)}$$
$$TSTORQ = -TT(1) - TT(2) - SFV(1)(AA1-AA2+AA4) \qquad \text{(c)}$$
$$+ SFV(2)\ (AA1 - AA2B + AA5)$$

$$\ddot{Z}SP(1) = -[SFV(1) + DN(1)]/MS(1) \quad (a)$$

$$\ddot{Z}SP(2) = -[SFV(2) + DN(2)]/MS(2) \quad (b) \qquad (B\text{-}164)$$

where the SFV, TRH, and FK forces are available from Equations (B-148), (B-154), and (B-139), respectively, and sin θL is available from Equation (B-143). The values of $\ddot{x}$, FX(1), FX(2), TT(1), TT(2), DN(1), DN(2), ZSP(1), and ZSP(2) are calculated elsewhere in the program and are input to the suspension model. FF(1) and FF(2) are frictional forces, also considered input to the model.

Thus the dynamic model is complete and we will now turn to static considerations. The MTRFSS model, as shown in Figure 2-19, is indeterminate with respect to static tire normal loads unless information describing the "preset" of the various torsional springs is known. The input parameter PRCTN1 provides this information. PRCTN1 is defined as the percentage of tire normal load (both axles) carried by the leading axle. Thus it can be shown that the parameters SRATIO and SCONST, which are defined by the equation

$$STORQ = SRATIO \cdot SSFV + SCONST \qquad (B\text{-}165)$$

are, for this suspension,

$$SRATIO = -(AA1-AA2A+AA4)\frac{PRCTN1}{100} + (AA1-AA2B+AA5)(1 - \frac{PRCTN1}{100}) \qquad (B\text{-}166)$$

$$SCONST = [\frac{PRCTN1}{100} WS2 - (1 - \frac{PRCTN1}{100})WS1][(AA1-AA2A+AA4) + (AA1-AA2B+AA5)] \qquad (B\text{-}167)$$

SRATIO and SCONST are calculated according to Equations (B-166) and (B-167) if the user enters PRCTN1 such that $0 \leq PRCTN1 \leq 100$. Optionally, the user may enter PRCTN1 outside of this range. In this case, the program will assume a "preset" of zero in the KTRTQ springs (Figure 2-19) under which condition the static model of the

MTRFSS becomes identical to that of the basic four spring suspension described earlier in Section B.4.

In either case, the static tire normal loads of the leading and trailing axles may be shown to be

$$NS1 = WS1 + \frac{STORQ - SSFV(AA1 - AA2B + AA5)}{(AA1-AA2B+AA5) - (AA1-AA2A+AA4)} \qquad (B\text{-}168)$$

$$NS2 = WS1 + WS2 - SSFV - NS1 \qquad (B\text{-}169)$$

B.8 The MTRFSS with a Leaf Spring-Type Lower Torque Rod

Figure 2-23 illustrates a common modification of the MTRFSS in which the lower torque rod function is performed by a leaf spring member. The addition of this leaf spring torque rod may be accommodated in the conceptual model of the MTRFSS by a change in the torque rod assembly model as shown in Figure B-28, where KTR is the linear spring rate of the leaf spring torque rod.

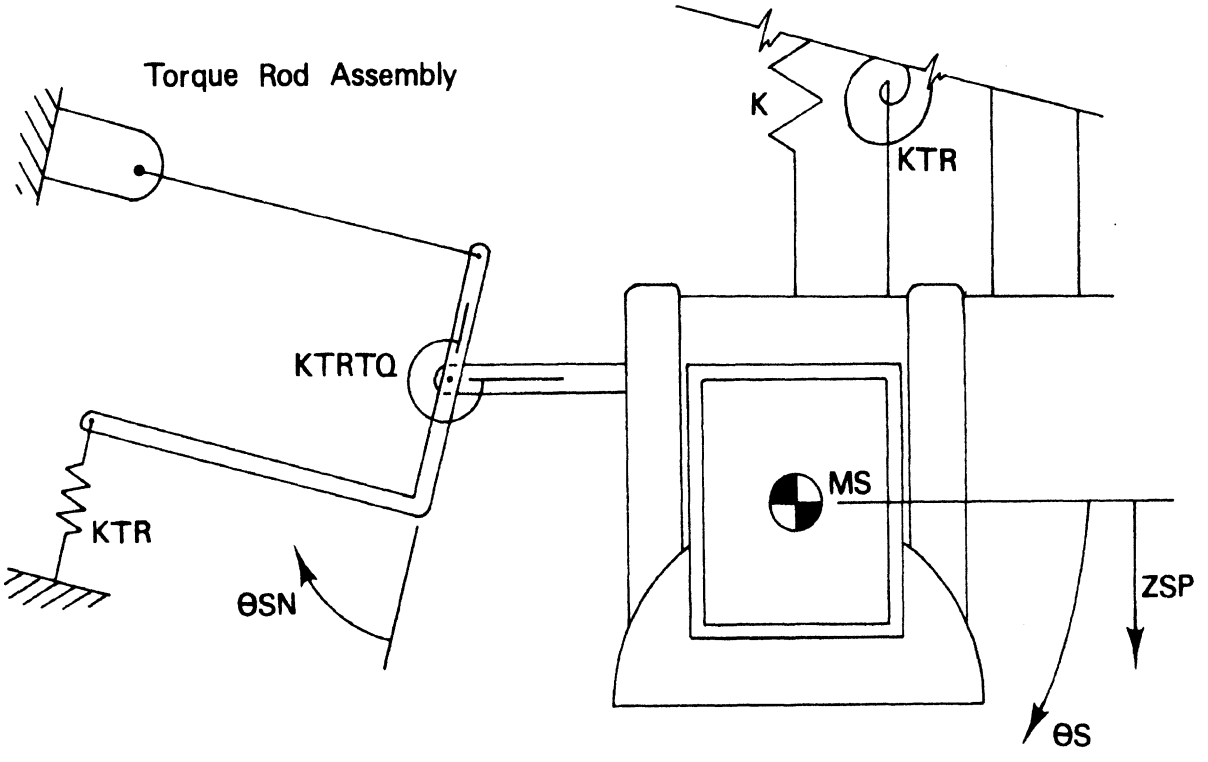

Figure B-28. Conceptual model of the MTRFSS with spring-type lower torque rod.

Mathematically, the use of a leaf spring torque rod results in changes to Equations (B-143) through (B-148) (of Section B.7), plus all following equations which are derived from these equations Equation (B-143) becomes

$$TRTQ + TRH\cdot[(1-c)\cdot d + (1-c)\cdot b\cdot \tan AA7] - P\cdot[b\cdot c\cdot \sin AA7 + (d + (1-c)\cdot b\cdot \tan AA7)\cdot \cos AA7] - FKTR\left[\ell - \frac{(1-c)\cdot b}{\cos AA7}\right] = 0 \qquad \text{(B-170)}$$

and (B-145) becomes

$$TRTQ + (1-c)\cdot d\cdot TRH + (1-c)\cdot b\cdot TRV - P(b\cdot \sin AA7 + d\cdot \cos AA7) - FKTR\cdot \ell = 0 \qquad \text{(B-171)}$$

Combining Equations (B-170) and (B-171) to eliminate P and solve for TRV yields

$$TRV = TRH \cdot \tan AA7 + \frac{FKTR}{\cos AA7} \qquad \text{(B-172)}$$

From the geometry of Figure B-28 we can show that for small values of θS

$$FKTR = \frac{KTR}{\cos AA7}(ZSP - AA9 \cdot \theta S) \qquad \text{(B-173)}$$

Substituting Equation (B-173) into (B-172)

$$TRV = TRH \cdot \tan AA7 + \frac{KTR}{\cos^2 AA7} \cdot (ZSP - AA9 \cdot \theta S) \qquad \text{(B-174)}$$

Equation (B-174) replaces Equation (B-147) in the analysis of Section B.7, resulting in appropriate changes to Equations (B-148), (B-152), and (B-153).

The static calculations for the suspension are identical to those for the MTRFSS. (In this case, the entry of PRCTN1 outside the range of 0 to 100 calls for an assumed zero preset in both the KTRTQ and KTR springs.)

B.9 Air Suspension Model

B.9.1 Introduction. This section is intended to explain the air suspension model of the Phase III simulation programs. There are a number of different air suspensions on the market. The model described here encompasses single and tandem axle designs using either four-bar- or trailing-arm-type linkages.

The air suspension model is conveniently divided into three parts:

1) the mechanical linkage system
2) the air spring
3) the air delivery system

These parts of the model will be dealt with successively in the next three sections. Section B.9.5 considers the interrelationships between the various parts of the model and Section B.9.6 discusses static considerations for the model.

B.9.2 The Mechanical Linkage System. The first linkage system to be modeled is the tandem four-bar type as illustrated in Figure 2.25. Dimensions relevant to the problem appear in the figure. Free-body diagrams of each link, showing all dynamic forces and moments acting on the links, appear in Figure B-29.

In the free bodies of Figure B-29, the dynamic tire normal forces (DN), viscous damping forces (FF), the air spring forces (FS), brake forces (FX), brake torques (TT), longitudinal decelerations (XDD), and their related D'Alembert forces (MS · XDD), are considered known "inputs" to the linkage, having been calculated earlier in other portions of the program. All other forces plus the vertical accelerations ($\ddot{Z}SP$) are unknown reactions to these forces.

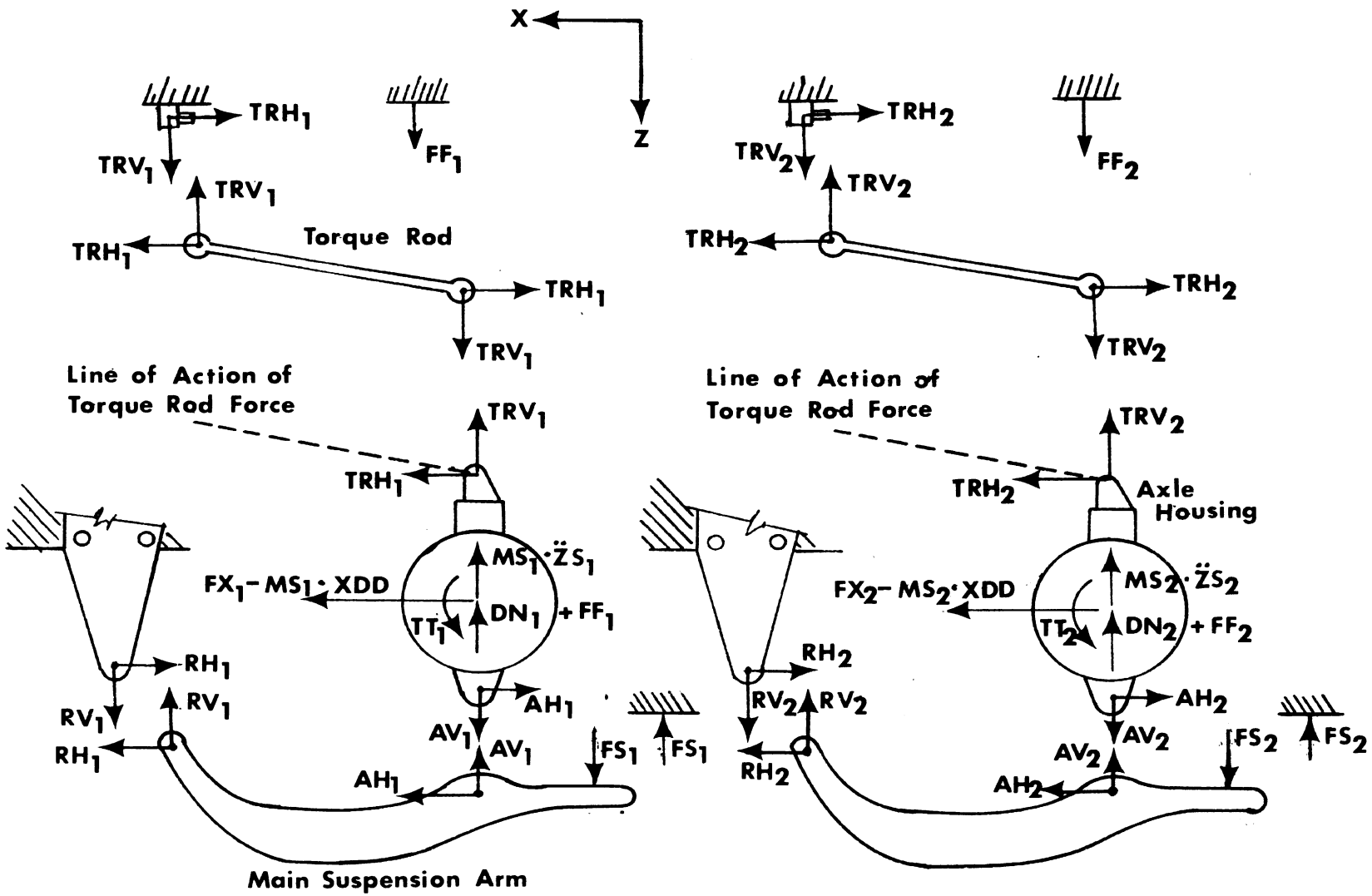

Figure B-29. Dynamic free-body diagram: tandem four-bar linkage air suspension

The assumptions on which the linkage model is based are:

1) Masses or moments of inertia are significant only with respect to vertical and longitudinal motion of the axle assembly.

2) The longitudinal accelerations of the unsprung masses are identical to that of sprung mass.

3) The mass center and axle center of each unsprung mass are coincident.

4) The pin connection between the main suspension arm and the axle housing lies directly below the axle center.

5) All pin connections are frictionless.

6) The air spring may transmit vertical force only.

7) Changes in geometry due to motions of the suspension and vehicle are ignored.

As outlined in Section B.1, the output of the suspension model required by subroutine FCT1 are the total vertical suspension force (TSFV), the total horizontal suspension force (TSFH), total suspension torque about the suspension reference point (TSTORQ), and the vertical accelerations of the unsprung masses ($\ddot{Z}SP(I)$, I = 1,2). (Note that the suspension reference point is defined as the leading axle center.) These quantities may be expressed as:

$$TSFV = SFV(1) + SFV(2) \qquad \text{(B-175)}$$

$$TSFH = SFH(1) + SFH(2) \qquad \text{(B-176)}$$

$$TSTORQ = TORQ(1) + TORQ(2) + SFV(2) \cdot AA1 \qquad \text{(B-177)}$$

where SFV, SFH, and TORQ are defined, respectively, as the total vertical axle force, total horizontal axle force, and the total axle torque about the axle center, and the subscripts (1) and (2)

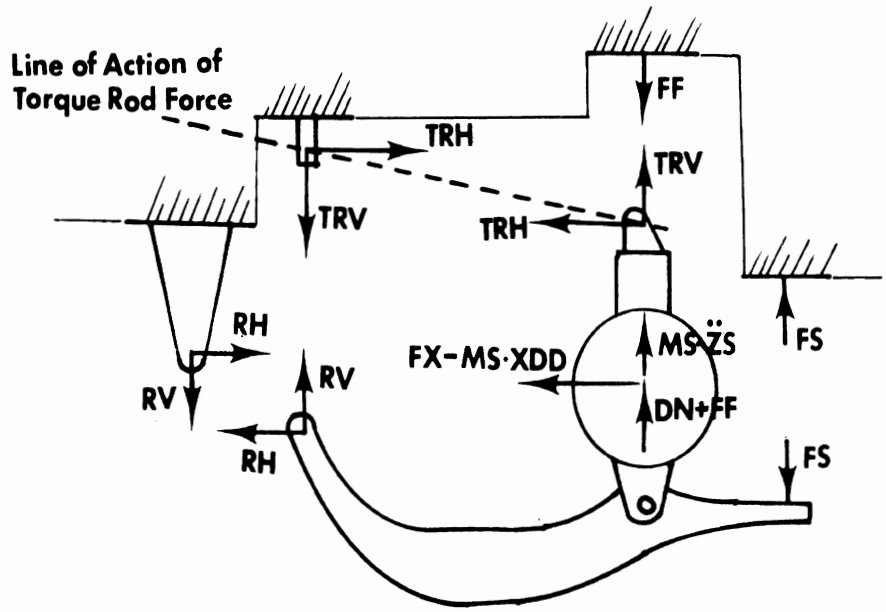

Figure B-30. Dynamic free-body diagram: Axle assembly of the four-bar linkage air suspension.

refer to leading and trailing axles, respectively. In the following analysis, equations for SFV, SFH, and TORQ, as well as $\ddot{Z}SP$, will be developed. Subscripts will be dropped from all notations since the analysis is applicable to either axle.

By definition:

$$SFV \equiv TRV + RV - FS + FF \tag{B-178}$$

$$SFH \equiv - TRH - RH \tag{B-179}$$

$$TORQ \equiv TRH \cdot AA5 - RV \cdot AA3 - RH(AA4 - AA3 \cdot tanAA7A) - FS \cdot (AA2-AA3) \tag{B-180}$$

Consider the free body of an entire axle assembly, Figure B-30. Summing moments about the axle center:

$$-TRH \cdot AA5 + RV \cdot AA3 + RH(AA4 - AA3 \cdot tanAA7A) + FS \cdot (AA2-AA3) + TT = 0 \tag{B-181}$$

Then from (B-180) and (B-181)

$$TORQ = -TT \tag{B-182}$$

and from the same free body, in the x direction:

$$TRH + RH + FX - MS \cdot XDD = 0 \tag{B-183}$$

Combining Equation (B-179) and (B-177)

$$SFH = FX - MS \cdot XDD \tag{B-184}$$

Applying Newton's second law to the main suspension arm in the z direction:

$$FS - RV - AV = 0 \tag{B-185}$$

and from Equations (B-178) and (B-185)

$$SFV = TRV - AV + FF \tag{B-186}$$

Applying Newton's second law to the axle housing in the z direction:

$$AV - TRV - MS \cdot \ddot{ZS} - DN - FF = 0$$

or

$$MS \cdot \ddot{ZS} = AV - TRV - DN - FF \tag{B-187}$$

and from Equations (B-184) and (B-185)

$$\ddot{ZS} = \frac{-(SFV + DN)}{MS} \tag{B-188}$$

It remains to determine the forces TRV and AV. With these two forces, Equations (B-175) through (B-180), (B-182), (B-184), (B-186), and (B-188) represent the entire solution for the required suspension model output variables.

Summing moments on the torque rod and setting equal to zero leads to

$$TRH = TRV/\tan AA7B \tag{B-189}$$

Summing moments on the axle housing, first about the axle center and then about the main arm pin, and setting equal to zero yields Equations (B-190) and (B-191), respectively.

$$TRH \cdot AA5 + AH \cdot AA4 + TT = 0 \tag{B-190}$$

$$TRH \cdot (AA4+AA5) + (FX - MS \cdot XDD) \cdot AA4 + TT = 0 \tag{B-191}$$

Rearranging (B-190)

$$TRH = \frac{-TT}{AA5} - \frac{AA4}{AA5} AH \tag{B-192}$$

Substituting (B-189) and (B-192), respectively, into (B-191) and rearranging yields:

$$TRV = -(FX - MS \cdot XDD) \frac{AA4 \cdot tanAA7B}{AA4 + AA5} - TT \frac{tanAA7B}{AA4 + AA5} \tag{B-193}$$

$$AH = (FX - MS \cdot XDD) \frac{AA5}{AA4 + AA5} - \frac{TT}{AA4 + AA5} \tag{B-194}$$

Now summing moments on the main arm about the body connection pin:

$$FS \cdot AA2 - AV \cdot AA3 + AH \cdot AA3 \cdot tanAA7A = 0 \tag{B-195}$$

Substituting (B-194) and (B-195) and solving for AV

$$AV = FS \frac{AA2}{AA3} + [(FX - MS \cdot XDD) \cdot AA5 - TT] \frac{tanAA7A}{AA4 + AA5} \tag{B-196}$$

Substituting (B-193) and (B-196) into (B-186)

$$SFV = -FS \frac{AA2}{AA3} - (FX - MS \cdot XDD) \cdot \left(\frac{AA5\ tanAA7A + AA4\ tanAA7B}{AA4 + AA5}\right)$$

$$+ TT \left(\frac{tanAA7A - tanAA7B}{AA4 + AA5}\right) + FF \tag{B-197}$$

In summary, the outputs from the suspension model are

$$TSFV = SFV(1) + SFV(2) \qquad (a)$$

$$TSFH = SFH(1) + SFH(2) \qquad (b)$$

$$TSTORQ = TORQ(1) + TORQ(2) + AA1 \cdot SFV(2) \qquad (c) \qquad (B\text{-}198)$$

$$\ddot{Z}S(1) = \frac{-(SFV(1) + DN(1))}{MS(1)} \qquad (d)$$

$$\ddot{Z}S(2) = \frac{-(SFV(2) + DN(2))}{MS(2)} \qquad (e)$$

where SFV(I), SFH(I), and TORQ(I) (I = 1,2) may be found from Equations (B-197), (B-184), and (B-182), respectively.

The preceding analysis for a tandem suspension composed of two four-bar linkage-type axles may be easily modified to account for trailing arm linkages (see Figure 2-26) at either or both axles.

Equation (B-198) remains applicable regardless of the linkage arrangement. Further, it can be shown that the equations for SFH and TORQ (Equations (B-184) and (B-182), respectively) remain unchanged for the trailing arm linkage. Thus, to adapt the analysis to the trailing arm arrangement, only the equation for SFV need be altered.

Using the notation from Figure 2-26 and B-31 (free-body diagram of a trailing arm axle), and the definition of SFV:

$$SFV = RV - FS + FF \qquad (B\text{-}199)$$

Equation (B-199) is, of course, identical to Equation (B-178) except for the omission of the vertical torque rod force, TRV.

Summing moments about the axle center in Figure 2.32 yields:

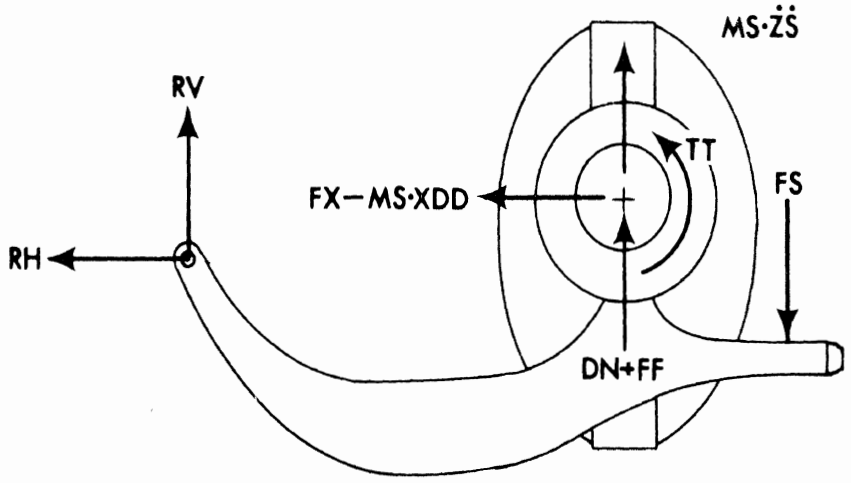

Figure B-31. Dynamic free-body diagram: Trailing arm air suspension.

$$RV \cdot AA3 + RH \cdot AA4 + FS(AA2-AA3) - TT = 0 \qquad \text{(B-200)}$$

where, from the summation of horizontal forces

$$RH = MS \cdot XDD - FX \qquad \text{(B-201)}$$

Combining the three preceding equations

$$SFV = -FS\left(\frac{AA2}{AA3}\right) + \frac{TT + (FX-MS \cdot XDD)AA4}{AA3} + FF \qquad \text{(B-202)}$$

Thus, if a trailing arm type axle is to be used, in either leading or trailing position, Equation (B-202) replaces Equation (B-197) as the definition of SFV (i.e., SFV(1) for leading axle or SFV(2) for trailing axle) in Equation (B-198).

Finally, the mechanical linkage analysis can be altered for a single-axle air suspension simply by setting all terms in Equation (B-198) with "(2)" subscripts to zero.

B.9.3 The Air Spring. Basic to the model of the air spring, whose description follows in this section, and to the model of the air delivery system described in Section B.9.4, is the assumption that the behavior of the entire air suspension system can be described as two independent thermodynamic processes. These processes are:

1. A constant mass, reversible polytropic (i.e., PV^n = const) process which is assumed to describe the action of the air in the spring at time (t) over the time period (t) to (t + Δt) where Δt is time step size used in the digital computer program.

2. A constant temperature process assumed to describe the effects of the various air flows in and out of the spring during the time period (t) to (t + Δt).

For the sake of semantic convention in the following discussions, the first process is attributed to the air spring; the second process is attributed to the air delivery system.

The nomenclature used in the following discussion includes:

h: air spring height

L: air spring load

P: air spring gauge pressure

P_a: air spring absolute pressure

P_{at}: atmospheric pressure

V: air spring internal volume

$(\ )_0$: the subscript 0 refers to the nominal (i.e., operating point) value of the variable. For example, L_0 is the nominal air spring load.

$\Delta(\ )$: the prefix, Δ, refers to a variation from the nominal value. For example, $\Delta L \equiv L - L_0$.

A_L: the effective air spring area with respect to load;

$$A_L \equiv \left.\frac{\partial L}{\partial P}\right|_{h=h_0} \tag{B-203}$$

A_V: effective air spring area with respect to volume;

$$A_V \equiv \left.\frac{dV}{dh}\right|_{h=h_0} \tag{B-204}$$

K_p: air spring constant pressure spring rate;

$$K_p \equiv - \left. \frac{\partial L}{\partial h} \right|_{P=P_0} \qquad \text{(B-205)}$$

An example of the air spring performance data [19] published by air spring manufacturers appears in Figure B-32. Example values of A_L, A_V, and K_p which derive from this data are given. Upon examining such air spring performance data, it is evident that the following assumptions are reasonable:

$$L = L(P,h) \qquad \text{(B-206)}$$

and

$$V = V(h) \qquad \text{(B-207)}$$

(Note the absence of P in Equation (B-207) implies that the internal volume of the air spring is not significantly affected by pressure. This, of course, is not exact.)

In addition, the statements of at least one air spring manufacturer [19] support the assumption of:

$$P_a V^n = C \qquad \text{(B-208)}$$

where C is a constant, and suggest that

$$n = 1.38 \qquad \text{(B-209)}$$

This value of n will be assumed here.

If it is further assumed that, within the range of interest about the operating point, linear approximations of Equations (B-206) and (B-207) are sufficiently accurate, then Equations (B-210) and (B-211) are applicable.

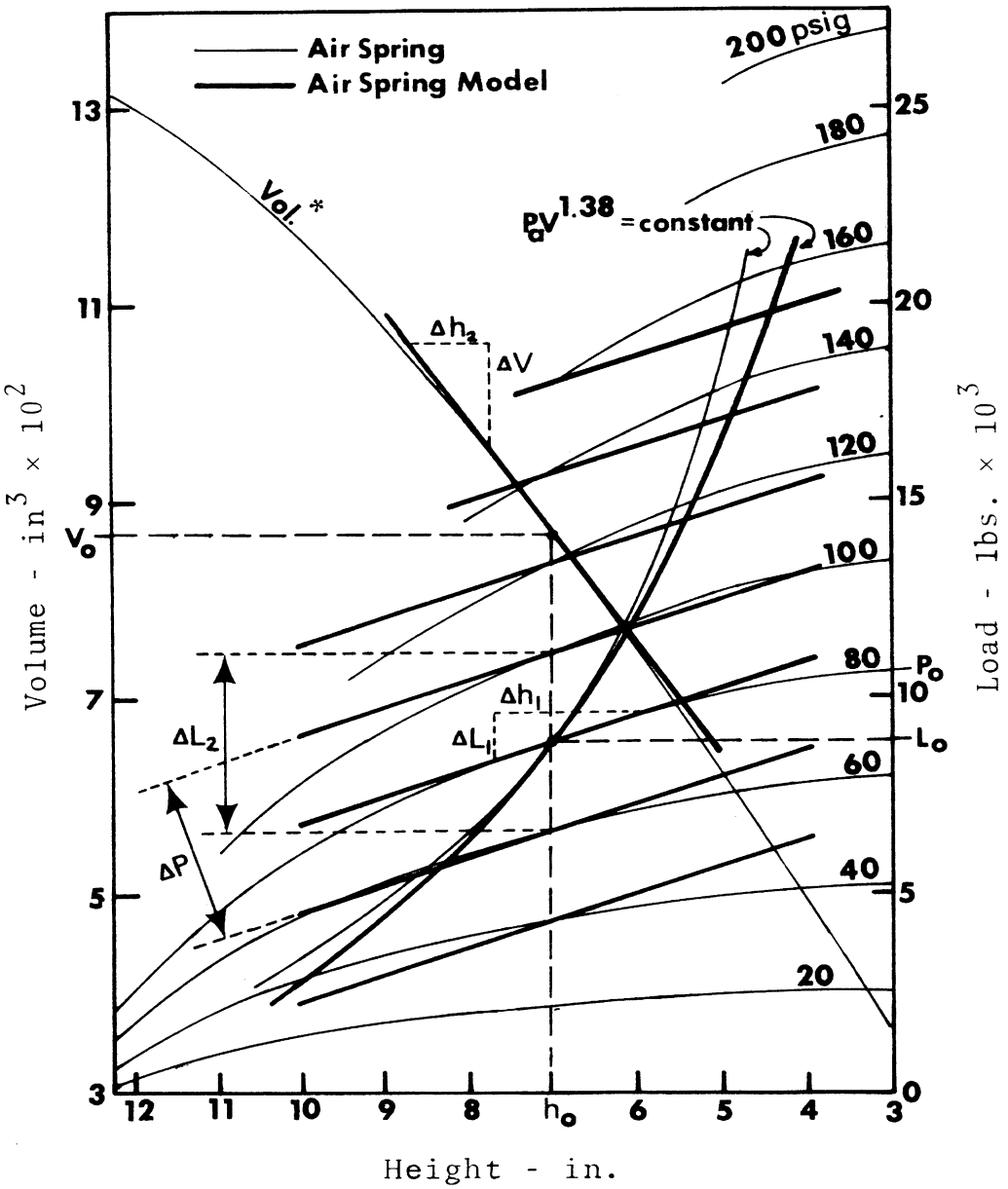

The Operating Point is defined by:

Nominal Volume ; $V_o = 870\ in^3$
Nominal Height ; $h_o = 7.0\ in$
Nominal Load ; $L_o = 8800\ lb$
Nominal Press ; $P_o = 80\ psig$

The Dynamic Characteristics are:

Effective Area, Volume;

$$A_V \equiv \left.\frac{dV}{dh}\right|_{h_o} = \frac{\Delta V}{\Delta h_2} = 120\ in^2$$

Effective Area, Load;

$$A_L \equiv \left.\frac{\partial L}{\partial P}\right|_{h_o} \approx \frac{\Delta L_2}{\Delta P} = 112\ in^2$$

Constant Pressure Spring Rate;

$$K_P \equiv -\left.\frac{\partial L}{\partial h}\right|_{P_o} = -\frac{\Delta L_1}{\Delta h_1} = 667\ \frac{lb}{in}$$

*This plot applies to volume vs. height axes only. All other plots apply to the load vs. height axes only.

Figure B-32. Example Air Spring Data and Model Characteristics

$$\Delta L = \left.\frac{\partial L}{\partial P}\right|_{h=h_0} \cdot \Delta P + \left.\frac{\partial L}{\partial H}\right|_{P=P_0} \cdot \Delta h \qquad \text{(B-210)}$$

$$\Delta V = \left.\frac{dV}{dh}\right|_{h=h_0} \cdot \Delta h \qquad \text{(B-211)}$$

Substituting Equations (B-203) and (B-205) into (B-210) and Equation (B-202) into (B-211) yields:

$$\Delta L = A_L \Delta P - K_p \Delta h \qquad \text{(B-212)}$$

and

$$\Delta V = A_V \Delta h \qquad \text{(B-213)}$$

Substituting nominal values of pressure and volume and a value of 1.38 for n into Equation (B-208):

$$C = (P_0 + P_{at})V_0^{1.38} \qquad \text{(B-214)}$$

Using this value for C and solving Equation (B-208) for P

$$P = \frac{(P_0 + P_{at})V_0^{1.38}}{V^{1.38}} - P_{at} \qquad \text{(B-215)}$$

and by the definition of ΔP

$$\Delta P = \frac{(P_0 + P_{at})V_0^{1.38}}{V^{1.38}} - P_{at} - P_0 \qquad \text{(B-216)}$$

From the definition of ΔV and Equation (B-213)

$$\Delta V = V - V_0 = A_V \cdot \Delta h \qquad \text{(a)}$$

or (B-217)

$$V = V_0 + A_V \cdot \Delta h \qquad \text{(b)}$$

Substituting Equation (B-217b) into (B-215) yields:

$$\Delta P = \frac{(P_0 + P_{at})V_0^{1.38}}{[V_0 + A_V \cdot \Delta h]^{1.38}} - P_{at} - P_0 \qquad \text{(B-218)}$$

Equations (B-212), (B-213), and (B-218) constitute a mathematical representation of the proposed air spring model. The input to the model is Δh, the change in air spring height, and the output is ΔL, the change in air spring vertical force. A graphical representation of this model appears in Figure B-32. Figure B-32 gives an example of the air spring model performance characteristics of an example air spring.*

In the figure, the lines of constant pressure and the plot marked "Vol." represent published data. The various straight lines are the model's approximation of this data according to the values of A_V, A_L, and K_p obtained for the arbitrarily chosen operating point. The two plots marked "$P_a V^{1.38}$ = Constant" are the results of applying the empirical data and the model characteristics, respectively, to this equation (i.e., each of these plots represents a solution to the simultaneous equations:

$$V = V(h) \qquad \text{(a)}$$

$$P_a V^{1.38} = \text{Constant} \qquad \text{(b)} \qquad \text{(B-219)}$$

$$L = L(P,h) \qquad \text{(c)}$$

*Firestone Airide ®, No. 21. [19].

The lighter plot results when Equations (a) and (c) are solved using actual air spring data; the darker line comes from employing the air spring model to solve Equations (a) and (c).

Note that in Figure B-32, the values of A_V, A_L, and K_p were determined by designating the operating point to be identical to the static condition. In certain situations, improved model behavior may be obtained by a slight variation of this procedure. For example, consider the case when this spring is being used on the rear of a straight truck being studied under braking only. Assuming that the operating point represents the static loading condition, it would generally be expected that loads on the spring would always be less than or equal to the nominal load and spring height would be greater or equal to nominal height. Consequently, the model would operate only to the left of and below the operating point. By choosing A_V to more nearly represent the slope of the "Vol." plot in this region, significant improvement in model performance in the same region can be gained. (See Figure B-33.)

Similar adjustment of A_L to more nearly represent the vertical spacing of the constant pressure lines in the region of interest will also improve performance. For the example spring considered here, K_p appears to be near optimum as shown. In general, the goal when choosing the values of A_V, A_L, and K_p is to obtain the most accurate linear approximations of the spring data (both "Vol." and constant pressure plots) as possible within the expected region of operation.

B.9.4 The Air Delivery System. The discussion of the previous section assumed no air flow into or out of the air spring. This, of course, is not the case. Figure B-34 diagrams the plumbing system of a typical tandem air suspension.* As

*Note that height regulating valves are indicated since this model is intended for use as a full suspension, not as tag axles.

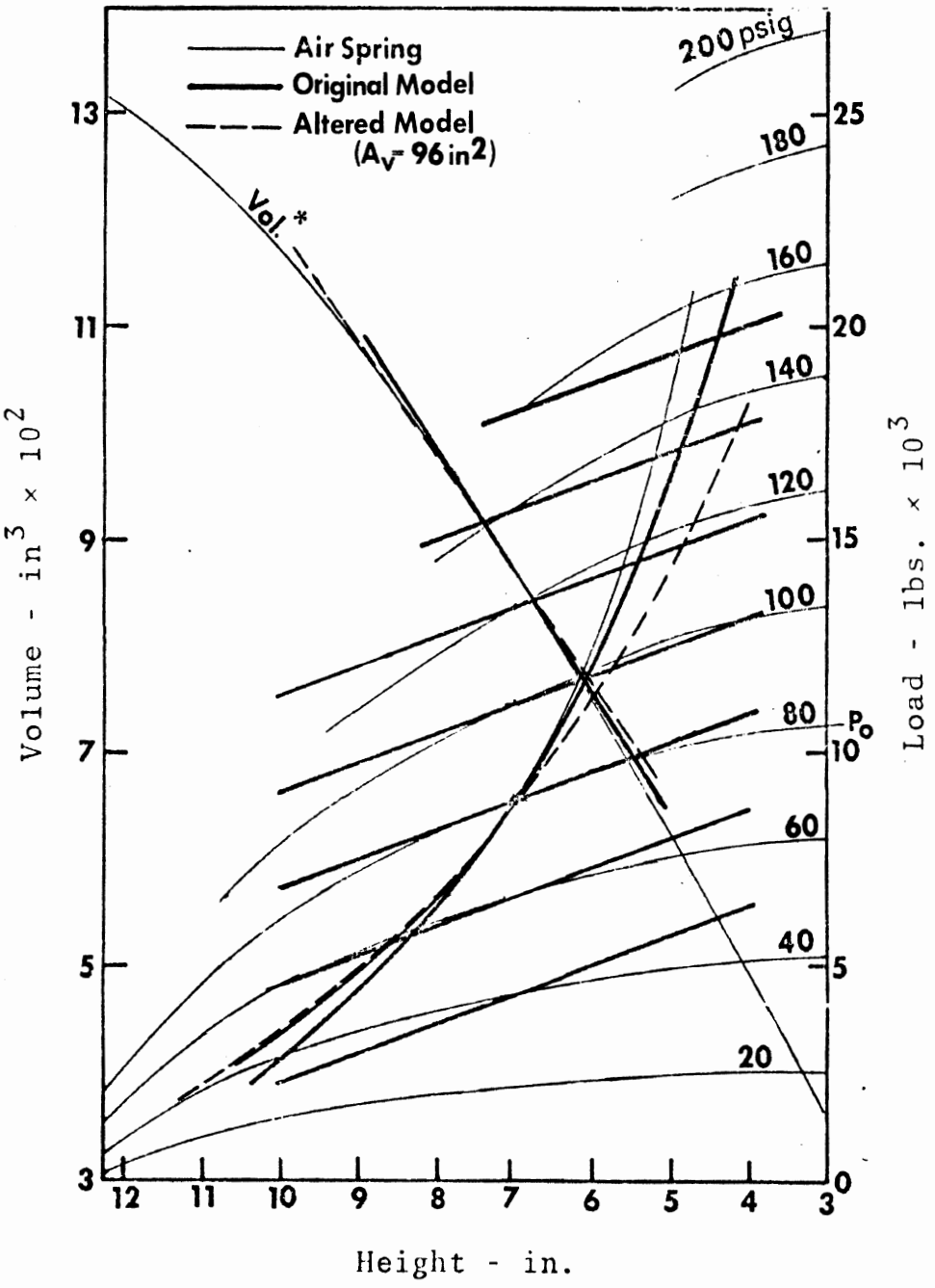

Figure B-33. Improved model performance within a limited operating range.

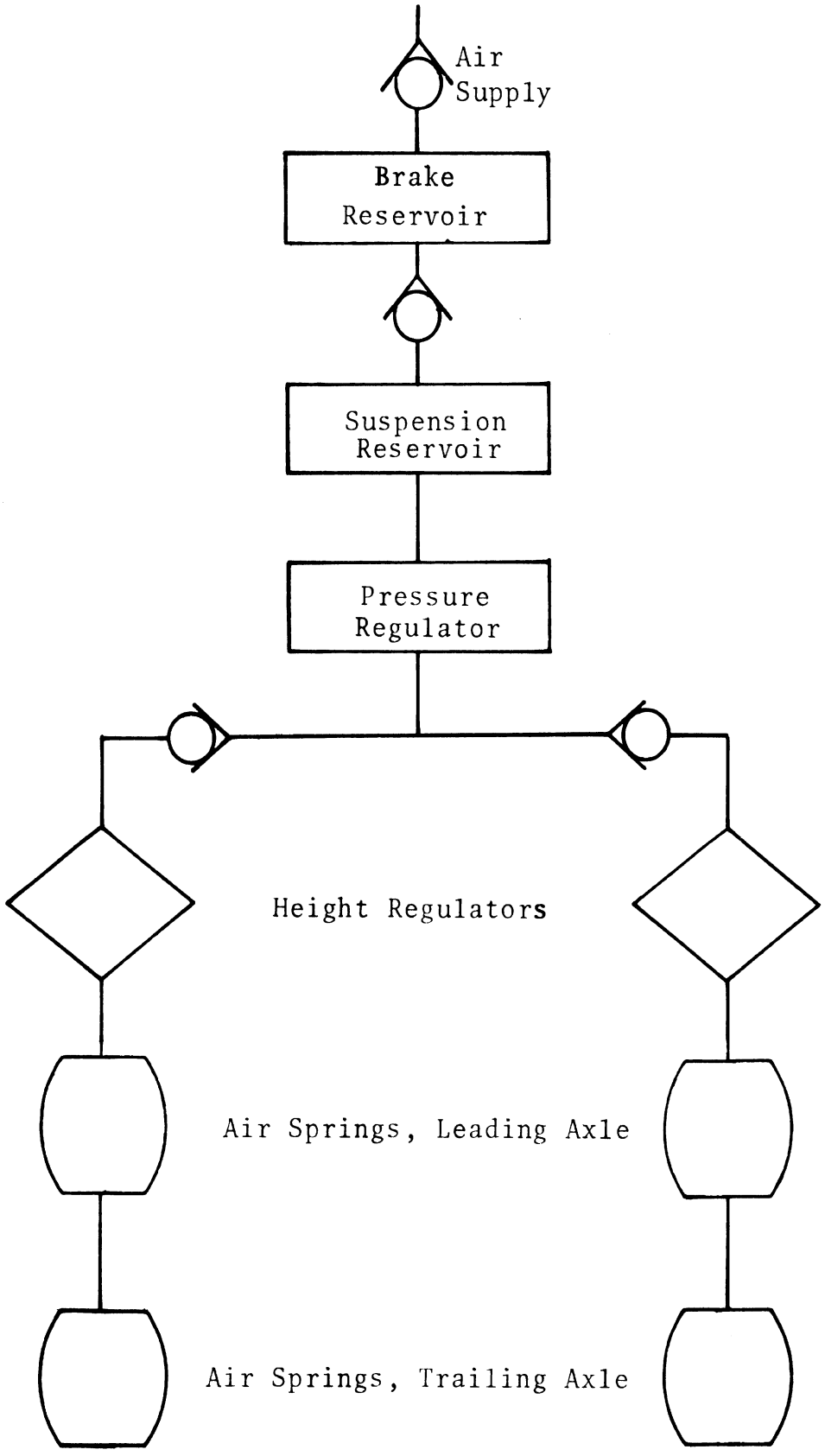

Figure B-34. Air Suspension Plumbing Diagram

shown, air may enter or exit an air spring via the height regulator or through its interconnections with the other spring on the same side of the vehicle.

Air flow through the height regulators is typically quite slow, but may have an effect on the pitch attitude of the vehicle near the end of a high-speed stop. More importantly, the interconnection between the two axles of a tandem may have a significant load leveling effect.

The same model is proposed for each of the several flow paths (to be enumerated later). Basic to this model are the assumptions that (1) during a single time step ($\Delta t = 0.0025$ sec) temperature in the air spring is constant, and (2) the mass flow of air in a given flow path may be described by:

$$\left(\frac{dM}{dt}\right)_i = C_i' \left(P_{e_i} - P\right) \qquad \text{(B-220)}$$

where

$\left(\frac{dM}{dt}\right)_i$: the mass rate of air flow into (positive) the spring via the particular flow path

P: the gauge air pressure in the spring

P_{e_i}: the gauge air pressure at the opposite end of flow path i (supply pressure, atmospheric pressure, or pressure in the other spring)

C_i': a constant property of the flow path i.

Then for either air spring, assuming the ideal gas law

$$(P + P_{at}) \cdot V = M \cdot R \cdot T \qquad \text{(B-221)}$$

where

P_{at} is atmospheric pressure

R is the gas constant

V is the air spring volume

T is the absolute temperature in the spring

M is the air mass in the air spring.

Then by differentiating

$$\frac{dM}{dt} = \frac{d}{dt}\left[\frac{(P + P_{at})V}{R \cdot T}\right] = \sum_{i=1}^{n} \left(\frac{dM}{dt}\right)_i \qquad \text{(B-222)}$$

where n is the number of flow paths.

Since R and T are constants, Equation (B-222) may be written

$$\sum_{i=1}^{n} \left(\frac{dM}{dt}\right)_i = \frac{1}{R \cdot T}\left[(P + P_{at})\frac{dV}{dt} + V\frac{dP}{dt}\right] \qquad \text{(B-223)}$$

Combining Equations (B-220) and (B-223) and rearranging:

$$\frac{dP}{dt} = \frac{1}{V}\left[\sum_{i=1}^{n} C_i(P_{e_i} - P) - (P + P_{at})\frac{dV}{dt}\right] \qquad \text{(B-224)}$$

where

$$C_i = C_i' \cdot R \cdot T \qquad \text{(B-225)}$$

The time step at which the HSRI simulation program proceeds (Δt = 0.0025 sec) is extremely small relative to the expected dynamic behavior of the air delivery system. Consequently, the simplest form of digital integration will be adequate for the solution of Equation (B-224). Therefore, from Equation (B-224)

$$\Delta P_D = \frac{1}{V_{AV}} \left[\sum_{i=1}^{n} C_i (P_{e_i} - P_{AV}) - (P_{AV} + P_{at}) \left(\frac{dV}{dt} \right)_{AV} \right] \Delta t \qquad \text{(B-226)}$$

where the subscript (AV) indicates an average value over the time step and the subscript (D) indicates "of the delivery system."

Determination of the values of V_{AV}, P_{AV}, and $\left(\frac{dV}{dt}\right)_{AV}$ to be substituted into the right-hand side of Equation (B-226) will be discussed in Section B.9.5. Suffice to say they will be approximations to their average values over the time step.

Figure B-28 illustrates all the flow paths available in the tandem air suspension model. As shown in the figure, there is an input and exhaust coefficient plus a switching mechanism associated with the air spring of each axle. Either of these regulators may be removed from the model by setting the appropriate flow coefficients to zero. A flow coefficient is also available to describe flow between the axles. Associated with each switching mechanism is a time lag as described in Section 2.1.8.

The details of the interrelationship between the air spring and air delivery system models will be covered in the following section. In general, the value of ΔP_D determined by this air delivery model will be used as a modifier to the value of ΔP associated with the air spring model. (See Equation (B-217).)

B.9.5 The Complete Model. In this section, the interrelationships between the three portions of the air suspension model will be described. A conceptual flow diagram of the model appears in Figure B-35. It may be helpful in understanding the material in this section to refer to this figure. Initially, the air spring and air delivery system models will be combined to form a total air system model. To complete the model, air and mechanical systems will then be combined.

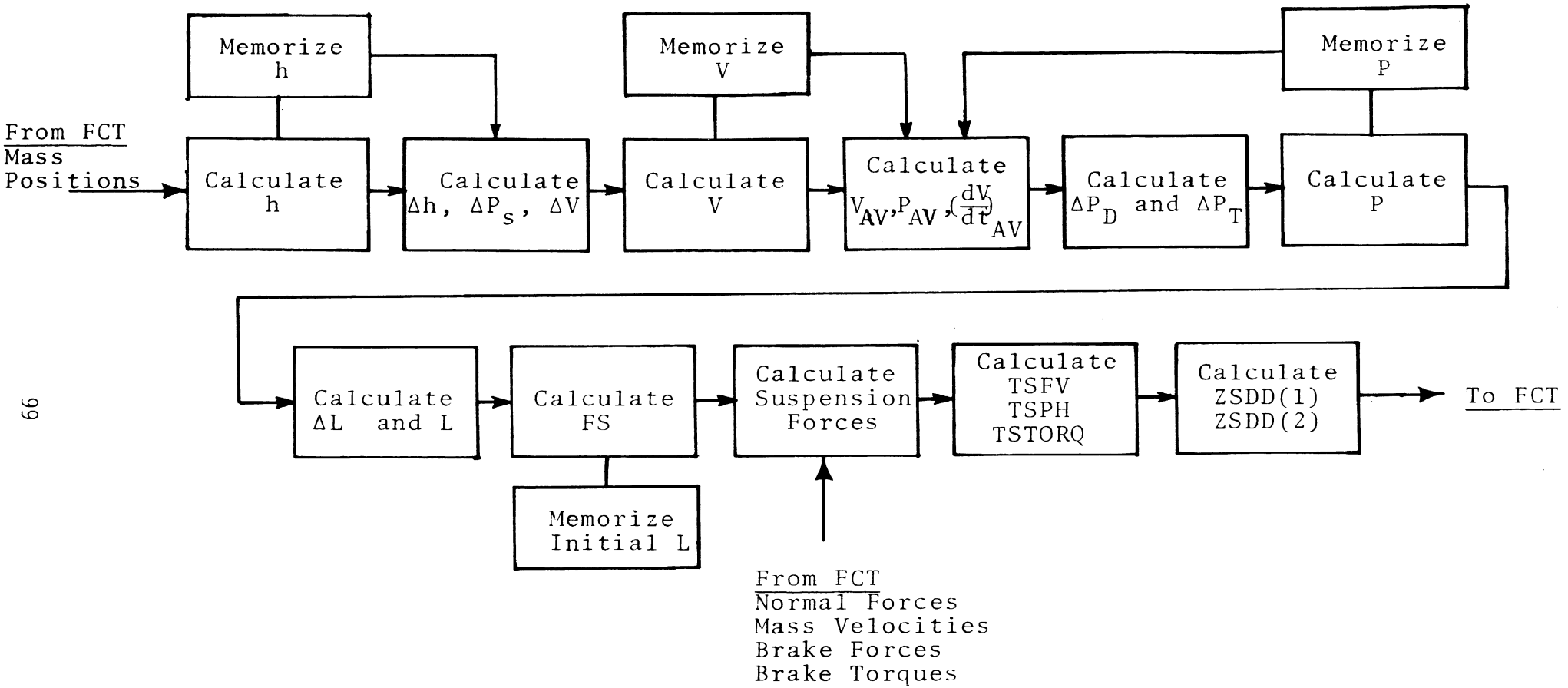

Figure B-35. Air Suspension Model Flow Diagram

To this point, the air system has been considered as two separate systems, the air spring and the air delivery system. Important to the interaction of these systems is the fact that, in general terms, the dynamic response of the air delivery system can be expected to be very much slower than that of the air spring-tire spring-unsprung mass system. (Indeed, it is this difference in response which has allowed the separation of the spring and delivery system.) Since this is the case, it can be expected that over the short time span of a single integration time step, the total change in air pressure in the air spring (ΔP_T) will be dominated by the effect of the air spring as indicated by Equation (B-217). (ΔP as calculated from Equation (B-217) will be designated ΔP_S, i.e., ΔP of the spring model, in this section.) By comparison, ΔP_D, the change in pressure due to the delivery system, will be small for any given time step. The more important effect of ΔP_D will be its accumulative effect over a longer period of time.

Now defining,

P_t: air spring pressure at the beginning of a time step

P_{AV}: average air spring pressure during the time step.

Then assuming the total air spring pressure change may be written

$$\Delta P_T = \Delta P_S + \Delta P_D \tag{B-227}$$

it follows that

$$P_{AV} = P_t + \Delta P_T/2 = P_t + \frac{\Delta P_S + \Delta P_D}{2} \tag{B-228}$$

But from the preceding discussion

$$\Delta P_D << \Delta P_S \tag{B-229}$$

and therefore it may be assumed

$$P_{AV} = P_T + \Delta P_S/2 \tag{B-230}$$

The average pressure, P_{AV}, of Equation (B-23) is then the value to be used in the right-hand side of Equation (B-226) to calculate ΔP_D.

In addition to P_{AV}, the right-hand side of Equation (B-226) also requires values of V_{AV} and $(dV/dt)_{AV}$. These values become available simply by performing the digital integration to determine the new positions of the sprung and unsprung masses (via HPCG) before solving Equation (B-226). With this done, the mass positions, and consequently the spring heights, are known both at the beginning and end of the particular time step. Then, Δh is also known for that time step, and from Equation (B-213) ΔV is known. By definition

$$(dV/dt)_{AV} = \Delta V/\Delta t \tag{B-231}$$

and

$$V_{AV} = V_t + \Delta V/2 \tag{B-232}$$

where V_t is the volume at the beginning of the time step.

At this point, sufficient information is available to calculate the total pressure change, ΔP_T, which, with Δh, is substituted into Equation (B-212) (replace ΔP with ΔP_T) to obtain the change in spring force, ΔL. Note that Equation (B-212) was derived independently of the assumed equation of operation ($P_a V^{1.38}$ = Const.) and is valid regardless of the source of ΔP or Δh.

The final step in the operation of the air system model is an adjustment of the "constant" in the equation.

$$P_a V^{1.38} = \text{constant} \tag{B-233}$$

Combining Equation (B-233) and (B-214) yields

$$P_a V^{1.38} = (P_0 + P_{at}) V_0^{1.38} \tag{B-234}$$

Note that the basic assumptions, given in the opening remarks of Section B.9.3, states that Equation (B-234) holds over a single integration time step. However, due to the action of the air delivery system, P_0 and V_0 must be updated between integration steps. As the solution according to the model progresses through a time step, ΔP_S is first found according to an equation derived from Equation (B-233). Next, this pressure change is altered by the amount, ΔP_D, and, thus, is no longer compatible with Equation (B-233). Consequently, to prepare the model for solution in the next time step the values of P_0 and V_0 must be updated. That is,

$$P_{0_{t+\Delta t}} = P_{0_t} + \Delta P_T \tag{a}$$

$$V_{0_{t+\Delta t}} = V_{0_t} + \Delta V \tag{b}$$

(B-235)

A more graphical representation of this operation appears in Figure B-36. The initial condition of the air spring model is represented by points A and A'. The value Δh is determined by (1) integration of the dynamic variables to obtain ZSP and (2) the geometry of the mechanical linkage. ΔP_S is determined by following the "operating line" ($P_a V^{1.38} = C_1$) to point B

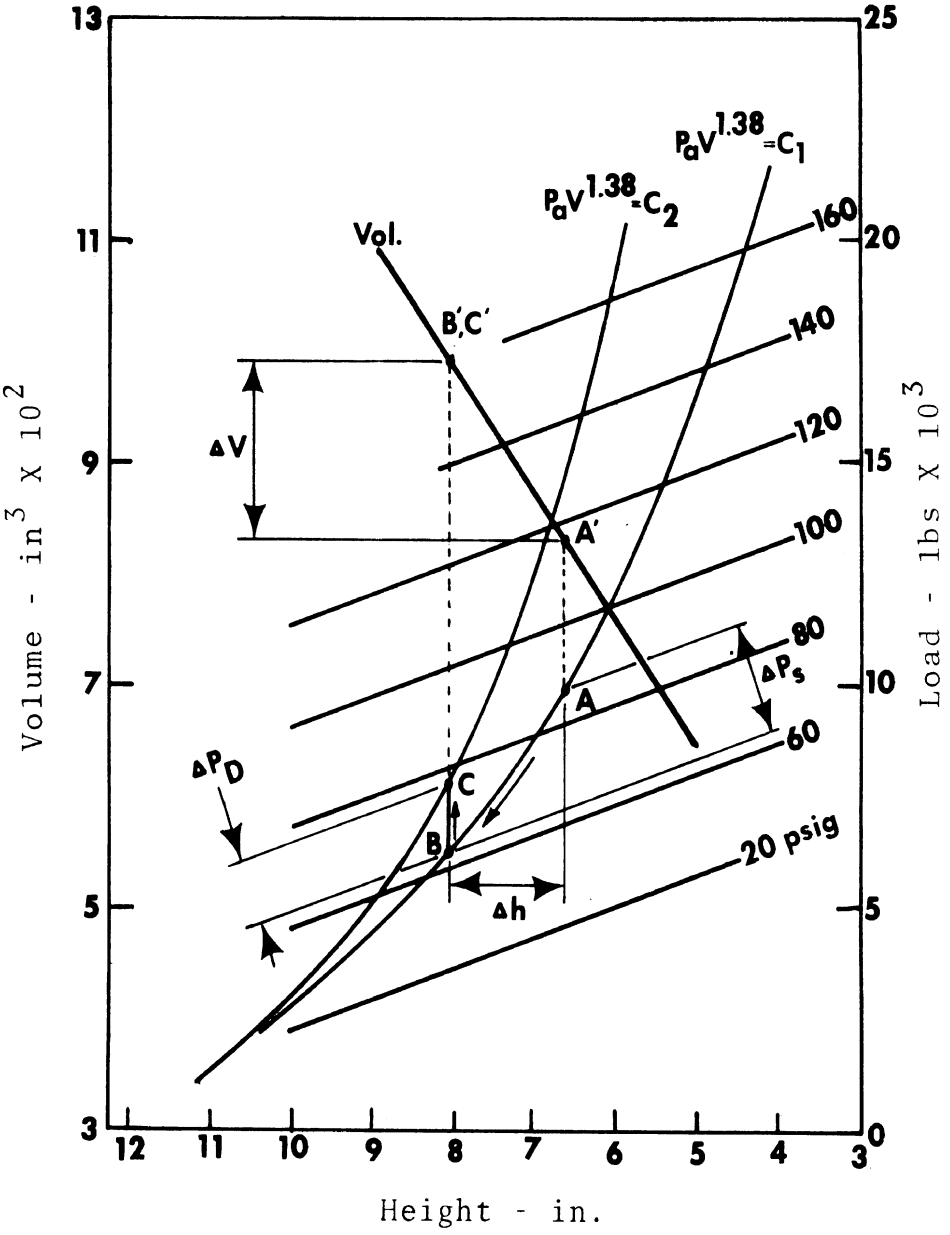

Figure B-36. Air Suspension Operation Over a Single Time Step

while ΔV is determined by following the "Vol." line to B'. ΔP_D is then calculated and the final condition of the air spring is determined by moving from point B to point C, a distance of ΔP_D along a line of constant h. (Constant h because it can change no more than Δh.) The condition of the air spring no longer agrees with the original operating line. Consequently, the values of P_0 and V_0 are updated to pressure and volume of points C and C', respectively (h_0 and L_0 are similarly updated), and a new operating line is established according to

$$P_a V^{1.38} = C_2 \tag{B-236}$$

where

$$C_2 = (P_0 + P_{at}) V_0^{1.38} \tag{B-237}$$

using the updated values of P_0 and V_0.

This completes the operation of the air system model. It remains only to relate the air spring load, L, and height, h, to the mechanical linkage model. Designating h_i and L_i as the initial (static) values of h and L, then from the geometry and notation of Figure B-28

$$h - h_i = \text{AA2/AA3 ZSP} \tag{B-238}$$

and

$$FS = L - L_i \tag{B-239}$$

Equations (B-238) and (B-239) complete the proposed model of the air suspension system. Equation (B-238) is used to compute Δh for input to the air system model. Equation (B-239) is used to compute the dynamic spring force needed by FCT to compute the derivatives for the next integration step.

B.9.6 Static Considerations. The preceding sections have described the various portions of the dynamic air suspension model. It remains to describe the calculations which determine the static normal tire loads, air spring load and air spring pressure.

Using the definitions given in Section B.1 and rigid body analysis, applied to the static free-body diagram of Figure B-37, it can be shown that

$$STORQ = SRATIO \cdot SSFV + SCONST \tag{B-240}$$

$$SSFV = WS1 + WS2 - NS1 - NS2 \tag{B-241}$$

$$STORQ = (WS2-NS2)AA1 \tag{B-242}$$

where WS1 and WS2 are the leading and trailing unsprung weights, respectively, and NS1 and NS2 are the static normal tire loads at the leading and trailing axles, respectively. Combining these three equations leads to:

$$NS1 = WS1 + SSFV \left[\frac{SRATIO}{AA1} - 1\right] + \frac{SCONST}{AA1} \tag{B-243}$$

$$NS2 = WS1 + WS2 - NS1 - SSFV \tag{B-244}$$

The values of SRATIO and SCONST are determined in two different ways, depending on whether the tandem axles are independent or dependent. If an air line interconnection exists between the air springs of the two axles (i.e., the input parameter CINTR is non-zero), the axles are "dependent" by virtue of the fact that the static air spring pressure at the two axles is identical. In this case, it can be shown that

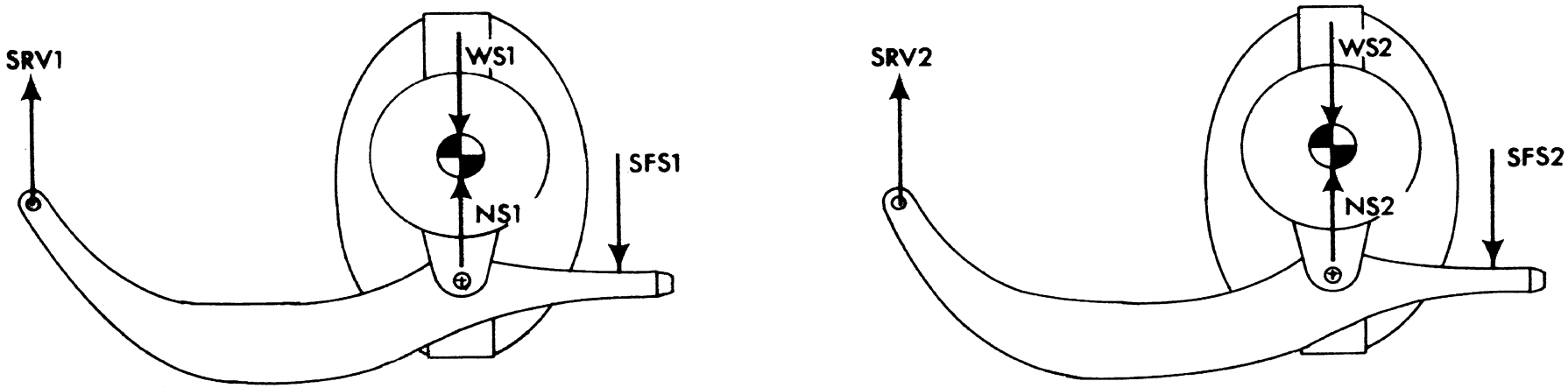

Figure B-37. Static Free-Body Diagram: The Air Suspension.

$$SRATIO = A_{L1} \cdot AA2(1)/AA3(1) + A_{L2} \cdot AA2(2)/AA3(2) \qquad (B\text{-}245)$$

and

$$SCONST = (L_{01} \cdot AA2(1)/AA3(1) + L_{02} \cdot AA2(2)/AA3(2) \cdot SRATIO - L_{02} \cdot AA1 \cdot AA2(2)/AA3(2) \qquad (B\text{-}246)$$

If the tandem axles are independent (CINTR = 0), then the static condition of the axles is indeterminate. In this case, the user must input the parameter, PRCTN1, which is the percentage of total tire normal load carried at the leading axle. In this case, it can be shown that

$$SRATIO = AA1(100-PRCTN1)/100 \qquad (B\text{-}247)$$

$$SCONST = -SRATIO \cdot WS2 - \frac{PRCTN1}{100-PRCTN1}(WS1+WS2) \qquad (B\text{-}248)$$

For either leading or trailing axles, the static air spring load (SFS) and pressure (SP) can be shown to be

$$SFS = (NS - WS)\frac{AA3}{AA2} \qquad (B\text{-}249)$$

$$SP = \frac{SL - L_0}{A_L} + P_0 \qquad (B\text{-}250)$$

where the "1" and "2" designations have been dropped since these equations are applicable to either axle.

APPENDIX C

THE SPRUNG MASSES

C.1 Introduction

This appendix reviews the mathematical models which are employed to simulate the motions of the vehicle's sprung masses. Models for the straight truck, tractor-semitrailer, and doubles combination vehicles will be considered.

Although a large variety of suspension options are available for use (at all suspension positions excluding the front), the sprung mass calculations are not altered by the use of different suspensions. As explained earlier, in Section 2 and Appendix B, each suspension model combines the various individual suspension forces into a common set of generalized suspension reactions composed of one vertical, one horizontal, and one moment reaction between suspension and sprung mass. Thus, a single set of sprung mass equations may be used regardless of the suspension types being simulated.

In the following two sections of this appendix, static and dynamic models will be discussed, respectively.

C.2 Static Considerations

The calculation of frequently used constants, including static loading and the effect of added payloads, must be accomplished before the actual simulation process begins. The calculation of static tire loads is accomplished in the suspension subprograms. These calculations have been covered in Appendix B. To determine the tire loads, the suspension subprograms must have available the static reactions present between the various suspensions and sprung masses (a generalized vertical force and generalized moment* about the suspension reference

*Generalized suspension reactions, both static and dynamic, have been defined in Section B.1 of Appendix B.

point* for each suspension). This section will develop the equations by which these static reactions are determined.

As discussed in Section 2, the user may enter parameters describing the sprung mass of the vehicle chassis and the payload separately, thus facilitating convenient changes in payload bewteen simulation runs. To enhance the utility of the program, static calculations are actually performed twice, once for the "empty" vehicle assuming the payload weight is zero, and once for the "loaded" vehicle, combining the effects of both chassis and payload. Thus, the mathematics used to combine the effects of these two masses will be covered first, followed by the static loading calculations which may be applied to either of the two static load calculations.

To illustrate the mechanism for combining the effects of chassis and payload masses, an empty straight truck configuration is used as an example; the mathematics for the articulated vehicle are analogous. Additionally, for the doubles combination vehicles, the mass of the dolly is treated as a second "payload" on the second trailer. (This mass is assumed to be located at the kingpin and to have zero pitch moment of inertia.) The empty truck and the payload to be added are shown in Figure C-1. The empty truck has sprung weight, W1, positioned at a point A1 inches behind the front axle as shown, and pitch moment of inertia, J1, about that point. The payload has weight, PW, and moment of inertia, PJ, about its center of gravity. If the combined weight and c.g. locations are designated with barred variables:

$$\bar{W}1 = W1 + PW \qquad (C\text{-}1)$$

The summation of moments yields

---

*The suspension reference point for each suspension type has been defined in Section 2.

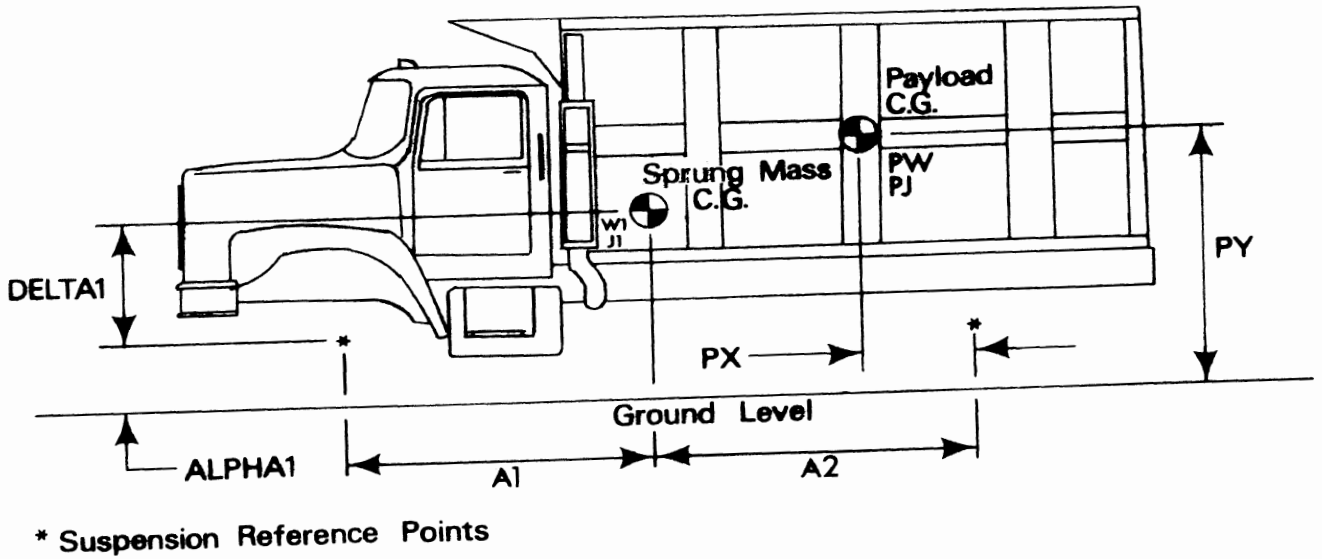

Figure C-1. Position of sprung mass and payload C.G.'s.

$$\overline{A2} = \frac{(PW)(PX) + W1(A2)}{\overline{W1}} \qquad (C\text{-}2)$$

$$\overline{DELTA1} = \frac{W1(DELTA1 + ALPHA1) + PW(PZ)}{\overline{W1}} \qquad (C\text{-}3)$$

The new configuration is shown in Figure C-2.

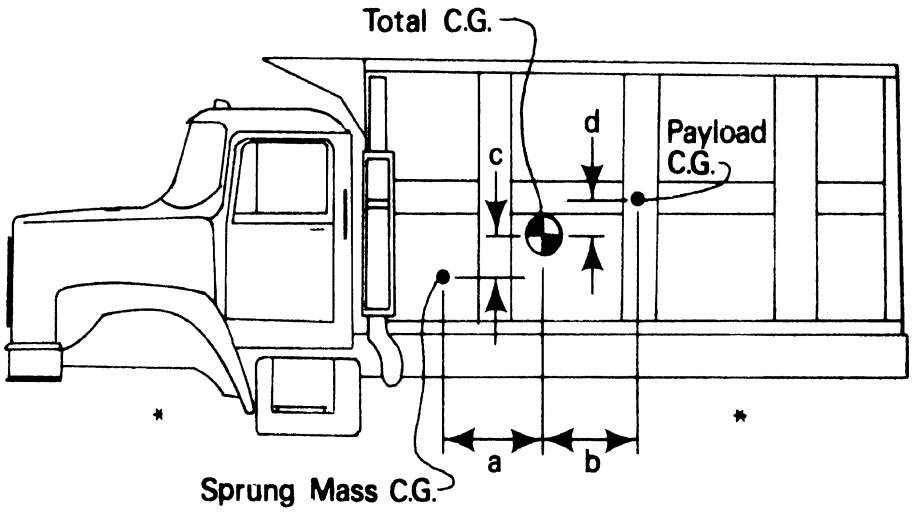

Figure C-2. Total sprung mass c.g.

The distances a, b, c, and d are found using the empty vehicle information and Equations (C-2) and (C-3).

$$a = \overline{A1} - A1 \tag{C-4a}$$

$$b = \overline{A2} - PX \tag{C-4b}$$

$$c = \overline{DELTA1} - DELTA1 \tag{C-4c}$$

$$d = PZ - ALPHA1 - \overline{DELTA1} \tag{C-4d}$$

The parallel axis theorem is applied to find the pitch moment of inertia of the combination of the empty truck plus the payload:

$$\overline{J1} = J1 + \frac{W1}{g}(a^2 + c^2) + PJ + \frac{WP}{g}(b^2 + d^2) \tag{C-5}$$

For the remainder of this appendix, the moment of inertia and mass center location parameters will appear without bars, with the understanding that the calculations given in Equations (C-1) through (C-5) have been completed if appropriate.

We may now determine the static suspension reactions for each of the three vehicle types. Consider first the straight truck sprung mass as shown in the static free-body diagram of Figure C-3. The forces and moments acting on the sprung mass are the sprung weight (W1), the generalized rear suspension vertical force (SSFV) and moment (STORQ) and the front suspension vertical force (SF1). (The front suspension, being a single-axle suspension, applies no static moment to the sprung mass.) By the definition of SRATIO and SCONST given in Section B.1 of Appendix B,

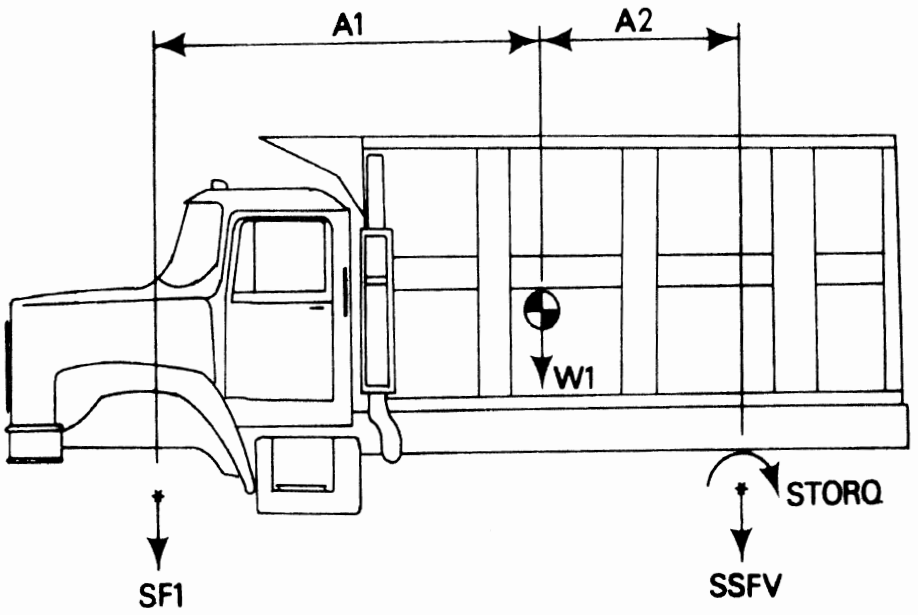

* Suspension Reference Points

Figure C-3. Static free-body diagram: Straight truck.

$$STORQ = SRATIO \cdot SSFV + SCONST \qquad (C\text{-}6)$$

where SRATIO and SCONST are properties of a given suspension and are calculated by the suspension programs as outlined in Appendix B. Summing moments about the front suspension reference point of Figure C-3 yields:

$$A1 \cdot W1 + (A1+A2)SSFV + STORQ = 0 \qquad (C\text{-}7)$$

Combining Equations (C-6) and (C-7) and solving for SSFV yields:

$$SSFV = \frac{A1 \cdot W1 - SCONST}{A1+A2+SRATIO} \qquad (C\text{-}8)$$

And from the summation of vertical forces

$$SF1 = -W1 - SSFV \qquad (C\text{-}9)$$

Equations (C-6), (C-8), and (C-9) provide solutions for the static suspension forces and moments.

The static analysis for the tractor-trailer is similar to that for the straight truck. Refer to the static free-body diagram of Figure C-4, in which subscripts (1) and (2) have been added to the SSFV and STORQ notations to designate the rear tractor and trailer suspensions, respectively. Summing moments on the trailer about the kingpin and combining the result with Equation (C-6) (with subscripts added) yields:

$$SSFV(2) = \frac{A3 \cdot W2 + SCONST(2)}{A3 + A4 + SRATIO} \qquad (C\text{-}10)$$

Summing vertical forces on the trailer and solving for the kingpin force results in

$$VS = W2 + SSFV(2) \qquad (C\text{-}11)$$

Then, summing moments on the tractor about the front suspension reference point and combining the result with Equation (C-6) (subscripts added) yields:

$$SSFV(1) = -\frac{W1 \cdot A1 + VS(A1+A2-BB) + SCONST(1)}{A1 + A2 + SRATIO(1)} \qquad (C\text{-}12)$$

Finally, from summing vertical forces on the tractor

$$SF1 = W1 + SSFV(1) + VS \qquad (C\text{-}13)$$

Equations (C-10) through (C-13) plus (C-6), with appropriate subscripts added, provide solutions for all the static suspension reactions of the tractor-trailer.

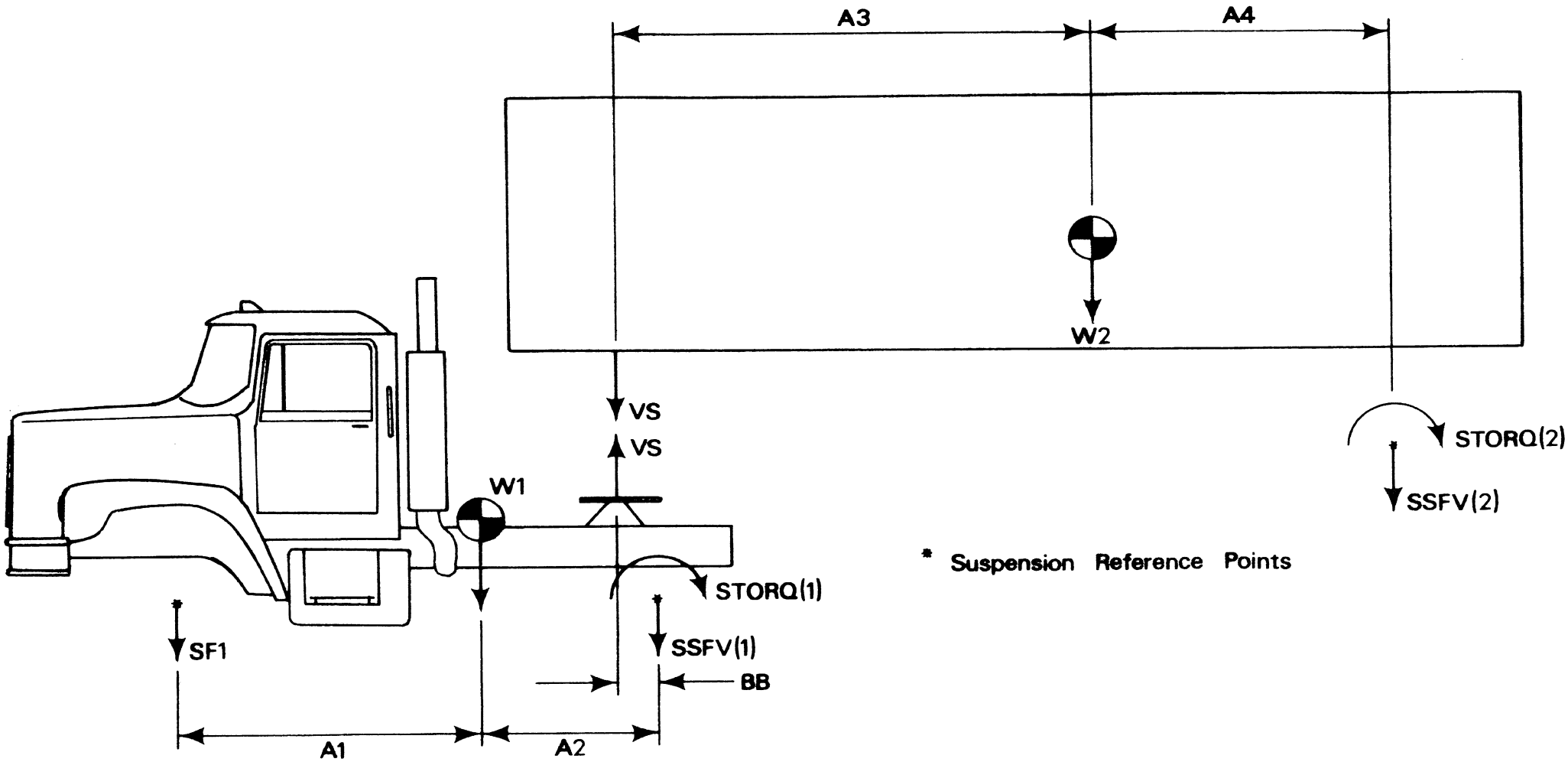

Figure C-4. Static free-body diagram: Tractor-trailer.

The static equations for the doubles combination result from an analysis analogous to that of the tractor-trailer. As for the tractor-trailer, the analysis starts with the rear-most unit and proceeds forward through each sprung mass element. Using the notation of Figure C-5, the following equations are obtained:

$$SSFV(4) = - \frac{A6 \cdot W3 + SCONST(4)}{A6+A7+SRATIO(4)} \qquad (C\text{-}14a)$$

$$VS3 = W3 + SSFV(4) \qquad (C\text{-}14b)$$

$$SSFV(3) = - \frac{A8 \cdot VS3 + SCONST(3)}{A8+BB2+SRATIO(3)} \qquad (C\text{-}14c)$$

$$VS2 = VS3 + SSFV(3) \qquad (C\text{-}14d)$$

$$SSFV(2) = - \frac{A3 \cdot W2+A5 \cdot VS2 + SCONST(2)}{A3+A4+SRATIO(2)} \qquad (C\text{-}14e)$$

$$VS1 = W2 + SSFV(2) + VS2 \qquad (C\text{-}14f)$$

$$SSFV(1) = - \frac{A1 \cdot W1+(A1+A2-BB1) \cdot VS1 + SCONST(1)}{A1+A2+SRATIO(1)} \qquad (C\text{-}14g)$$

$$SF1 = W1 + SSFV(1) + VS1 \qquad (C\text{-}14h)$$

In Equation (C-14), the subscripts (1) through (4) refer to the tractor rear suspension through the rear trailer suspension (moving rearward along the vehicle), respectively. With the same subscripts added to Equation (C-6), these two equations provide solutions for all the static suspension reactions for a doubles combination vehicle.

It is interesting to note that the static dolly fifth wheel force (VS3) requires correction if it is to correspond to the actual compressive force on the face of the fifth wheel of the real vehicle. Because the dolly mass is treated as a "payload" for the second trailer (see Section C.1), VS3 is in "error" by

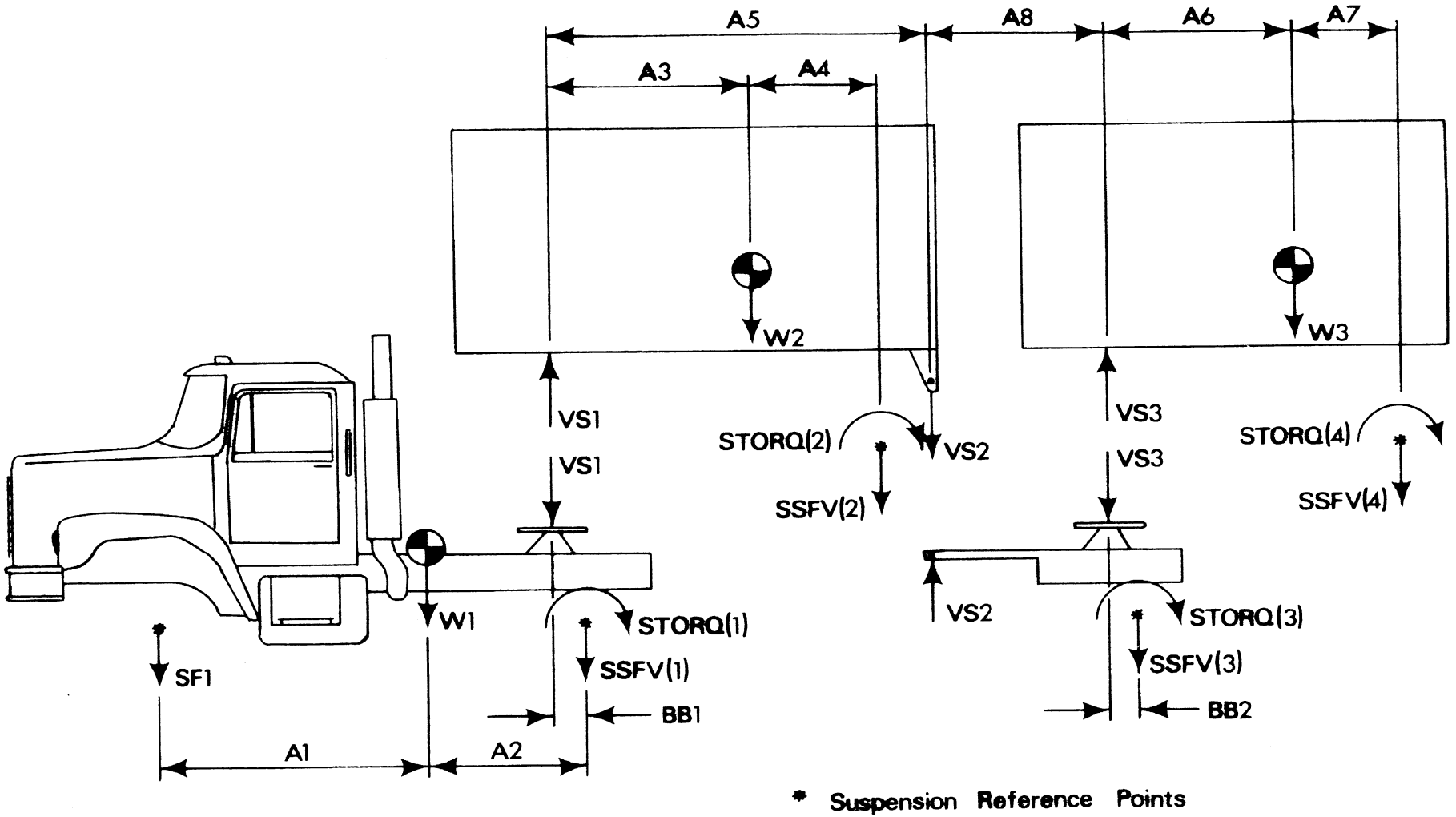

Figure C-5. Static free-body diagram: doubles combination.

the quantity W4 (dolly sprung weight). Defining the "real" dolly fifth wheel force as $\overline{VS3}$, it can be shown that:

$$\overline{VS3} = VS3 - W4 \qquad \text{(C-15)}$$

C.3 The Dynamic Sprung Mass Models

In this section, all the dynamic equations of the doubles combination vehicle simulation will be outlined. This vehicle type has been chosen because it is, of course, the most complex of the three vehicle types which can be simulated with the Phase III programs. The dynamic equations for the tractor-trailer and straight truck may be derived from the doubles equations simply by dropping those equations and terms which are not applicable, or are not defined, for these simpler vehicles.

All the dynamic equations of the doubles combination vehicle, except that for longitudinal deceleration, are derived by applying Newton's second law to the free-body diagram of Figure C-6 and using the dimensional notation of Figure C-7. The longitudinal deceleration equation is obtained by applying Newton's second law to the entire vehicle, assuming that all masses of the vehicle are constrained to have the same longitudinal deceleration. The equations which are derived are:

Deceleration:

$$\frac{GVW}{32.2}\ XDD = \sum_{I=1}^{KAXLE} FX(I) \qquad \text{(C-16)}$$

where GVW is the total weight of the vehicle, FX(I) is the total brake force at axle I, KAXLE is the total number of axles on the vehicle, and XDD is the longitudinal acceleration of the vehicle.

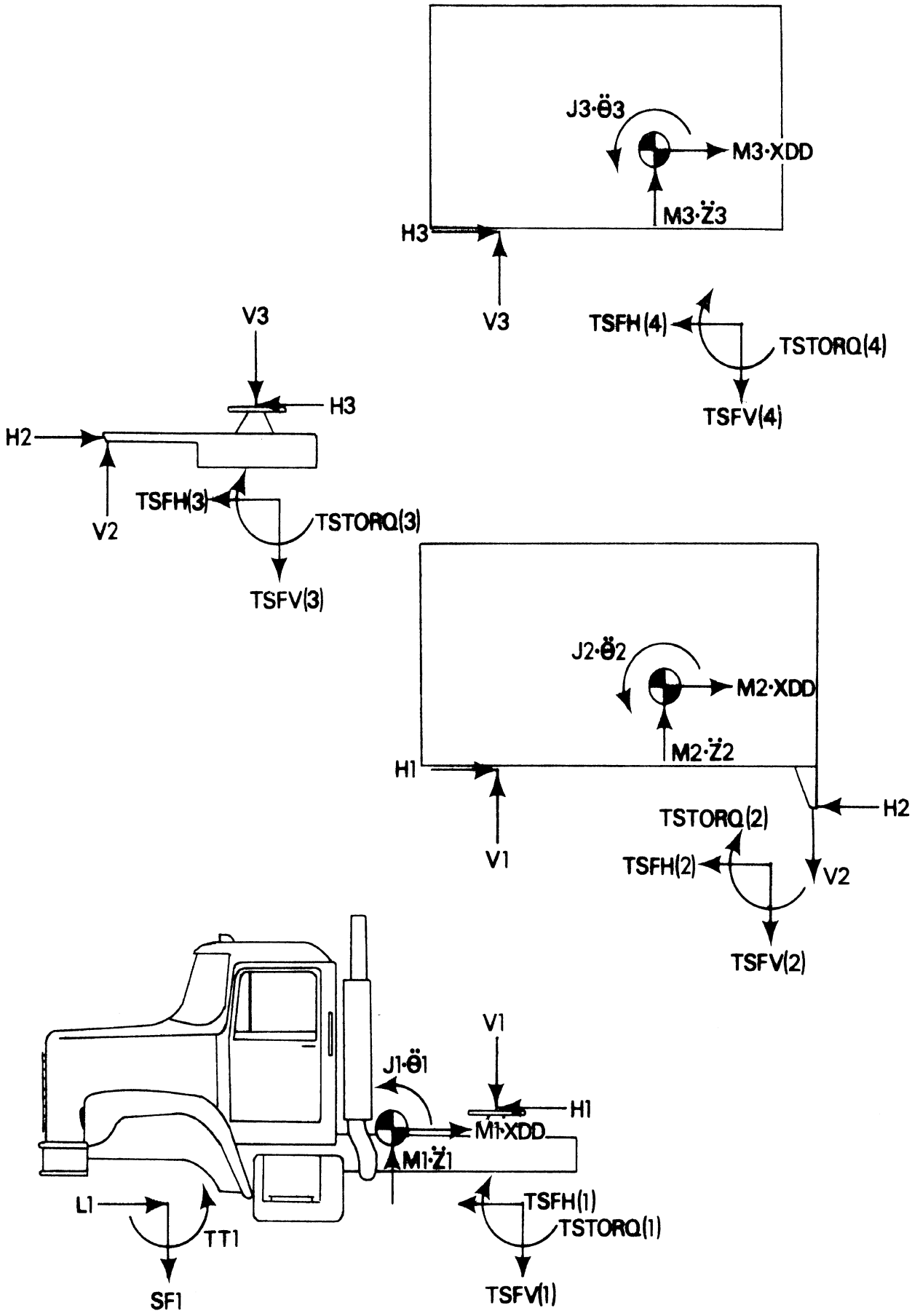

Figure C-6. Dynamic free-body diagram: doubles combination

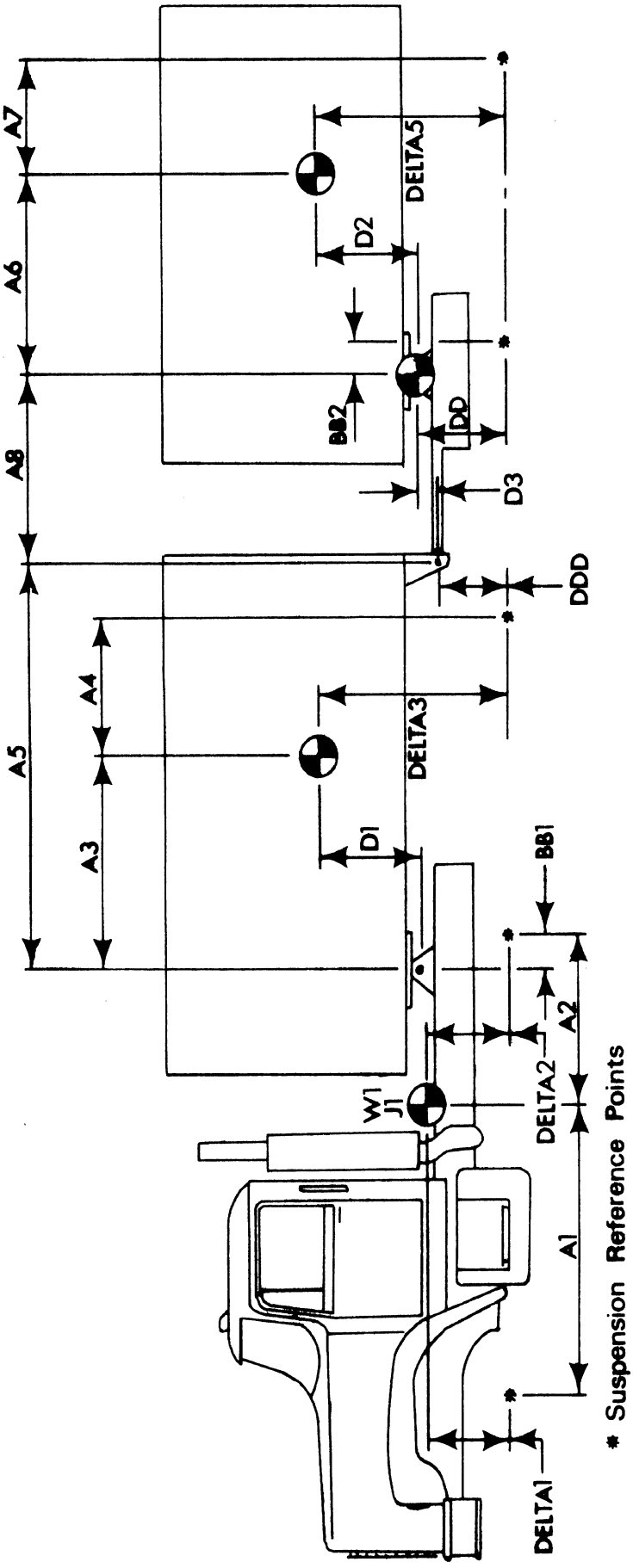

Figure C-7. The doubles combination vehicle.

Dolly Fifth Wheel Forces:

$$H3 = TSFH(4) - M3 \cdot XDD \qquad (C\text{-}17)$$

$$V3 = [H3 \cdot D3 - TSTORQ(3) - TSFV(3) \cdot (A8+BB2) - TSFH(3) \cdot (DD-D3)]/A8 \qquad (C\text{-}18)$$

Dolly Hitch Forces:

$$H2 = H3 + TSFH(3) \qquad (C\text{-}19)$$

$$V2 = V3 + TSFV(3) \qquad (C\text{-}20)$$

Tractor Fifth Wheel Forces:

$$V1 = KF \cdot [-Z1 - \theta 1 \cdot (A2-BB1) + Z2 - \theta 2 \cdot A3] \qquad (C\text{-}21)$$

where KF is the rate of the tractor fifth wheel, vertical spring. See Reference [1] for a discussion of KF.

Second Trailer Motions:

Bounce:

$$M3 \cdot \ddot{Z} = TSFV(4) - V3 \qquad (C\text{-}22)$$

Pitch:

$$I3 \cdot \ddot{\theta}3 = V3 \cdot A6 - H3 \cdot D2 + TSFV(4) \cdot A7 + TSFH(4) \cdot DELTA5 \qquad (C\text{-}23)$$

First Trailer Motions:

Bounce:

$$M2 \cdot \ddot{Z}2 = V2 - V1 + TSFV(2) \qquad \text{(C-24)}$$

Pitch:

$$I2 \cdot \ddot{\theta}2 = V1 \cdot A3 - H1 \cdot D1 + V2 \cdot (A5-A3) + H2 \cdot (DELTA3-DDD) + TSFV(3) \cdot A4 + TSFH(2) \cdot DELTA3 + TSTORQ(2) \qquad \text{(C-25)}$$

Tractor Motions:

Bounce:

$$M1 \cdot \ddot{Z}1 = SF1 + TSFV(1) + V1 \qquad \text{(C-26)}$$

Pitch:

$$J1 \cdot \ddot{\theta}1 = -L1 \cdot DELTA1 - SF1 \cdot A1 - TT1 + TSFH(1) \cdot DELTA2 + TSFV(1) \cdot A2 + TSTORQ(1) + (A2-BB1) \cdot V1 - H1 \cdot D1 \qquad \text{(C-27)}$$

Similar to the case in the static calculations, the dynamic dolly fifth wheel forces which are calculated in Equations (C-19) and (C-20) vary from the dynamic fifth wheel forces of the real vehicle due to the combining of dolly and second trailer inertial properties. We can determine the "real" values of the dolly fifth wheel forces, which we denote as barred quantities, from the free-body of the dolly in which the dolly maintains its mass (see Figure C-8).

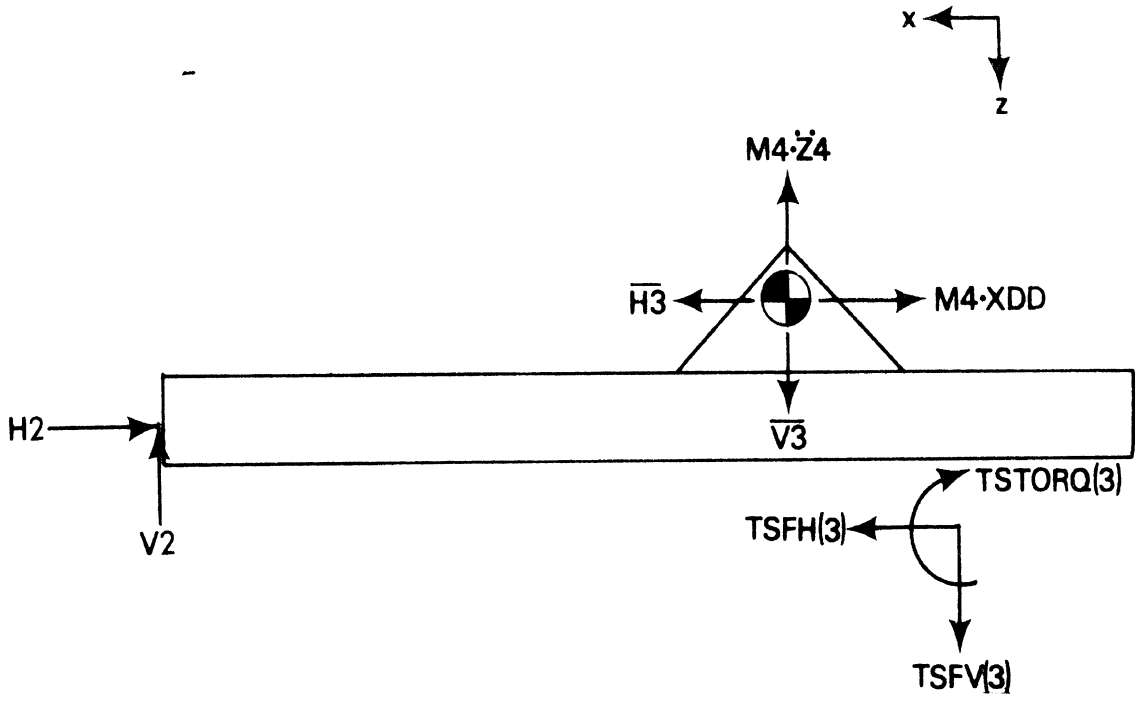

Figure C-8. Dynamic free-body diagram: The dolly with sprung mass.

Applying Newton's second law in the x and z direction, respectively, yields

$$\overline{H3} = M4 \cdot XDD + H2 - TSFH(3) \qquad (C\text{-}28)$$

$$\overline{V3} = M4 \cdot \ddot{Z}4 + V2 - TSFV(3) \qquad (C\text{-}29)$$

Substituting Equation (C-19) into (C-28) and (C-20) into (C-29)

$$\overline{H3} = H3 + M4 \cdot XDD \qquad (C\text{-}30)$$

$$\overline{V3} = V3 + M4 \cdot \ddot{Z}4 \qquad (C\text{-}31)$$

Since M4 is located at the connection between the dolly and second trailer, the vertical acceleration of M4 can be expressed

as a function of Z3 and $\theta 3$ and their derivatives. It can be shown that for small values of $\theta 3$,

$$\ddot{Z}4 = \ddot{Z}3 - (D2 \cdot \theta 3 + A6)\ddot{\theta}3 - D2 \cdot \theta 3^2 \qquad \text{(C-32)}$$

Note that it was assumed implicitly in Equation (C-30) that

$$\ddot{X}4 = XDD \qquad \text{(C-33)}$$

This derives from the assumption stated above that all masses are constrained to have the same longitudinal deceleration.

APPENDIX D

THE BRAKE MODELS

D.1 Introduction

Calculation of brake torque using the brake modules rather than tables of torque versus line pressure can be selected by specifying for NUM(2), the number of points in the torque-line pressure table for the first axle. Subroutine BRAKE will then be called to read in the appropriate parameters for the brakes on each axle. The various brake types the user can specify are: no brakes, S-cam, single or dual wedge, duo-servo, duplex, and disc.

D.2 Brake Torque Calculation

The brake torque produced at the I^{th} axle is calculated by means of the following equation [1]:

$$T(I) = PB(I) \cdot Q(I) \cdot BF(I) \qquad (D\text{-}1)$$

where

- T(I) is the attempted brake torque on the I^{th} axle
- PB(I) is the effective line pressure at the brake minus the pushout pressure
- Q(I) is the brake system constant
- BF(I) is the brake factor, defined as the ratio of drum drag to the actuating force of the brake shoes [2].

For hydraulic brake systems,

$$Q(I) = 2A_{wc}\,\eta_c r \qquad \text{(D-2)}$$

where

A_{wc} = area of wheel cylinder

η_c = mechanical efficiency of the brake

r = drum radius

For air brakes,

$$Q(I) = 2A_c\,\eta_m\, r\,\rho \qquad \text{(D-3)}$$

where

A_c = brake chamber area

η_m = mechanical efficiency between brake chamber and shoe actuation

ρ = lever ratio between brake chamber and brake shoe.

For S-cam brakes, the lever ratio is given by

$$\rho = \frac{\ell_s}{2\ell_c} \qquad \text{(D-4)}$$

where

ℓ_s = effective slack adjuster length

ℓ_c = effective cam radius.

For wedge brakes, the lever ratio is related to the wedge angle, α:

$$\rho = \frac{1}{2\,\tan(\alpha/2)} \qquad \text{(D-5)}$$

If the brakes are in good mechanical condition, the mechanical efficiencies exhibited by S-cam and wedge brakes range from 0.70 to 0.75 and 0.80 to 0.88, respectively [3].

The value of the brake factor for the various types of drum and disc brakes required in Equation (D-1) is calculated by means of analytical expressions in which brake factor is given as a function of brake type, brake geometry, and the coefficient of friction between the lining and the drum or disc. Brake factor-lining friction coefficient relationships for three commonly used brake types are given in Figure D-1 [1].

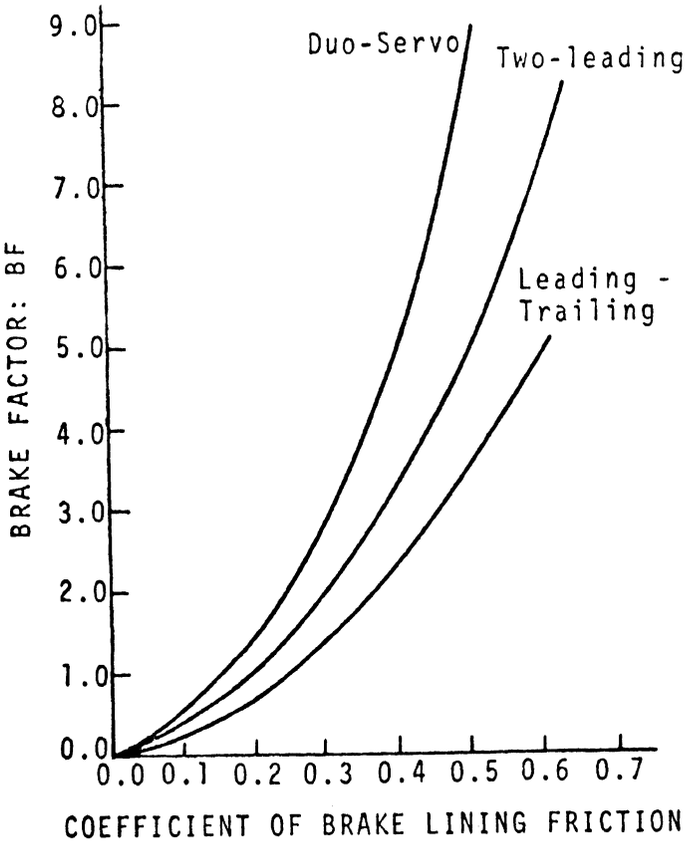

Figure D-1. Typical brake factor-lining friction curves for typical drum brakes.

D.3 Brake Factor Calculations

This section contains a description of the brake factor calculations for the several types of brakes used in the program [4,5]. Except for disc brakes and duo-servo self-actuating brakes, the calculations are made for each shoe, and the total brake factor is the sum of the brake factors calculated for each shoe. The three types of brake shoes available in the program are: a pinned leading shoe, a pinned trailing shoe, or a leading shoe supported by an abutment. The following three equations are used for calculation of brake factors for these individual shoes:

Pinned Leading Shoe (see Figure D-2)

$$BF = \frac{\mu D}{E - \mu G} \tag{D-6}$$

where

$D = HB/RD$

$ALPH3 = ALPHO + 2.0 \cdot ALPH1$

$$E = \frac{APRIM}{RD}\left[\frac{ALPHO - SIN(ALPHO) \cdot COS(APLH3)}{4.0 \cdot SIN(ALPHO/2) \cdot SIN(ALPH3/2)}\right]$$

$$G = 1 + \frac{APRIM}{RD} \cdot COS(ALPHO/2) \cdot COS(ALPH3/2)$$

μ = coefficient of friction of the linings

and all other angles and dimensions are as shown in Figure D-2.

Pinned Trailing Shoe (see Figure D-2)

The expression for the brake factor for the pinned trailing shoe is the same as Equation (D-6) except for a sign change in the denominator:

$$BF = \frac{\mu D}{E + \mu G} \tag{D-7}$$

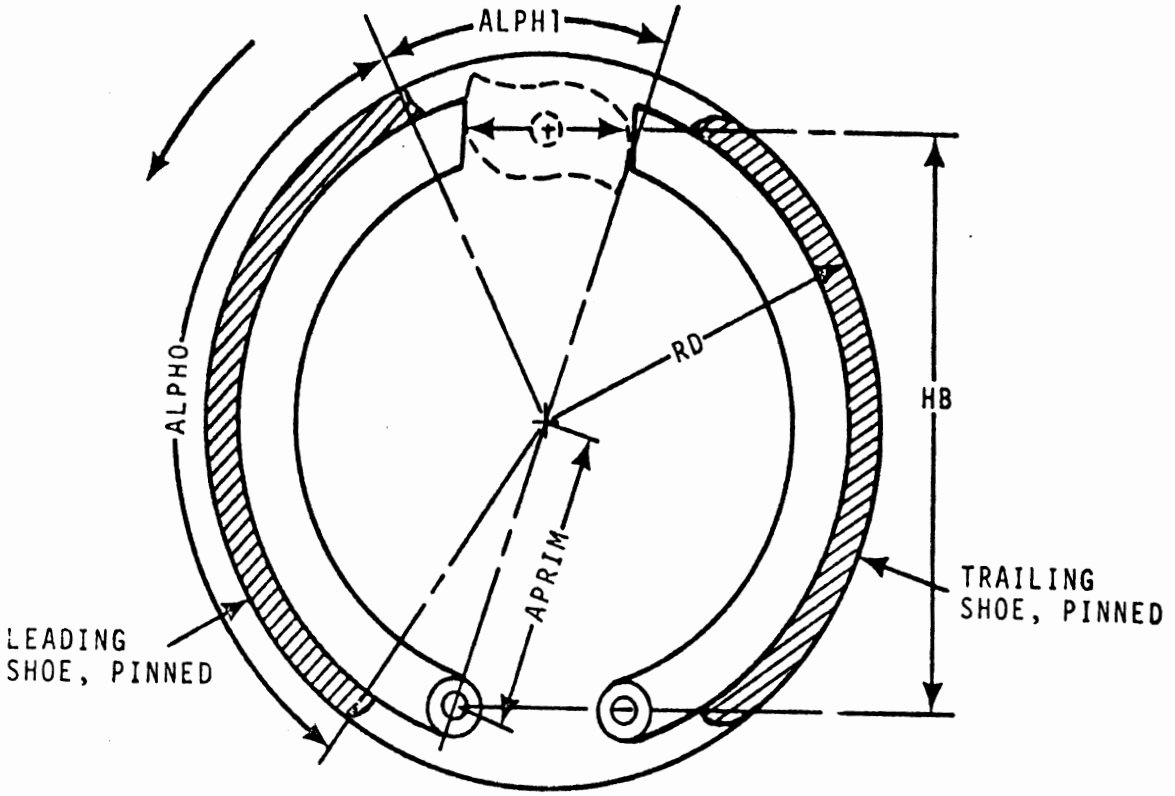

Figure D-2. Leading shoe-trailing shoe brake.

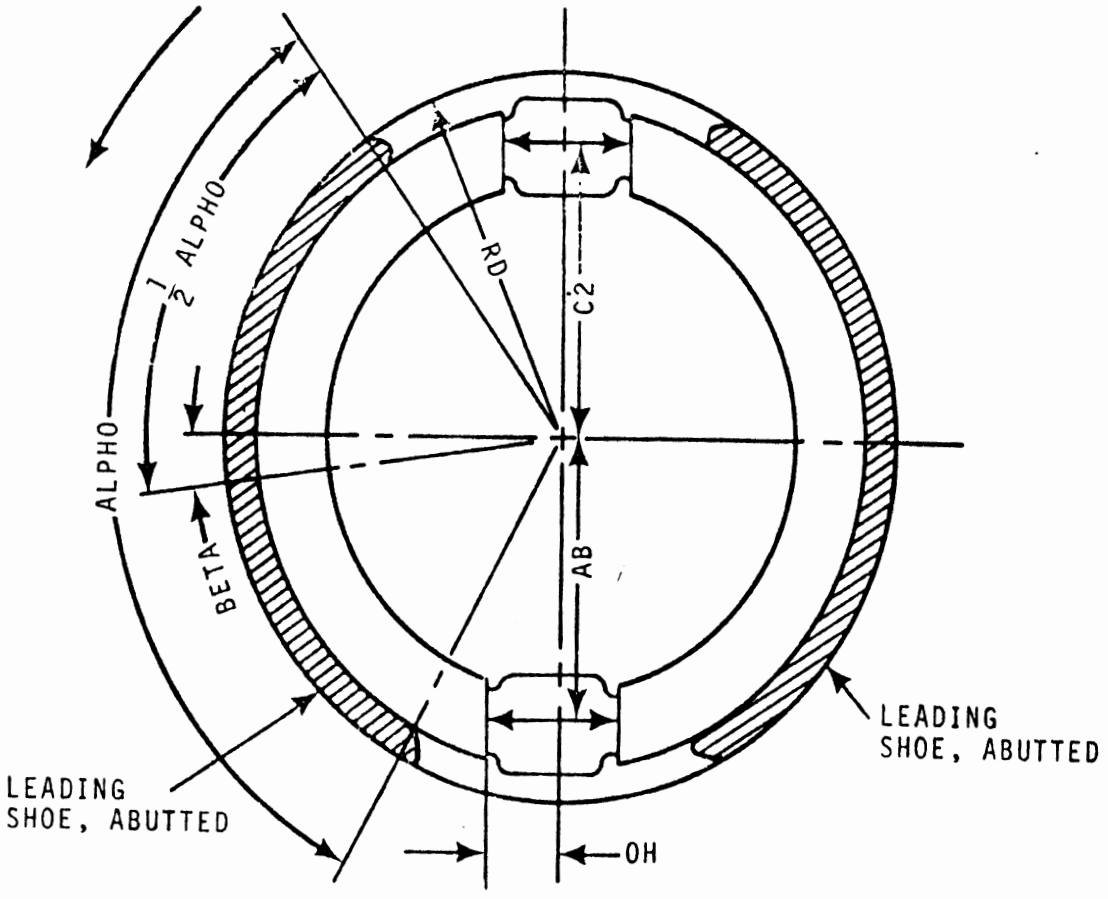

Figure D-3. Two leading shoe brake.

Leading Shoe Supported by an Abutment

$$BF = \frac{\mu D + \mu^2 E}{F2 - \mu G + \mu^2 H2} \qquad (D\text{-}8)$$

where in this case:

$$D = \left[\frac{C2}{RD} + \frac{AB}{RD} + 0.25\,\frac{OH}{RD}\right] \cdot COS(BETA) + 0.25 \cdot \frac{C2}{RD} \cdot SIN(BETA)$$

$$E = 0.25 \cdot \frac{C2}{RD} \cdot COS(BETA) - \left[\frac{C2}{RD} + \frac{AB}{RD} + 0.25 \cdot \frac{OH}{RD}\right] \cdot SIN(BETA)$$

$$M = \frac{ALPHO + SIN(ALPHO)}{4.0 \cdot SIN(ALPHO/2)}$$

$$F2 = MM\left[\frac{AB}{RD} + 0.25\,\frac{OH}{RD}\right]$$

$$G = COS(BETA) + 0.25 \cdot SIN(BETA)$$

$$H2 = MM\left[\frac{AB}{RD} + 0.25\,\frac{OH}{RD}\right] - (0.25\ COS(BETA) - SIN(BETA))$$

Angles and dimensions are as shown in Figure D-3.

The equations used in the program to calculate the brake factors are (with the exception of disc brakes) combinations of the above three equations.

For S-cam brakes, the program sums the brake factors calculated for the leading and trailing shoes using:

$$BF = \frac{\mu D}{E - \mu G} + \frac{\mu D}{E + \mu G} \qquad (D\text{-}9)$$

where the first term is from Equation (D-6) (a pinned, leading shoe) and the second term is from Equation (D-7) (a pinned, trailing shoe).

For each of the shoes of a 2-wedge brake, the program calculates the brake factor using Equation (D-8). The brake is

assumed to consist of two identical leading shoes whose ends are supported by abutments. Thus the total brake factor is:

$$BF = 2\left[\frac{\mu D + \mu^2 E}{F2 - \mu G + \mu^2 H2}\right] \qquad \text{(D-10)}$$

For a single wedge brake, the brake factor is calculated as if the leading and trailing shoes are pinned as in Equation (D-9).

For the duo-servo self-actuating brake, the program calculates the brake factor for each shoe separately and then combines them to solve for the total brake factor. The primary shoe is considered equivalent to the leading shoe supported by an abutment, whose brake factor can be calculated using Equation (D-8).

$$BF1 = \frac{\mu D + \mu^2 E}{F2 - \mu G + \mu^2 H2} \qquad \text{(D-11)}$$

The brake factor for the secondary shoe is calculated in two steps. First, the secondary shoe is assumed to be a pinned leading shoe and BF2 is calculated using Equation (D-6):

$$BF2 = \frac{\mu D2}{E2 - \mu G2} \qquad \text{(D-12)}$$

Since the brake factor is the drum drag divided by the actuating force on the shoe from the wheel cylinder, the brake factor, BF2 (for the secondary shoe), must be corrected due to the fact that, not only is there the actuating force from the wheel cylinder, but there is also the (tangential) force generated by the friction between the primary shoe and the drum, which adds to the force actuating the secondary shoe. In order to give the brake factor in terms of the actuating force from the wheel cylinder, BF2 must be multiplied by

$$\frac{\text{Actual actuating force on secondary shoe}}{\text{Force from wheel cylinder}} = \frac{C2}{AB} + \frac{BF1 \cdot RD}{AB} \qquad (D\text{-}13)$$

The brake factor for the whole brake is given as:

$$BF = BF1 + BF2 \ \frac{C2}{AB} + \frac{BF1 \cdot RD}{AB} \qquad (D\text{-}14)$$

For a 2-leading shoe brake, the shoes are assumed to be supported by abutments rather than pins and the brake factor is calculated the same as for a 2-wedge brake using Equation (D-10).

The brake factor for a disc brake is:

$$BF = 2 \ \frac{F_{tangential}}{F_{wheel\ cylinder}} \qquad (D\text{-}15a)$$

or

$$BF = 2 \ \frac{\mu F_{wheel\ cylinder}}{F_{wheel\ cylinder}} \qquad (D\text{-}15b)$$

which reduces to

$$BF = 2\mu \qquad (D\text{-}15c)$$

D.4 User Input for Brake Modules

The sequence of data input for using the brake modules is shown in Figure D-4. The parameter NUM(2) is read by subroutine INPUT. If NUM(2) has a value of -1, subroutine BRAKE is called to read the input data for the brake modules.

The parameters describing the brakes are read axle by axle. The brake type for axle I, IBRT(I), is read first. If this is zero, signifying no brake, the program moves on to the next axle without attempting to read any data. If there is a brake on

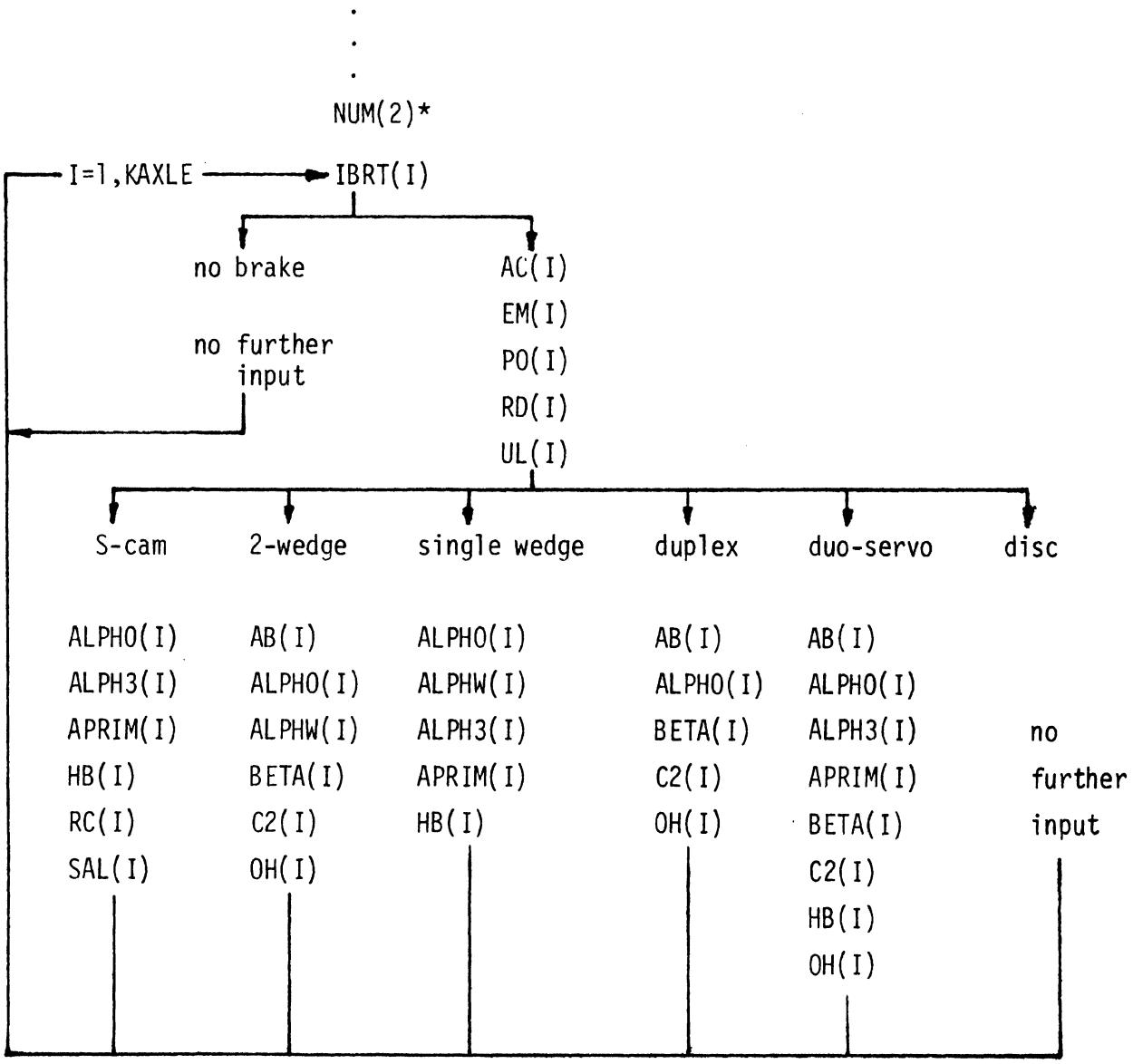

*All input formats are F11.4 except NUM(2) which is I2 and IBRT(I) which is I1.

Figure D-4. Input data list for brake modules.

axle I, the five parameters common to all the brake types are first read. Then the program branches to read parameters detailing the specific brake type. After all the parameters for an axle have been read, the parameters for the next axle are read. When all axles have been dealt with, subroutine BRAKE returns control to subroutine INPUT.

Definitions of the input parameters are listed in Table D-1.

D.5 References

1. Murphy, R.W., Limpert, R., and Segel, L., Bus, Truck and Tractor-Trailer Braking System Performance, Final Report for Contract FH-11-7290, National Highway Traffic Safety Administration, Dept. of Transportation, March 1971.

2. North, M.R. and Oliver, S.J., Transient Load Transfer in an Articulated Vehicle Under Braking Conditions, M.I.R.A. Report No. 1967/7, June 1967.

3. Alfred Teves K.G., Ate Brake Handbook, Frankfurt-Main, Germany, 1960, pp. 131-135.

4. Strien, H., "Computation and Testing of Automotive Brakes," Dissertation, Technical University, Braunschweig, Germany, 1949.

5. Stroh, G.B., Lawrence, M.H., and Deibal, W.T., "Effects of Shoe Force Geometry on Heavy Duty Internal Shoe Brake Performance," SAE Paper No. 680432, May 1968.

Table D-1. Input Data Definitions

NUM(2)	Number of entries in torque vs. line pressure table for axle 1. Set this parameter to -1 to select the brake module option.
IBRT	Brake type identifier 0 = no brake 1 = S-cam 2 = 2-wedge 3 = single-wedge 4 = duo-servo 5 = duplex 6 = disc
AC	Brake chamber area (in^2) (wheel cylinder area for duo-servo, duplex, and disc brakes)
EM	Mechanical efficiency
PO	Pushout pressure (psi)
RD	Drum radius (in) (mean braking radius for disc brake)
UL	μ; unfaded lining coefficient of friction
ALPHO	See Figs. D-2, D-3
ALPH3	ALPHO + 2*ALPH1 (deg)
APRIM	(in)
HB	(in)
AB	(in)
BETA	(deg)
C2	(in)
OH	(in)

Table D-1 (Cont'd)

RC	Cam radius (in)
SAL	Slack adjuster length (in)
ALPHW	Wedge angle (deg)
KAXLE	Number of axles on vehicle

APPENDIX E

THE ANTILOCK MODEL

Three sets of antilock data are listed in this appendix, accompanied by corresponding pressure and wheel slip time histories representative of each data set. (Figures E-1 through E-3.) The time histories which are shown for each data set reflect the approximate behavior which a user should expect. These basic characteristics will vary according to the tire data, brakes, and loads employed.

```
01          ILOCK
-1          IALOPT1
01           OPTION1
3
2.
4.
1.
-1.
-85.
5
45.
2.
47.
3.              1.
1.              1.
 1.
-16.
16.
-1.
-8.
2
23.
1.
1.
-.5
3
5
45.
2.
47.
 3.             1.
1.              1.
-1.
16.
-16.
1.
8.
2
4.
1.
1.
-20.
2
4.
1.
1.
-290.
0.              0.          0.          0.
0
1.
1.
5.
1.
1.
5.
0.              50.
0.              50.
13.             13.         13.
```

```
6.7          6.7          6.7
.02          .02
.010         .010
100
100
-1
-1
-1
-1
.001
01           IALOPT2
01           IALOPT3
.025         TINC
0.0          TRUCK
```

Antilock Data Set #2

```
01       ILOCK
-1       IALOPT1
01       OPTION1
3
5
3.
45.
2.                        6.
47.           1.          6.
1.            1.          36.
-1.
1.
-22.          -12.                    -16.
 20.           12.
-4.           -7.                     -16.
2                                      .5
4.
1.
-1.
-72.
3
42.
1.
23.
1.
-.1
1000.
3
5
3.
45.
2.                        6.
47.           1.          6.
1.            1.
1.
-1.
```

```
  20.          10.                    -16.
 -20.         -10.                     -16.
 7.
 2.
 4.
 1.
 1.


-20.
2
42.
1.
1.
-.1
0.           0.          0.          0.
2
1
1.
5.
4
35.
27.
2.                       36.
21.          1.          36.
1.
-1.
200.         100.                    1.5
-200.        -100.                   1.5
0.           50.
-5.           2.5
12.5          12.5          12.5
14.          14.            0.
1
1.
5.
4
35.
27.
2.                       36.
21.          1.          36.
1.
-1.
200.         100.                    1.5
-200.        -100.                   1.5
0.           50.
-5.           2.5
0.           0.          0.
0.           0.          40.
.015          .01
.010         .010
100
100
-1
-1
```

```
01
5
3.
45.
2.                          6.
47.          1.             6.
1.           1.
-1.
1.
-20.         -10.                      -16.
20.           10.                     -16.
-6.
.02
4


1.
1.
41.
41.          4.
0.
-.1
50.
1.
.02
0
-1
.001
01           IALOPT2
01           IALOPT3
.025         TINC
0.0          TRUCK
```

Antilock Data Set #3

```
01          ILOCK
-1          IALOPT,
01          OPTION,
2
3
4.
1.                      -5.
23.
-1.
-80.        -1000.                  -35.
2000.
5
45.
2.
47.
3.          1.
1.          1.          36.
1.
-16.
16.
-1.
-15.        -8.                     1.5
4
5
45.
2.
47.
3.          1.
1.          1.
-1.
16.
-16.
1.
10.
2
4.
1.                      -5.
1.
-20.        -1000.                  -35.
```

```
148       2
149       34.
150       1.
151       -1.
152       0.10
152,25    2
152,5     4.
152.6     1.
152,7     1.
152.8     -200.
153       0.          0.          0.          0.
154       2
155       1
156       1.
157       5.
158       2
159       2.
159.25    12.
160       1.
160.25    -1.
161       0.          50.
162       0.          .35
163       14.         14.         14.
164       12.         12.          0.
165       1
166       1.
167       5.
168       2
169       2.
170       12.
171       1.
172       -1.
173       0.          50.
174       0.          .35
175       0.          0.          0.
176       0.          0.          40.
177       .00         .00
178       .010        .010
179       100
180       100
181       01
182       3
183       7.                      36.
185       1.
186       31.                     36.
187       0.          1.                      1.5
189       -2.
190       1.0         0.                      1.5
191       4
194       1.
194.25    1.
194.5     7.                      23.
194.6     41.         7.          23.
195       0.
196       0.
197       .35         0.                      .9
198       -.35        0.                      .9
204       -1
219       01
220       2
```

```
1.
32.
.9
-1.
.04
0
0
-1
.020
01          IALOPT2
01          IALOPT3
.025        TINC
0.0         TRUCK
```

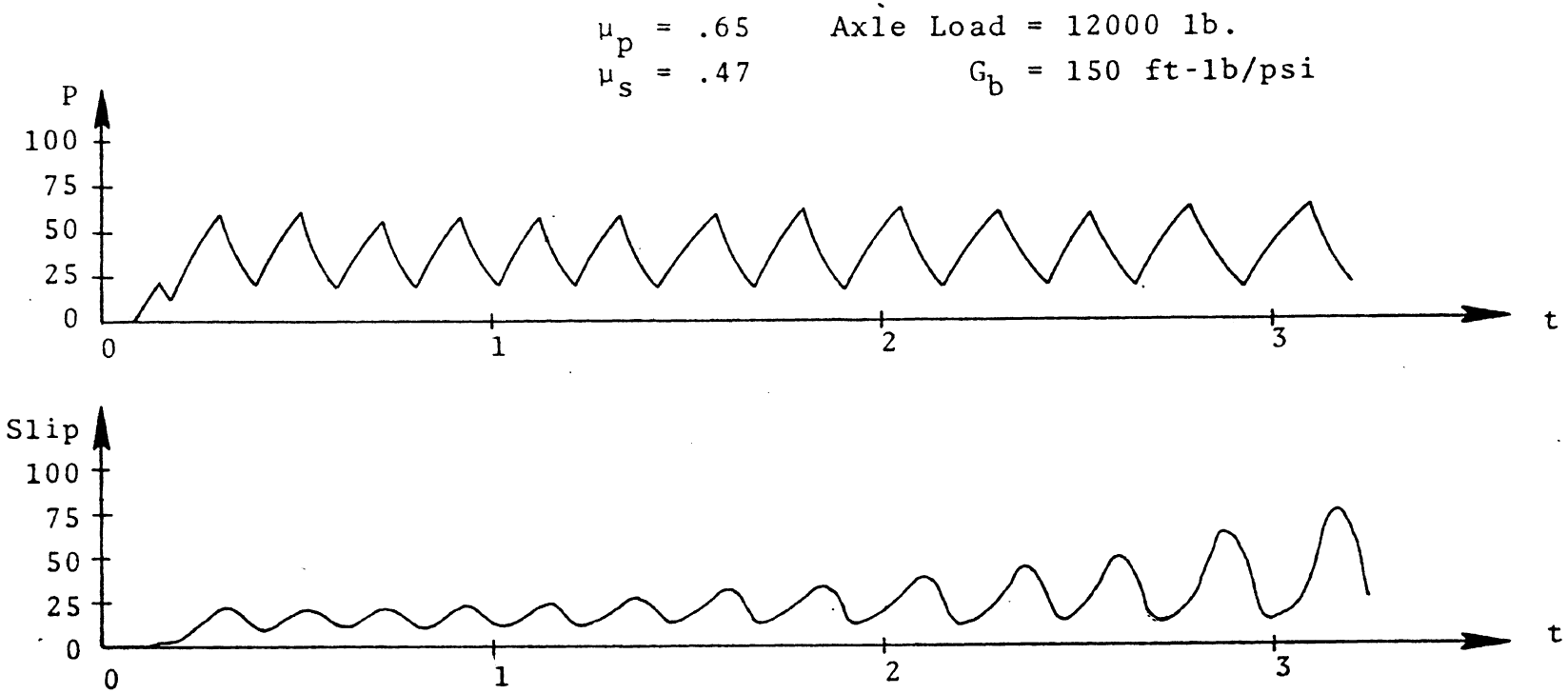

Figure E-1
SIMULATION RESULT --- Data Set #1

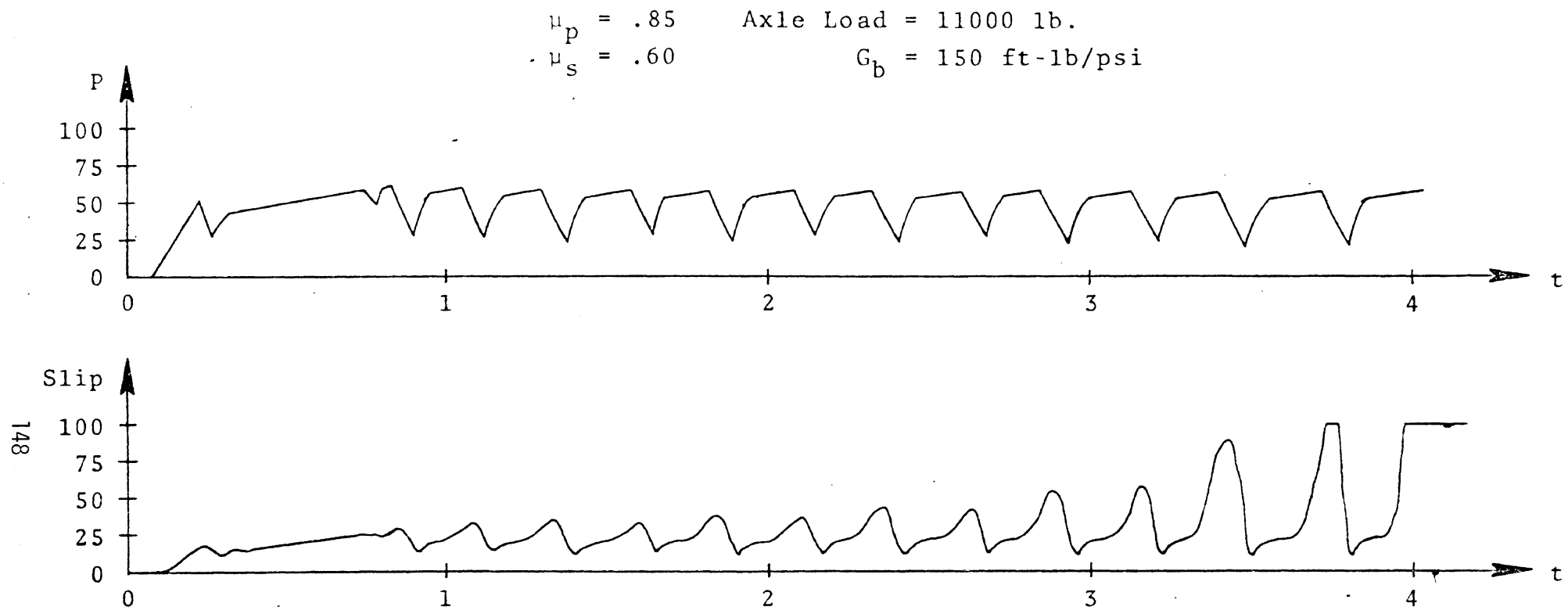

Figure E-2

SIMULATION RESULT --- Data Set #2

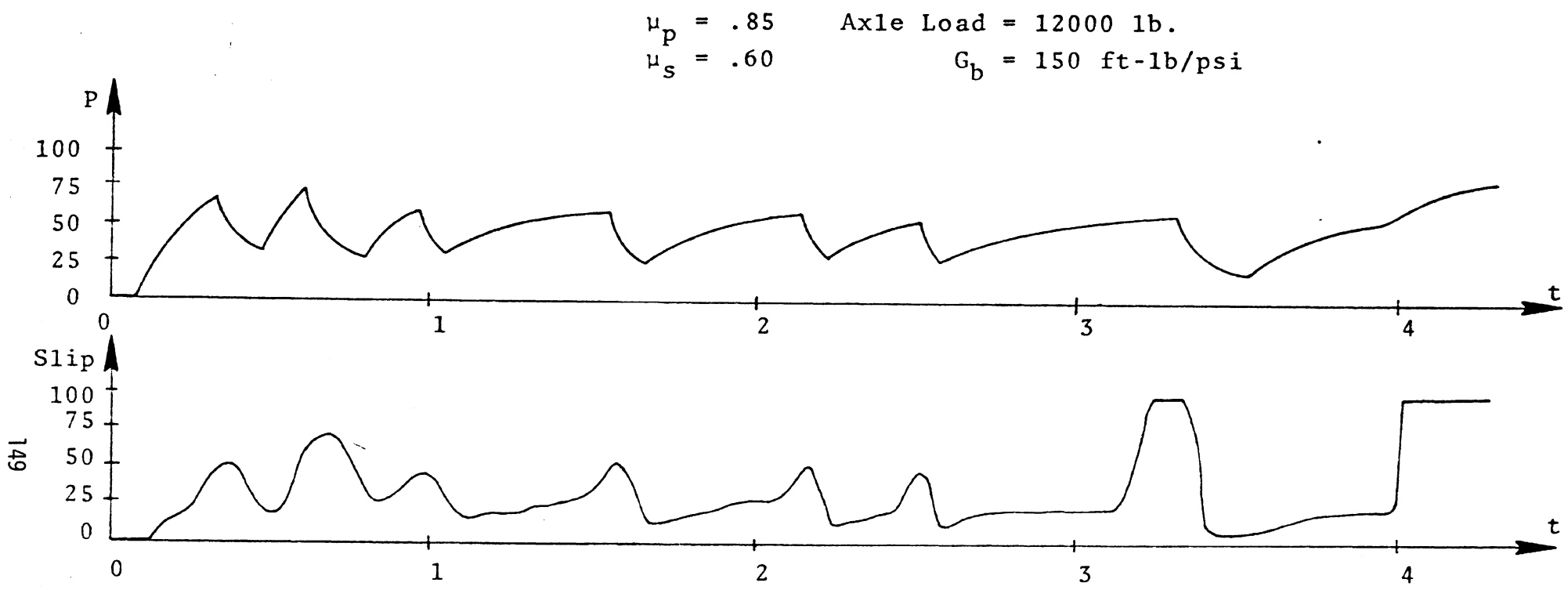

Figure E-3

SIMULATION RESULT --- Data Set #3

APPENDIX F

OPTIONAL FIFTH WHEEL MODELS

The original Phase III Tractor-Trailer Braking Performance Program employed a somewhat unique model of the fifth wheel coupling. This model assumes a rigid coupling at the fifth wheel in the fore/aft direction, but a compliant coupling between tractor and trailer in the vertical direction. (See Eq. C-21 and Reference [1].) The purpose of the vertical motion spring is to mathematically decouple the equations of motion of tractor and trailer, thus avoiding the need for matrix solution of these equations. The spring is not intended to model real compliance in the fifth wheel. Thus, this spring rate is not an input parameter, but is fixed within the program based on a compromise between stiffness and system frequency as they reflect on accuracy and digital integration requirements, respectively.

While employing the Phase III tractor-trailer program for preliminary ride studies, one user discovered that unrealistic pitch and bounce motions of the vehicle could be predicted. The fifth wheel spring, in concert with suspension springs, apparently contributed to unrealistic sprung mass oscillations in the 10 Hz range. It does not appear that the problem resulted from the modeling concept, but rather from the choice of spring rate. In the original program, the fifth wheel spring rate was a fixed value established within the program.

Two steps have been taken to remedy this problem in the most recent program version. First, the original fifth wheel model has been altered in two ways. These are: (1) The fifth wheel spring rate is now calculated by the program. Its value is chosen (dependent on other inertia and geometric parameters) to be rather high, but within the limits acceptable to the digital integration routine used in the programming. (2) Damping has been added to the fifth wheel model. The damping coefficient is also calculated by the program and is approximately 70% of critical.

The second change to the program is the inclusion of a "matrix solution" option. If this option is chosen, the fifth wheel is no longer modeled as compliant, but as a rigid coupling in all directions. In this scheme, the pitch and bounce motion of tractor and trailer are coupled, requiring, at each time step, simultaneous solution of the four associated equations of motion. This model, while providing an optional method of problem solution, also provides a "check" on the fifth wheel spring model.

A comparison of three solutions of the same "problem," using the three fifth wheel models (i.e., the old spring model, the new spring model, and the matrix solution) is shown in Figure F-1. The "problem" involves a five-axle tractor-trailer, freely rolling at 50 ft/sec, encountering a step (down) of 0.1 ft in an otherwise smooth road surface. The figure displays tractor bounce acceleration and displacement.

The figure shows clearly that the "old spring" model is very oscillatory. The acceleration trace is so dominated by the 10 Hz mode that only peak accelerations have been shown. However, the new spring model and the matrix inversion solution agree very well and both eliminate the unrealistic 10 Hz oscillation. Early in the solution, predictions by these two models disagree somewhat, but are qualitatively quite similar. Immediately following clearance of the road disturbance by the last axle, the solutions become virtually identical.

It would be only conjecture to say which solution is "better" at this point. Fifth wheels are neither rigid, as the matrix solution assumes, nor as compliant (or viscous) as the spring solution assumes. Further, for ride considerations, it is very likely that the rigid body assumptions (no frame compliance) of the general model introduce greater errors than either of the newer fifth wheel models.

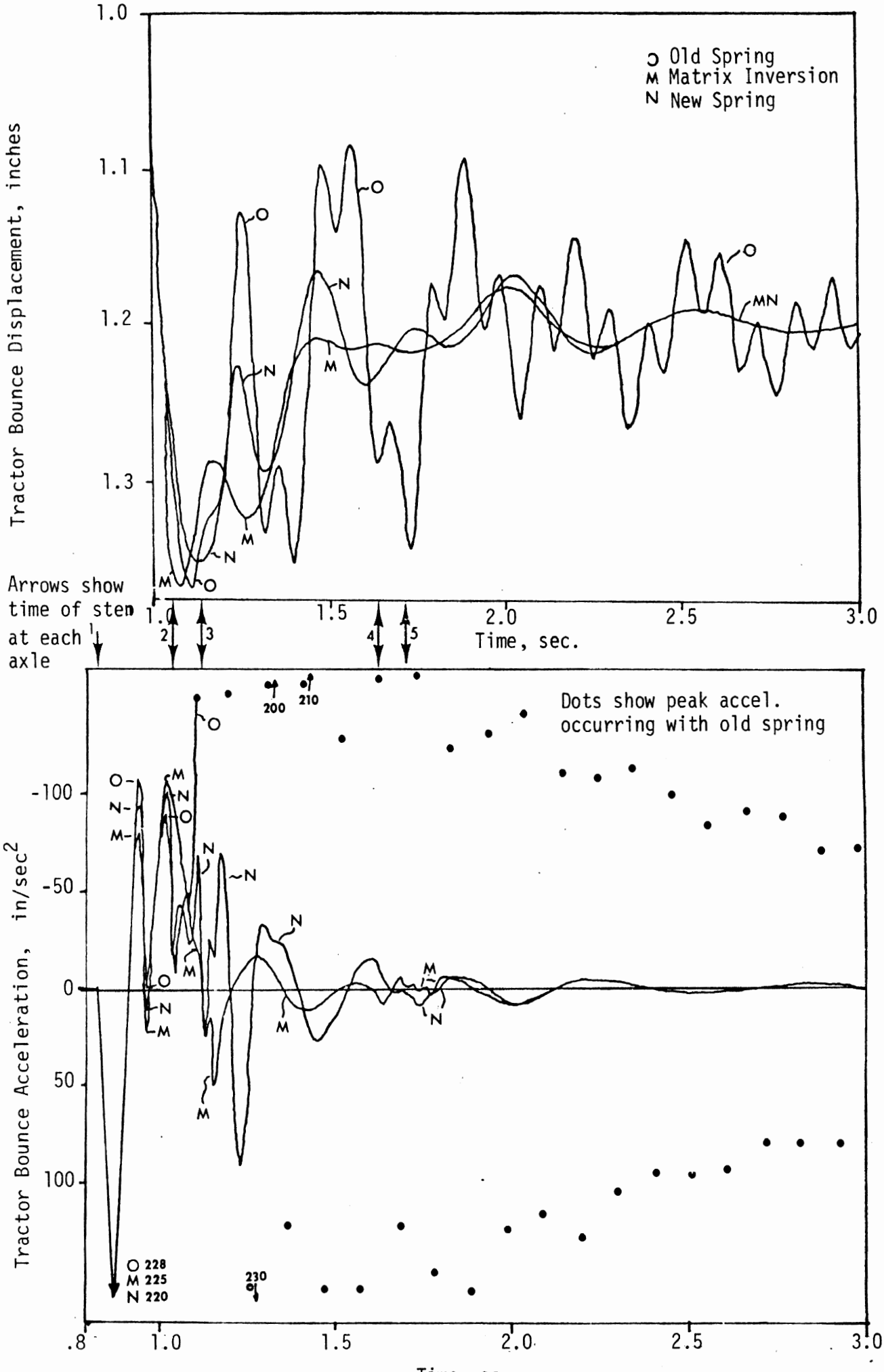

Figure F-1. Comparison of problem solution by the three fifth wheel models.

The program changes require that the subprograms MINV and GMPRD be made available. Both of these subprograms are available in the IBM Scientific Subroutine Package which most users will have on line. Both subprograms are called from FCT1 when (and only when) the matrix solution is chosen. MINV is called only once from the initialization portion (entry point FCT1) of FCT1. GMPRD is called at each integration time step from the active portion (entry point FCT) of FCT1.

The new spring model introduces no changes from the user's point of view, i.e., program manipulation is exactly as in the past. The matrix solution requires that a negative number be entered for TIMF, the maximum real time for simulation (sec). For example, if TIMF is entered as (+3.0), the simulation will run for 3 seconds real time and solution will be per the new spring model; if TIMF is entered as (-3.0), the simulation will run for 3 seconds real time and solution will be per the matrix inversion model.